DISSECTING LEAF DORSIVENTRAL POLARITY IN MAIZE

A Dissertation

Presented to the Faculty of the Graduate School

of Cornell University

In Partial Fulfillment of the Requirements for the Degree of

Doctor of Philosophy

by

Ryan Nathaniel Douglas

May 2010

DISSECTING LEAF DORSIVENTRAL POLARITY IN MAIZE

Ryan Nathaniel Douglas, Ph. D.

Cornell University 2010

Leaves are produced from the flank of the shoot apical meristem and are asymmetric from inception. Mutations perturbing dorsiventral cell-fate acquisition may cause the formation of radially symmetric leaves that lack adaxial/abaxial (upper/lower) polarity. However, mutations in the maize (*Zea mays*) gene *ragged seedling2* (*rgd2*) condition radial leaves that maintain dorsiventral polarity. A positional cloning approach revealed that *rgd2* encodes an ARGONAUTE7 (AGO7)-like protein. In *Arabidopsis,* AGO7 forms a complex with microRNA390 (miR390) to cleave the non-protein coding *tas3* transcript. The cleavage product is stabilized and converted to double-stranded RNA (dsRNA). The dsRNA is then cleaved into 21-nucleotide long fragments termed *t*a-siARFs. The ta-siARFs then target transcripts of the putative abaxial identify factor *auxin response factor3* (*arf3*) for degradation by AGO7. Previous studies with the abaxialized maize mutant leafbladeless1 (lbl1) implicated a role for *t*a-siARF function in establishing dorsiventral polarity. Although RGD2 and LBL1 function are required for reduced accumulation of *arf3a*, *arf3a* transcripts are spatially restricted to the abaxial regions of leaf primordia independently of *t*a-siARF biogenesis. Additionally, RGD2 function is required to regulate the accumulation and localization the abaxial identity factor miR166 in shoot apices. These data suggest combined over-accumulation of *arf3a* and miR166 are insufficient to confer abaxialized leaf phenotypes in maize. A revised model for the role of small RNAs during dorsiventral patterning of maize leaves is discussed.

A maize gene of unknown function (AC211276.4_FG008; *punctate vascular expression1* (*pve1*)) was previously identified as being markedly down-regulated in rgd2 mutants. The coding region and putative gene structure of *pve1-R* is described. Quantitative reverse transcriptase-PCR confirmed that *pve1* accumulates to lower levels in rgd2 apices and showed its accumulation is diminished in lbl1 mutants, suggesting *pve1* regulation is downstream of *t*a-siARF biogenesis. Finally, to investigate potential downstream effects of *t*a-siARF biogenesis on a genomic scale, laser microdissection was coupled with Illumina RNA sequencing to search for differential regulation of predicted target genes that may be controlled by miR390, miR166 and/or *t*a-siARF. This research furthers our understanding of leaf development in maize.

BIOGRAPHICAL SKETCH

Ryan Nathaniel Douglas was born in St. Louis, Missouri in 1983. He graduated from Brentwood High School in Brentwood, Missouri in 2001. Following high school, he attended Truman State University in Kirksville, Missouri. Ryan graduated from Truman State University in 2005 with a Bachelor of Science in biology.

To my parents and Diana

ACKNOWLEDGMENTS

Thank you to Diana for her understanding, patience, and willingness to move to New York. Thanks to my parents for giving me every opportunity to succeed and for helping me along the way.

Thanks to my doctoral mentor, Mike Scanlon, for taking me into his lab and then passing down decades of wisdom both in the lab and in the fields (maize and baseball). Thank you to my undergraduate mentors, Brent Buckner and Diane Janick-Buckner, for introducing me to the world of maize genetics. Thank you to my committee members, Tom Brutnell, Wojtek Pawlowski and Jian Hua, for their helpful discussions and suggestions for this research.

My lab mates, particularly John Woodward, Katie Petsch and Josh Strable, deserve thanks for aiding me in the lab and in the maize field. I thank Chris Bozza for assisting me during field seasons. Dan Wiley was instrumental in mapping *ragged seedling2*. Dave Henderson and Marja Timmermans offered insightful comments regarding the *t*a-siARF biogenesis pathway. I am indebted to Jean Koski, Nick Vail, and Janet Myrick of the Guterman Greehouse staff at Cornell University for keeping my plants alive even when I forgot about them. The staff in the Plant Biology office, Pat Welch, Tara Nihill and Karin Jantz, were incredibly helpful throughout my time at Cornell.

Finally, I wish to thank the National Science Foundation and the Plant Biology department at Cornell University for providing funding.

TABLE OF CONTENTS

LIST OF FIGURES

LIST OF TABLES

Introduction

Introduction

Perhaps the most distinguishing morphological feature of plants is their leaves. Maize (*Zea mays*) leaves consist of four main anatomical parts: the proximal sheath, the ligule, the auricle and the distal blade (Figure 1.1). The sheath wraps around the stem and younger leaves, while the blade is flattened in the mediolateral axis (midrib to margin) and is adapted for light capture and gas exchange. The ligule and auricle are found at the blade sheath boundary; the ligule is an adaxial (upper) membranous structure and has been hypothesized to function in protecting younger leaves from water, dust and pathogens or possibly to have a secretory function (Freeling and Lane, 1994; Chaffey, 2000). The leaves of the eudicotyledon *Arabidopsis thaliana* consist of only two main parts: the proximal petiole and the distal lamina, with a pair of stipules at the base of the petiole (Figure 1.1). While leaves in maize and *Arabidopsis* may appear very different at the macroscopic level, many of the molecular mechanisms involved in forming the leaves are conserved between the genera.

The process of leaf formation begins in the shoot apical meristem (SAM). The SAM has two major functions: (1) to maintain itself and (2) to initiate lateral organs (Brooks et al., 2009). Determining which cells will maintain the SAM and which will become founder cells for new leaf primordia is a crucial aspect of SAM function. Generally, the SAM maintains itself with a group of "stem cells" in a central zone (CZ), which replenish cells in the peripheral zones (PZ) that give rise to the above-ground lateral organs of the plant (Figure 1.2). Eudicotyledonous plants such as *Arabidopsis* have a three-tiered SAM. The outer two layers of the SAM (L1 and L2), the tunica, divide anticlinally, while the underlying corpus (L3) has more random planes of division.

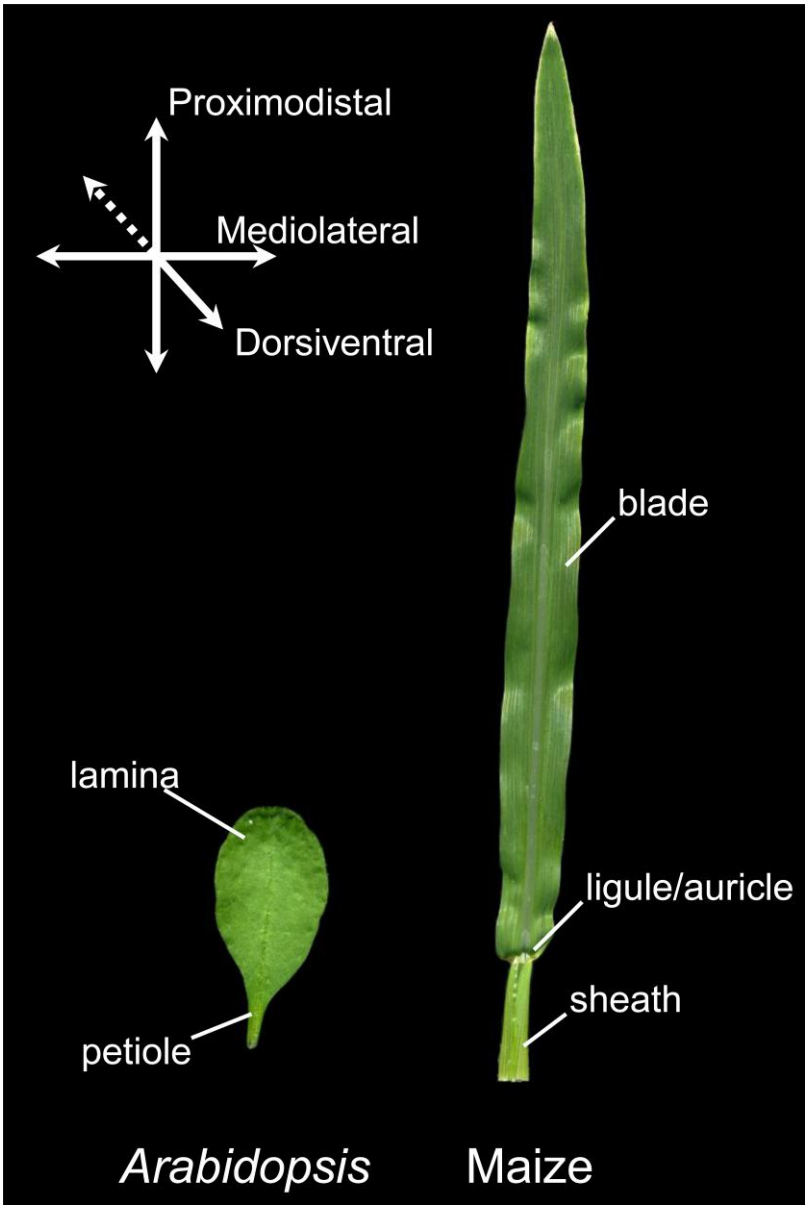

Figure 1.1. Leaf morphology.

Arabidopsis and maize leaves are morphologically distinct. *Arabidopsis* leaves consist of a proximal petiole and distal lamina, while maize leaves have a proximal sheath and a distal blade with a ligule and auricle at the sheath-blade boundary. Blades are flattened in the mediolateral axis (medial midrib to lateral margin) to harvest light energy. Leaves also have distinct adaxial (upper surface) and abaxial (lower surface) tissues, which comprise the dorsiventral axis.

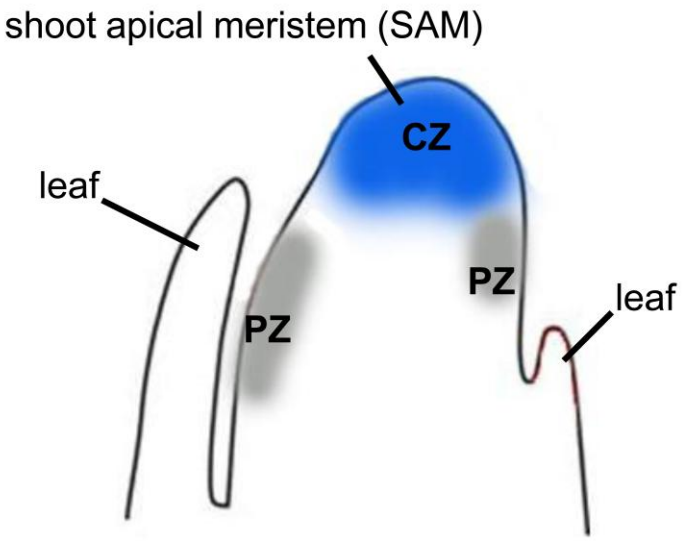

Figure 1.2. Maize shoot apex.

The shoot apex consists of the shoot apical meristem (SAM) and leaf primordia. The SAM consists of the central zone (CZ; blue area) where meristem identity is maintained and peripheral zones (PZ; gray areas) where leaf founder cell recruitment occurs.

Monocotyledons like maize only have a one cell layer tunica (L1) overlaying the corpus (L2) (Brooks et al., 2009).

Maintaining the shoot apical meristem

In *Arabidopsis* the maintenance of the SAM relies heavily, but not exclusively, on the *WUSCHEL (WUS)-CLAVATA (CLV1, CLV2, CLV3)* genetic pathway (Schoof et al., 2000). *WUS* is required to maintain a "stem cell" niche, while the CLV proteins restrict the area of *WUS* accumulation (Laux et al., 1996; Schoof et al., 2000). *Arabidopsis clv* mutants have enlarged meristems with a larger than normal CZ, and *CLV* genes are required to maintain the boundary between the CZ and the PZ (Clark et al., 1997; Jeong et al., 1998; Fletcher et al., 1999; Reddy and Meyerowitz, 2005). *CLV3* was identified as a small 96-amino acid long peptide ligand that acts non-cell autonomously (Fletcher et al., 1999; Sharma et al., 2003), while *CLV1* and *CLV2* were identified as receptor-like proteins (Clark et al., 1997; Jeong et al., 1998). More recently, the functional CLV3 ligand was found to be 13-amino acids long and shown to directly bind the CLV1 receptor (Ohyama et al., 2009; Ogawa et al., 2008). CLV1 is a fully functional leucine-rich repeat receptor kinase, but CLV2 lacks an intracellular kinase domain. CLV2 interacts with CORYNE, which consists of a transmembrane domain and an intracellular kinase, to form a functional receptor kinase to transmit CLV3 signals independently, but in parallel to, CLV1 receptors (Müller et al., 2008; Zhu et al., 2009). The maize genes *thick tassel dwarf1* (*td1*) and *fasciated ear2* (*fea2*) have been shown to encode functional homologs of *CLV1* and *CLV2*, respectively (Taguchi-Shiobara et al., 2001; Bommert et al., 2005). Similar to *clv1* and *clv2* mutants in *Arabidopsis*, *td1* and *fea2* maize mutants have larger inflorescence meristems than non-mutant siblings, suggesting a mechanism similar to the *Arabidopsis WUS-CLV* pathway is operating in maize inflorescences.

The CLV signaling pathway is required for proper regulation of *WUS* in *Arabidopsis,* which encodes a homeodomain transcription factor required for SAM maintenance; loss-of-function *wus* mutants fail to maintain a CZ in the SAM (Mayer et al., 1998). *WUS* is believed to function in a feedback loop with *CLV3*; *WUS* accumulation increases when *CLV3* is silenced and decreases when *CLV3* expression is activated (Fletcher et al., 1999; Brand et al., 2000; Schoof et al., 2000; Müller et al., 2006). This feedback loop is believed to work in a manner such that *WUS* promotes *CLV3* accumulation, whereupon CLV3 moves from the L1/L2 to the CZ to decrease *WUS* accumulation via the CLV1 receptor. When *WUS* has been sufficiently depleted it can no longer promote *CLV3* accumulation, which halts *WUS* repression. With no functioning CLV pathway to repress *WUS,* the cycle can begin anew and thus regulate the amount of cells comprising the CZ of the SAM. This negative feedback loop functions to maintain a pool of stem cells in the SAM core that is balanced by the loss of SAM cells during organogenesis.

Meristematic cells are maintained in an indeterminate growth state by homeodomain-containing *KNOX* (*KNotted-like homeobOX)* genes such as *SHOOTMERISTEMLESS* (*STM*), *BREVIPEDICELLUS* (*BP*), *KNAT1* (*knotted1-like homeobox gene*), *KNAT2*, and *KNAT6* in *Arabidopsis* and *KNOTTED1* (*KN1*), *LIGULELESS3* (*LG3*), *GNARLEY* (*GN*) and *ROUGH SHEATH1* (*RS1*) in maize (Long et al., 1996; Mele et al., 2003; Lincoln et al., 1994; Byrne et al., 2002; Kerstetter et al., 1997; Muehlbauer et al., 1999; Foster et al., 1999; Schneeberger et al., 1995). KN1 has been implicated in maize as being required for meristem initiation and/or maintenance as *kn1* mutants containing loss-of-function alleles often have shoots that do not proceed past the coleoptilar stage (Kerstetter et al., 1997; Vollbrecht et al., 2000). In some maize inbreds with large SAMs, such as B73, *kn1* loss-of-function mutants are able to produce a SAM and generate phenotypically normal

leaves (Vollbrecht et al., 2000). However, some *kn1* mutant plants produce additional leaves in the axils of otherwise normal leaves, suggesting that *KN1* function is required for establishing proper leaf-SAM boundaries (Kerstetter et al., 1997). In order for founder cell recruitment to occur, these *KNOX* genes must be turned off in the PZ to allow a switch to determinate growth. Similarly, the *Arabidopsis* homolog of *KN1*, *STM*, is believed to play a similar role in maintaining/initiating *Arabidopsis* meristems and separating leaves from the SAM because *stm* mutants produce only two fused cotyledons (Long et al., 1996).

In addition to loss-of-function alleles, several dominant alleles of maize *KNOX* genes have been recovered. *Kn1* dominant mutants exhibit ectopic "knots" of sheath, ligule and auricle in the blade, *Gn1-R* shows ectopic carpals in flowers and *Lg3* mutants have ligule displaced into the leaf blade (Sinha and Hake, 1994; Foster et al., 1999; Fowler and Freeling, 1996). The phenotypes caused by these dominant mutations are hypothesized to have been caused by the timing of their misexpression (Muehlbauer et al., 1997). The *Kn1-DL* dominant mutation causes misexpression of *KN1* in distal portions of the leaf blade, which causes midrib termination and leaf bifurcation. These phenotypes suggest that *KN1* function may be involved in setting up proximodistal polarity in maize leaves in addition to SAM maintenance (Ramirez et al., 2009).

Establishing organ boundaries

The second main function of the SAM is to generate above-ground lateral organs. Several genes play roles in both maintaining the SAM and in allowing the production of lateral organs. For example, the *KN1*-like gene *STM* is required to create proper boundary separation between the SAM and initiating leaf primordia via interactions with the *Arabidopsis CUP-SHAPED COTYLEDON1/2/3* (*CUC*) genes, NAC-domain transcription factors similar to the petunia (*Petunia sp.*) gene *NO*

APICAL MERISTEM (Souer et al., 1996; Aida et al., 1997; Aida et al., 1999; Vroemen et al., 2003). All *CUC* transcripts accumulate in boundary regions between the presumptive SAM and cotyledons during embryogenesis, and later between the SAM and initiating leaves where they function to inhibit growth (Aida et al., 1999; Vroemen et al., 2003). Similarly, the NAC-domain transcription factor *GOBLET* is required to separate leaflet boundaries in the compound tomato leaves (Berger et al., 2009). The *CUC* genes are believed to function redundantly as *cuc* single mutants have essentially no mutant phenotype, but *cuc* double mutants lack an embryonic SAM and have two fused cotyledons (Aida et al., 1997). Genetic and molecular techniques revealed that *STM* expression requires *CUC1/2* function, and thus the *CUC* genes are required for SAM initiation in *Arabidopsis* (Aida et al., 1999). However, once *STM* expression initiates in the presumptive SAM, *CUC2* function is not required to maintain *STM* expression (Aida et al., 1999). *STM* and *CUC2* may function in a feedback-loop, as *stm* mutants lose *CUC2* accumulation in the normal boundary regions that separate the presumptive SAM from the cotyledons, which suggests *STM* function is required to both initiate SAM identity and to separate the SAM from the cotyledons in *Arabidopsis* (Aida et al., 1999). In addition to requiring *STM* function for proper localization, a search for enhancers of the *cuc2-1* mutant phenotype revealed that *CUC* accumulation is dependent on the SWI/SNF chromatin-remodeling ATPases *SPLAYED* (*SYD;* only *CUC2*) and *AtBRM*, although this regulation is independent of the *STM*-related pathway and it is unclear if *SYD* and *AtBRM* maintain or initiate *CUC* accumulation in boundary regions (Kwon et al., 2006). The *KNOX* gene *KNAT6* has also been shown to be involved in the *STM-CUC* pathway, as *CUC1* and *CUC2* are required for *KNAT6* expression and *knat6;stm* double mutants have more severely fused cotyledons than *stm* single mutants (Belles-Boix et al., 2006).

Auxin also plays an important role in defining where leaf-meristem and leaf-

leaf boundaries are established. An auxin maximum forms at the presumptive site of the incipient leaf primordium (P0), and the flow of auxin is directed by *PIN-FORMED1* (*PIN1*) (Reinhardt et al., 2003). *PIN1* is an auxin efflux carrier that is polarly-localized by the regulator *PINOID* (*PID*) (Gälweiler et al., 1998; Friml et al., 2004). Both *pin1* and *pid* single mutants occasionally exhibit moderate cotyledon phenotypes (abnormal number, size and/or shape), but cotyledons are almost always present (Bennett et al., 1995). In contrast, *pin1;pid* double mutants often lack cotyledons (Furutani et al., 2004). In *pin1;pid* double mutant embryos *CUC1* and *CUC2* accumulation domains expanded into regions of the embryo that normally became cotyledons (Furutani et al., 2004). This suggests that *PIN1* and *PID*, and thus auxin, function to repress *CUC* accumulation and prevent it from accumulating outside of boundary regions in the embryo and developing leaf primordia. The over-accumulation of *CUC* in *pin1;pid* double mutants likely inhibits cell division enough that cotyledons simply are not produced (Furutani et al., 2004).

CUC gene accumulation is regulated by several distinct pathways, including by small RNA molecules called microRNAs (miRNAs). miRNAs are approximately 21-nucleotide long RNA molecules that function in post-transcriptional gene silencing by guiding the cleavage of mRNAs or repressing translation (Fagard et al., 2000; Lanet et al., 2009). Long single-stranded RNAs that form imperfect hairpin loops are transcribed from noncoding regions of the genome to form primary miRNAs (pri-miRNAs), and the pri-miRNAs are cleaved into short double-stranded RNAs by a complex including DICER-LIKE1 (DCL1) and HYPONASTIC LEAVES1 (McManus et al., 2002; Reinhart et al., 2002; Kurihara et al., 2006). The dsRNAs are exported from the nucleus to the cytoplasm where they are incorporated into a complex including ARGONAUTE1 (AGO1) to cleave the appropriate target mRNA (Figure 1.3; Fagard et al., 2000). miR164 is required to spatially regulate the transcript

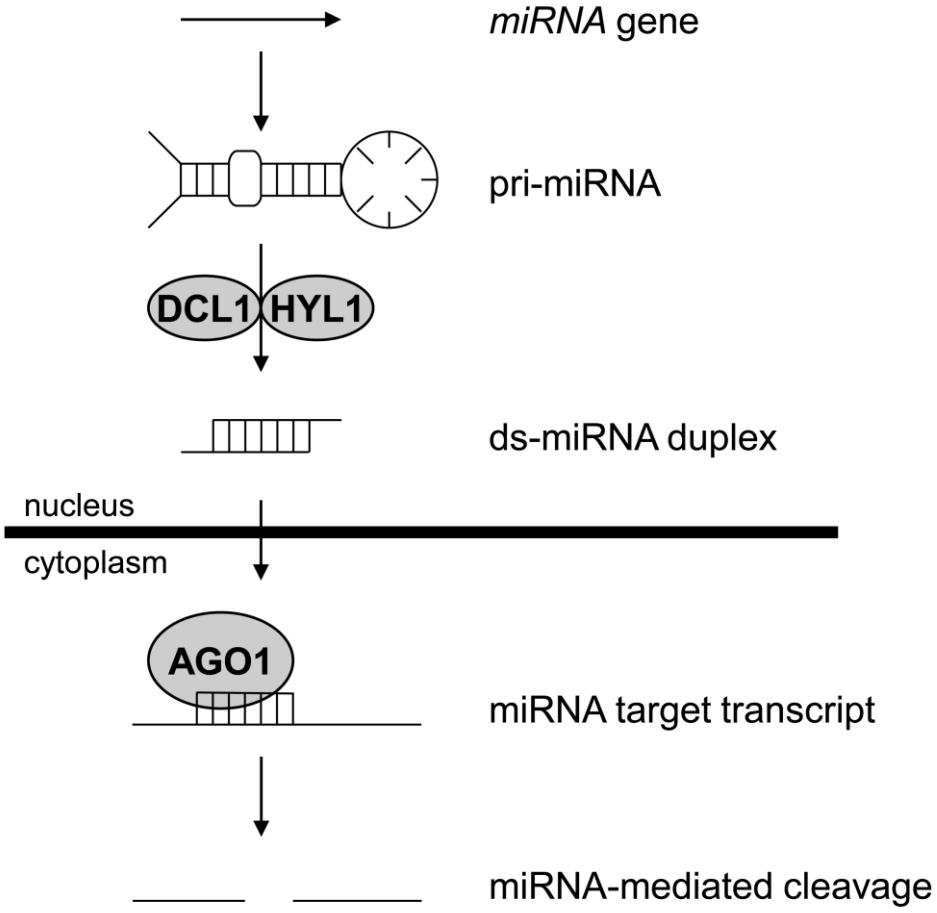

Figure 1.3. microRNA biogenesis.

MicroRNA (*miRNA*) genes are transcribed and form an imperfect stem-loop structure called a pri-miRNA. The pri-miRNA is convered into a double-stranded (ds) miRNA duplex by DICER-LIKE1 (DCL1) and HYPONASTIC LEAVES1 (HYL1) that is exported from the nucleus to the cytoplasm. Once in the cytoplasm the miRNA forms an RNA-induced silencing complex (RISC) with ARGONAUTE1 (AGO1) and the RISC binds a complimentary sequence on a target transcript. The target transcript is then cleaved by the RISC.

accumulation pattern of *CUC1* and *CUC2* in *Arabidopsis* (Laufs et al., 2004; Mallory et al., 2004). *CUC1* and *CUC2* transcript levels are diminished and a *cuc1;cuc2* double mutant phenotype is recapitulated when miR164 is over expressed (Laufs et al., 2004; Mallory et al., 2004). Similarly, when miR164-resistant versions of *CUC1* and *CUC2* are expressed there are defects in organ boundary formation (Laufs et al., 2004; Mallory et al., 2004). The many levels of *CUC* gene regulation indicate its importance in forming proper SAM-cotyledon, SAM-leaf and leaf-leaf boundaries.

Despite the importance of *CUC* genes for forming boundaries, they are not the only genes known to have a role in establishing organ boundaries. Two BTB/POZ-domain proteins, BLADE-ON-PETIOLE1 (BOP1) and BOP2, have been found to interact with LATERAL ORGAN BOUNDARY (LOB)-domain proteins to help define organ boundaries, and both *BOP* gene transcripts accumulate around SAM-leaf boundaries (Ha et al., 2004; Norberg et al., 2005; Ha et al., 2007; Jun et al., 2010). Another gene known to affect boundary formation is *ARABIDOPSIS THALIANA HOMEOBOX GENE1* (*ATH1*), a BELL-type homeodomain protein (Gómez-Mena and Sablowski, 2008). *ATH1* transcripts accumulate throughout the SAM, early leaf primordia and at the base of developing leaves, and *ath1* exhibit rosette leaves that are partially fused on the abaxial side of the leaf base (Gómez-Mena and Sablowski, 2008).

The role of phytohormones in leaf initiation

The pyhtohormones cytokinin, auxin and gibberellin play important roles in determining where a new leaf primordium will emerge from the SAM (reviewed in Shani et al., 2006). Cytokinin levels are high in the CZ of the SAM and low in the PZ where founder cell recruitment occurs; KNOX function may establish this concentration gradient. KNOX proteins, which are excluded from regions of the PZ undergoing founder cell recruitment, enhance cytokinin levels by increasing the

expression of *ISOPENTENYL TRANSFERASE7*, a cytokinin biosynthesis gene (Yanai et al., 2005). Cytokinin is a promoter of cell division and the cytokinin signaling pathway may serve as a mechanism for KNOX-mediated indeterminate growth of the CZ (Riou-Khamlichi et al., 1999). A KNOX protein in tobacco also keeps levels of the plant growth regulator gibberellin low by directly inhibiting expression of the *GA20 oxidase* gene, which is required for gibberellin biosynthesis (Sakamoto et al., 2001; Hay et al., 2002). In maize, KN1 proteins directly activate expression of *GA2OX1*, a gene required to inactivate gibberellin (Bolduc and Hake, 2009).

In contrast to cytokinin, auxin and gibberellin levels are high in the PZ where founder cell recruitment takes place. The polar transport of auxin by the efflux transporter PIN1 and the influx transporter AUXIN RESISTANT1 sets up the gradient of auxin required for leaf initiation (Gälweiler et al., 1998; Yamamoto and Yamamoto, 1998; Reinhardt et al., 2003). Generally, PIN1, which is capable of a rapidly changing accumulation pattern (Friml et al., 2002), localizes to the apical side of cells in the meristem and transports auxin towards the apex of the meristem, but PIN1 localization changes in the area of the incipient leaf primordium (P0). When PIN1 accumulates near the P0 it points towards the primordium rather than the meristem apex. This increases the auxin concentration at the P0 and is correlated with leaf initiation. Auxin has been shown to reduce accumulation of *KNOX*-like transcripts in *Arabidopsis*, which has the secondary effect of lowering the levels of cytokinin and increasing gibberellin levels in the PZ (Hay et al., 2006; Yanai et al., 2005; Sakamoto et al., 2001). As the levels of auxin and gibberellin increase, the amount of KNOX proteins and cytokinin levels decrease, thus promoting founder cell recruitment.

Auxin turns the *KNOX* genes off initially, but as auxin levels gradually decrease in the leaf primordium *KNOX* genes will reactivate without the action of the ARP family of MYB-domain containing transcription factors *PHANTASTICA (PHAN;*

Antirrhinum majus)/ASYMMETRIC LEAVES1 (AS1; Arabidopsis)/ROUGH SHEATH2 (RS2; maize) (Waites and Hudson, 1995; Byrne et al., 2000; Timmermans et al., 1999; Tsiantis et al., 1999; Phelps-Durr et al., 2005). *AS1* is expressed in the leaf founder cells in the PZ as well as the adaxial surface of leaf primordia (Byrne et al., 2000). Maize RS2 protein was shown to interact with HIRA, a WD-40 repeat containing protein that may direct changes in chromatin arrangement (Phelps-Durr et al., 2005). It is believed that PHAN/AS1/RS2 and HIRA work together to change the chromatin state at *KNOX* loci to maintain *KNOX* gene silencing throughout leaf development. In maize, leaf founder cell recruitment begins at the site of the presumptive midrib and proceeds laterally around the SAM until two overlapping leaf margins are formed (Scanlon, 2000). In order for founder cell recruitment to begin, *KNOX* genes must first be down regulated by auxin (Hay et al., 2006). The site of the presumptive midrib is thus determined by an auxin maximum and PIN1 localization (Reinhardt et al., 2000; Reinhardt et al., 2003). PIN1 localizes primarily in the L1 in the *Arabidopsis* SAM and in the epidermis and vasculature in leaf primordia (Reinhardt et al., 2003). However, near the P0 the localization of PIN1 orients the flow of auxin toward the leaf primordium rather than the apex, suggesting that auxin is funneled through the L1 to P0 to initiate leaf formation (Reinhardt et al., 2003). Maize PIN1 does not accumulate throughout the L1, but it does accumulate in the L1 near the P0 and it accumulates in the presumptive provascular strands of young leaf primordia (Lee et al., 2009).

PIN1 and auxin play important roles in determining phyllotaxy. As PIN1 funnels auxin into new leaf primordia, auxin sinks are created and the production of additional leaves in the immediate vicinity is discouraged. When the required auxin threshold for new leaf formation is crossed at a minimum distance from pre-existing leaf primordia PIN1 will relocalize to form a new auxin sink (Reinhardt et al., 2003).

Maize has alternate phyllotaxy, with one leaf per node and leaves initiating 180° apart. The maize gene *ABERRANT PHYLLOTAXY1* (*ABPHYL1*), which encodes a cytokinin-inducible type A response regulator that accumulates at the P0, is required to regulate SAM size and leaf phyllotaxy, as *abphyl1* mutants initiate two leaves per node in a decussate pattern (Jackson and Hake, 1998; Giulini et al., 2004). Although cytokinin-inducible type A response regulators are generally believed to be negative regulators of cytokinin signaling, several have been found to be positive gene regulators (Osakabe et al., 2002; Leibfried et al., 2005). *ABPHYL1* is necessary for *PIN1* accumulation (and thus auxin distribution), and deficient *PIN1* accumulation may cause delays in leaf initiation allowing for abnormal amounts of SAM growth between nodes (Lee et al., 2009). The enlarged SAM in *aphyl1* mutants may allow two auxin maxima to form, as opposed to only one in non-mutant meristems, and cause the production of two leaves per node (Jackson and Hake 1998; Giulini et al., 2004). Since cytokinin is required to promote *ABPHYL1* accumulation, and *ABPHYL1* is required for *PIN1* accumulation, cytokinin and auxin are inexorably linked in the establishment of phyllotaxy in maize (Lee et al., 2009).

TERMINAL EAR1 (*TE1*), a maize RNA-binding gene, has also been implicated in establishing proper phyllotaxy (Veit et al., 1998). *In situ* hybridizations have shown *TE1* to accumulate in a horseshoe-like pattern at the base of each leaf primordium, with the opening of the horseshoe positioned at the site of the presumptive midrib for each primordium (Veit et al., 1998). The accumulation pattern of *TE1* rotates 180° with each successive phytomer and correlates with the alternate phyllotaxy of maize (Veit et al., 1998). Since *te1* mutants have shortened internodes and deviations from alternate phyllotaxy, it has been proposed that TE1 functions to repress leaf development and thus regulate phyllotaxy (Veit et al., 1998). However, potential targets for TE1 binding have not yet been identified and the exact function of

TE1 remains unknown.

The three main axes of leaf development

Leaves develop with three main axes: the proximodistal (proximal sheath to distal blade tip in maize), mediolateral (medial midrib to lateral margin) and dorsiventral (bottom to top or abaxial to adaxial) (Figure 1.1). As a leaf grows away from the SAM division and differentiation of cells ceases first at the tip and along the midrib, and proceeds toward the base and margins along the proximodistal and mediolateral axes, respectively. Regulation of cell division is vital to formation of leaves as seen in the *Arabidopsis jaw-D, jagged* (*jag*), and *leafy petiole* (*lep*) mutants (Palatnik et al., 2003; Dinney et al., 2004; Ohno et al., 2004; van der Graaff et al., 2000). *JAW* encodes miR319a and targets TCP transcription factors, which are required for timing the transition between cellular division and differentiation in leaves (Palatnik et al., 2003). When miR319a is over expressed, as it is in *jaw-D* mutants, leaf morphology is greatly altered due to mistimed cessation of cell division along margins and midrib regions (Palatnik et al., 2003). JAG is a C_2H_2-type zinc finger transcription factor that represses cellular differentiation in leaves and flowers (Dinney et al., 2004; Ohno et al., 2004). The distal regions of *jag* mutant leaves and petals do not fully develop, suggesting that *JAG* function is required to repress distal cell division until differentiation is complete (Dinney et al., 2004; Ohno et al., 2004). *LEP* encodes a member of the AP2/EREBP transcription factor family that is involved in patterning the proximodistal axis of leaves (van der Graaff et al., 2000). Activation tagging of *LEP* caused the leaf petiole to be replaced by leaf blade tissue, suggesting that LEP is required to initiate blade formation and thus for the establishment of the distal domain of the leaf (van der Graaff et al., 2000).

One maize gene, *WAVY AURICLE IN BLADE1* (*WAB1*), has been implicated in both proximodistal and mediolateral leaf patterning. Dominant *Wab1* mutants have

narrow blades with patches of sheath and auricle tissue pushed distally into the blade caused by misexpression of LG1, a SQUAMOSA-PROMOTER BINDING protein (Hay and Hake, 2004; Foster et al., 2004). While *WAB1* is required for mediolateral patterning in the blade, it does not appear to play a role in patterning the sheath (Hay and Hake, 2004; Foster et al., 2004). In addition to mediolateral patterning, *WAB1* is also required for the proper accumulation of *LG1*, which acts cell autonomously to promote ligule and auricle development (Becraft et al., 1990; Hay and Hake, 2004; Foster et al., 2004). *WAB1* has not yet been cloned, so how it functions to regulate *LG1* accumulation and to mediate mediolateral patterning remains unknown.

Similar to *WAB1*, the duplicate maize genes *NARROW SHEATH1* (*NS1*) and *NS2* are involved in mediolateral leaf patterning. However, unlike *WAB1*, *NS* gene functions are required for mediolateral patterning of the sheath and blade (Scanlon et al., 1996). By utilizing clonal sector analysis, the *NS* genes were predicted to be required for proper founder cell recruitment in marginal domains, as well as to function in two foci along the flanks of the SAM (Scanlon and Freeling, 1997; Scanlon, 2000). Remarkably, when the *NS* genes were identified as homologues of *Arabidopsis PRESSED FLOWER*, a *WUS*-like homeodomain gene, they were found to accumulate in two foci on the flanks of the SAM and in the margins of leaf primordia (Nardmann et al., 2004). *NS* genes seem to function to establish competency to recruit founder cells for marginal leaf domains rather than specifying lateral identity in leaves (Nardmann et al., 2004).

As a leaf primordium develops from the initial founder cells there is an inherent dorsiventral asymmetry; the adaxial surface of the primordium is adjacent to the SAM and the abaxial side of the primordium is opposite the SAM. Experiments have suggested this asymmetry is set up by a signal emanating from the SAM to the adaxial half of the leaf primordium, as when the incipient leaf primordium is dissected

away from the SAM an abaxialized radial leaf develops (Sussex 1951; Reinhardt et al., 2005). Interestingly, an adaxialized radial leaf is seen in gain-of-function mutations of *PHABULOSA* (*PHB*), and *PHAVOLUTA* (*PHV*), two *Arabidopsis* class III homeodomain-leucine zipper (*HD-ZIP III*) genes (McConnell et al., 2001). In addition to *PHB* and *PHV* there are three other *HD-ZIP III* genes, which are required for adaxial identity in *Arabidopsis*: *REVOLUTA* (*REV*), *ATHB8* and *ATHB15/CORONA* (Figure 1.4). With the lone exception of *rev*, loss-of-function mutations do not produce noticeable phenotypes in single *hd-zip III* mutants, likely due to genetic redundancy. *rev* loss-of-function mutants lack axillary meristems and have a loss of xylem and interfasicular fibers (Ostuga et al., 2001). Prigge et al. (2005) looked at various double, triple, and quadruple *hd-zip III* mutants to dissect distinct roles for each gene. It was found that *REV* and *PHB* play significant roles in meristem formation and organ polarity, while *PHV* has a major role only in organ polarity. *ATHB15/CNA* is important for meristem regulation, and plays an antagonistic role to *PHB, PHV* and *REV* in meristem formation and organ polarity. *ATHB8* is required for vasculature to differentiate from procambial cells (Baima et al., 2001; Donner et al., 2009). *In situ* hybridizations have shown that *PHB, REV, PHV* and *ATHB15/CNA* are all expressed early in embryogenesis, and then restrict their accumulation domains to the center of the SAM, the vasculature, and the adaxial regions of leaf primordia (McConnell et al., 2001; Ostuga et al., 2001). *PHB* accumulates in distinct rays that connect the center of the SAM to the adaxial region of leaves, but the implications of this novel expression pattern remain unknown (McConnell et al., 2001). Like its homologue *REV*, the maize gene *ROLLED LEAF1* (*RLD1*) accumulates in the SAM as well as in adaxial areas of leaf primordia (Juarez et al., 2004a). Although it is also a dominant allele, *Rld1-O* does not exhibit an adaxialized radial leaf phenotype like its *Arabidopsis* homologues. *Rld1-O* mutants

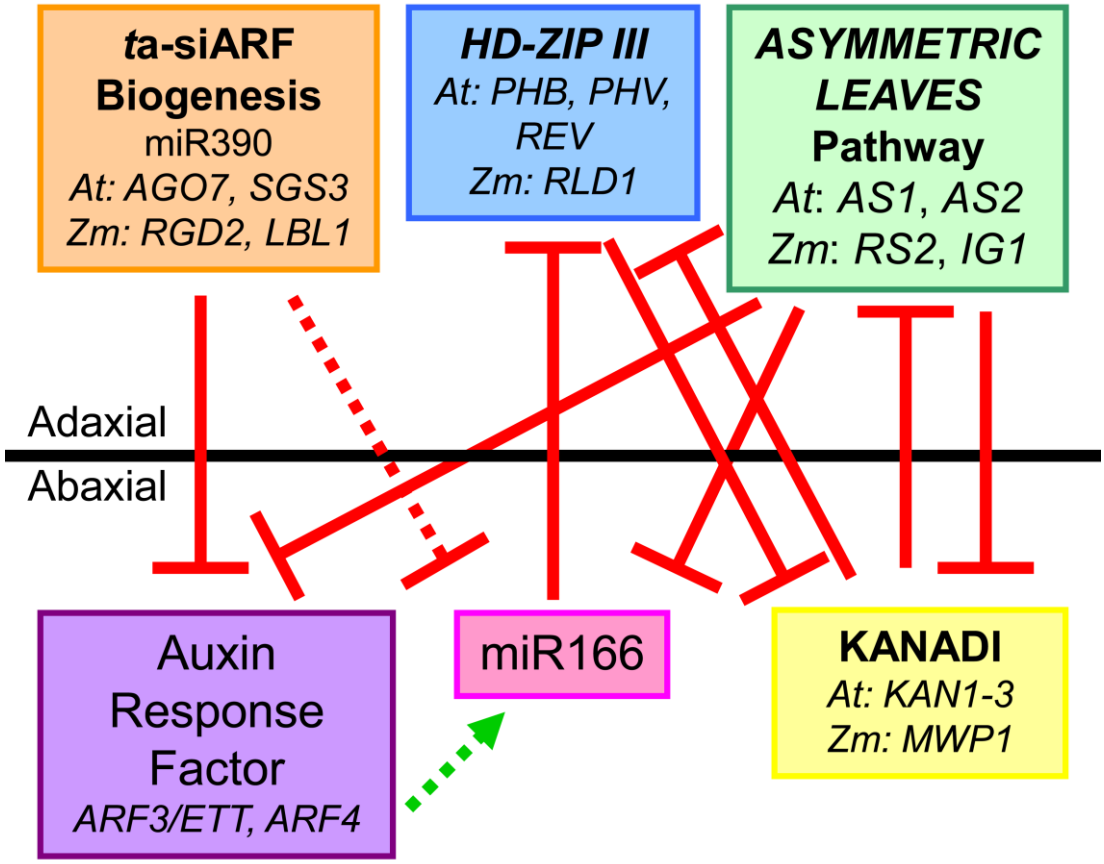

Figure 1.4. Genetic and molecular interactions involved in establishing dorsiventral leaf polarity in maize and *Arabidopsis*.

See text for references. Modified from Husbands et al., 2009.

have a partial loss of dorsiventral polarity that causes the leaves to curl upwards and have a net gain of adaxial tissue types in the blade (Juarez et al., 2004a).

The dominant *Rld1-O*, *phb* and *phv* mutations contain missense mutations in a sterol/lipid binding (START) domain (McConnell et al., 2001; Juarez et al., 2004a), which led researchers to believe HD-ZIP III proteins could be receptors for the elusive adaxializing signal from the SAM suggested by earlier experiments (Sussex 1951). However, with the discovery of miRNAs it was soon revealed that the START domains of *REV*, *PHB* and *PHV* contain sequences complementary to miR165 and miR166, and mutant phenotypes associated with the dominant mutations are caused by altered miRNA recognition sites rather than amino acid changes in the START domain (Mallory et al., 2004). In the dominant *phb-3d* and *Rld1-O* mutant alleles a single nucleotide change in the miR165/166 complementary site is enough to abolish AGO1-mediated cleavage of the *PHB* mRNA transcript, which leads to ectopic accumulation of *PHB* and *RLD1* transcripts and adaxialized radial leaves (Mallory et al., 2004; Juarez et al., 2004a). Not surprisingly, miR166 accumulates in abaxial regions of leaf primordia, where *HD-ZIP III* gene accumulation is not detected (Juarez et al. 2004a; Kidner and Martienssen, 2004). When a single nucleotide change that maintains the proper amino acid sequence, but changes the miR165/166 binding site, is introduced into the cDNA encoding *PHB,* the resulting phenotype is identical to the dominant *phb-3d* mutant. Also, when a *35S*::*PHB* construct is introduced into wild-type plants there is essentially no adaxialization phenotype. These findings strongly suggest that miR165 and miR166 are key regulators of *HD-ZIP III* transcript accumulation in *Arabidopsis* (Figure. 1.4) (Zhou et al., 2007; Mallory et al., 2004).

KANADI (*KAN1*, *KAN2*, and *KAN3*) genes are members of the GARP family of transcription factors that are expressed in abaxial regions of leaf primordia, the phloem, and in a disc below the SAM (Kerstetter et al., 2001; Eshed et al., 2004).

KAN proteins are abaxial identity factors that mutually repress the *HD-ZIP III* gene products and *AS2* expression (Figure 1.4) (Eshed et al., 2004; Emery et al., 2003; Candela et al., 2008; Wu et al., 2008). Over-accumulation of *KAN* genes in *Arabidopsis* arrests the SAM by repressing *HD-ZIP III* gene accumulation (Emery et al., 2003). Also, when a *pAS1::KAN2* construct is placed into wild-type plants the accumulation of *PHB* is reduced and the leaves become radial and abaxialized (Eshed et al., 2004). Single *kan* mutants do not show leaf polarity defects, but when two, or all three, *kan* genes are knocked out polarity defects appear (Eshed et al., 2004). In *kan1;kan2* double mutants and *kan1;kan2;kan3* triple mutants, leaves were radially symmetric and had adaxial epidermal features; some leaves had ectopic outgrowths on the abaxial surface and adaxialized flowers. The maize gene *MILKWEED POD1* (*MWP1*) is a *KAN* homologue that accumulates throughout young leaf primordia, but becomes restricted to abaxial regions of the sheath in older leaves (Candela et al., 2008). MWP1 is required to maintain abaxial identity in leaves, as *mwp1* mutants display ectopic outgrowths on the abaxial surfaces of husk leaves and vegetative sheaths (Candela et al., 2008).

Ectopic outgrowths may be explained by the Waites-Hudson Model, which was developed from work with the *phan* mutant of *A. majus* (Waites and Hudson, 1995). Severe *phan* mutants often have abaxialized radial leaves and amphicribral (phloem surrounding xylem) vascular bundles, whereas wild-type plants have dorsiventrally flattened leaves and collateral (xylem is adaxial and phloem is abaxial) vascular bundles. Since there is no adaxial tissue in the radial leaves observed in *phan* mutants, Waites and Hudson (1995) suggested the juxtaposition of adaxial and abaxial tissue types is required for mediolateral development. Further evidence supporting this model included ectopic outgrowths where epidermal swapping (a patch of adaxial tissue appearing on the abaxial surface) occurred (*mwp1*), the radial leaf phenotypes

seen in the *Arabidopsis kan1;kan2* and *phb-1d* mutants and work with the maize mutant *leafbladeless1* (*lbl1*). *lbl1* is reported to have abaxialized radial leaves with roughly amphicribral vascular bundles, similar to *phan* mutants (Timmermans et al., 1998). The Waites-Hudson model is adequate to explain most of the radial leaf phenotypes seen in plants, but the model stumbles when presented with the maize mutant *ragged seedling2* (*rgd2*). *rgd2* mutants have radial leaves, but the radial leaves maintain proper dorsiventral anatomy and contain collateral vascular bundles as opposed to being abaxialized or adaxialized with aberrant vascular bundle polarity (Henderson et al., 2005).

PHAN, *AS1* and *RS2* were previously mentioned as homologues that repress *KNOX* genes in leaf primordia. Another *Arabidopsis* protein involved in repressing *KNOX* genes, and enhancing *HD-ZIP III* genes, is the LOB-domain containing protein ASYMMETRIC LEAVES2 (AS2) (Lin et al., 2003; Fu et al., 2007). The maize homolog of *AS2*, *INDETERMINATE GAMETOPHYTE1* (*IG1*), may also be an adaxial identity factor; in certain genetic backgrounds *ig1* mutants yield ectopic outgrowths on the adaxial surface of the flag leaf (the final vegetative leaf) (Evans, 2007). AS1 and AS2 are believed to function in the same pathway, and they work to promote adaxial identity by repressing *KAN* genes and by interacting with HISTONE DEACETYLASES (HDACs) to exclude miR165/166 from adaxial regions of leaf primordia (Figure 1.4) (Serrano-Cartagena et al., 1999; Iwakawa et al., 2007; Ueno et al., 2007). HDACs remove acetyl groups from histones, allowing them to be methylated, which can lead to a change in the chromatin state and subsequent gene inactivation (reviewed in Wagner, 2003). When Ueno et al. (2007) treated *as1* or *as2* single mutants with HDAC inhibitors they saw an abaxialized radial leaf phenotype and ectopic miR166 accumulation. These results suggest that HDACs, perhaps in a complex with AS1/AS2, help establish dorsiventral leaf polarity in *Arabidopsis* by

regulating the chromatin state at *miR165/166* precursor gene loci. The *AS2* promoter has also been shown to be under the control of BOP1 and BOP2 in proximal adaxial regions of leaves, indicating that BOP proteins are involved in both proximodistal patterning and dorsiventral polarity (Jun et al., 2010). AS1 and AS2 also repress *YABBY* genes (*FILAMENTOUS FLOWER, YABBY2* and *YABBY3*), which are a family of abaxial identity and lateral outgrowth promoters in *Arabidopsis* (Siegfried et al., 1999; Iwakawa et al., 2007). In maize, *YABBY* genes exhibit adaxial accumulation, and seem to be involved in growth, not in establishing dorsiventral polarity (Juarez et al., 2004b).

AS1 and AS2 work in synergy with a *trans*-acting small interfering RNA (*t*a-siRNA) pathway to repress *AUXIN RESPONSE FACTOR3/ETTIN* (*ARF3*/*ETT*) and *ARF4*, which promote abaxial identity in *Arabidopsis* by promoting *YABBY* gene expression (Garcia et al., 2006; Iwakawa et al., 2007; Li et al., 2005). *t*a-siRNAs are similar to miRNAs and require many of the same proteins for their biosynthesis, but the two classes of small RNAs have different origins. The biogenesis of *t*a-siRNAs begins with the miRNA-directed cleavage of a noncoding *ta-siRNA* transcript. The cleavage product is converted into a dsRNA, which is incorporated into an AGO complex and cleaves the *t*a-siRNA target gene. *TAS3* is one of three *t*a-siRNA gene family members in *Arabidopsis* (Allen et al., 2005). The *TAS3* transcript is cleaved by miR390 with the help of AGO7/ZIPPY (ZIP), and the resulting product is converted into dsRNA by RNA-DEPENDENT RNA POLYMERASE6 (RDR6) and SUPPRESSOR OF GENE SILENCING3 (SGS3) (Allen et al., 2005; Adenot et al, 2006; Fahlgren et al., 2006; Montgomery et al., 2008). The dsRNA is then cleaved by DCL4 into functional 21-base pair *t*a-siRNAs. The *t*a-siRNAs then function in a manner similar to miRNAs in that they target a specific transcript, in this case *ARF3* and *ARF4*, and the target transcripts are cleaved with the aid of AGO1 (Allen et al.,

2005; Montgomery et al., 2008). In *Arabidopsis*, *sgs3, rdr6, dcl4* and *ago7*/*zip* mutants exhibit a precocious switch from juvenile to adult staged leaves; they lack dorsiventral polarity defects (Peragine et al., 2004; Gasciolli et al., 2004; Xie et al., 2005; Hunter et al., 2003).

ARF3/ETT and *ARF4*, targets of *t*a-siRNA regulation, encode DNA binding proteins that are responsive to auxin and promote a switch from juvenile and adult stage leaf traits in *Arabidopsis* (Sessions et al., 1997; Hunter et al., 2006). The ARF family of transcription factors binds auxin response elements in the promoters of auxin responsive genes. When auxin is present the ARFs are bound by Aux/IAA repressors to regulate the target gene (reviewed in Guilfoyle and Hagen, 2007). Interestingly, ARF3/ETT lacks a carboxy-terminal dimerization domain (CTD) believed to be required for ARF-Aux/IAA dimerization (Okushima et al., 2005). Despite the lack of a CTD, ARF3 may directly interact with SEUSS in *Arabidopsis* to regulate floral development (Pfluger and Zambryski, 2004). Exactly how ARF3/ETT and ARF4 function in vegetative leaves remains unknown. Although *arf3/ett* or *arf4* single mutants lack a dorsiventral polarity phenotype in leaves, *arf3;arf4* double mutants do have slight defects in leaf polarity (Figure 1.4) (Pekker et al., 2005). When *ARF3/ETT* is over-expressed, the *ago7/zip* mutant phenotype is recapitulated, suggesting that the precocious switch to adult stage leaves in *ago7/zip* mutants is due to an over-abundance of *ARF3/ETT* (Hunter et al., 2006).

The maize gene *LBL1* is a homologue of *Arabidopsis SGS3* (Nogueira et al., 2007). In striking contrast to *Arabidopsis sgs3* mutants, which only display a phase-change vegetative phenotype, *lbl1* mutants lose dorsiventral polarity and have abaxialized radial leaves (Timmermans et al., 1998). *lbl1* mutants are deficient in *t*a-siRNA biogenesis because *t*a-siRNAs are unable to be produced without the proper machinery to turn single-stranded *TAS3* cleavage products into dsRNA. With this

decrease in *t*a-siRNAs there is an expected increase in *ARF3a* transcript levels, but there is also a surprising change in miR166 levels (Nogueira et al., 2007). In *Arabidopsis* there are only two *miR166* loci, but in maize there are at least nine *miR166* loci (*miR166a* to *miR166i*) with distinct accumulation patterns in the shoot apex (Zhou et al., 2007; Nogueira et al., 2007; Nogueira et al., 2009). One *miR166* locus (*miR166a*) is repressed in *lbl1*, but two *miR166* loci (*miR166c* and *miR166i*) have enhanced transcript levels and have ectopic accumulation in the adaxial regions of leaf primordia (Nogueira et al., 2007). Work with *Arabidopsis* has also suggested that SGS3 may have functions outside of the *t*a-siRNA biogenesis pathway to regulate *AGO1* accumulation (Mallory and Vaucheret, 2009).

It has been hypothesized that the *t*a-siARF biogenesis pathway is of primary importance for regulating leaf dorsiventral polarity in maize, while the interplay of *HD-ZIP III* and *KAN* genes are more important in *Arabidopsis* (Figure 1.4) (reviewed in Kidner and Timmermans, 2007). Work with the *lbl1* mutant has suggested that *t*a-siARFs may regulate the accumulation of miR166 in the maize shoot apex, and thus influence dorsiventral polarity (Nogueira et al., 2009). The maize mutants *lbl1* and *rgd2* have similar macroscopic phenotypes, but they are reported to have very disparate phenotypes in regards to leaf dorsiventral polarity (Timmermans et al., 1998; Henderson et al., 2005). Whereas *lbl1* mutants have completely abaxialized radial leaves, *rgd2* mutants exhibit radial leaves with no net loss of dorsiventral polarity (Timmermans et al., 1998; Henderson et al., 2005). When *rgd2-R;lbl1-rgd1* double mutants were constructed, a synergistic phenotype was observed; no SAM was present in mature kernels (Henderson et al., 2006). This result strongly suggests that LBL1 and RGD2 operate in separate, but overlapping, pathways.

Purpose of study

Despite these advances in the understanding of leaf development much remains to be discovered, particularly in monocotyledons such as maize. The Waites-Hudson model predicts that whenever adaxial and abaxial tissue types are juxtaposed in species with bifacial leaves a mediolateral outgrowth will form (Waites and Hudson, 1995). In essence, this model states that leaves are flattened in the mediolateral axis when both adaxial and abaxial tissue types are both present. Despite several mutants in multiple species providing evidence to support this model, there is at least one exception (Waites and Hudson, 1995; McConnell et al., 2001; Henderson et al., 2005; Evans et al., 2007; Nagasaki et al., 2007; Candela et al., 2008). The maize *rgd2* mutant has leaves with adaxial *and* abaxial tissue types, but with radial symmetry and thus no mediolateral development away from the midrib (Henderson et al., 2005). This observation suggests that either the Waites-Hudson model is insufficient to explain mediolateral development or that RGD2 function is required for competency to understand that the two tissue types are in juxtaposition.

Although it has a clear role in leaf development, the identity and function of *RGD2* are unknown. The elucidation of RGD2 identity and function may help establish its role in the interaction between the mediolateral and dorsiventral axes of leaf development. Since RGD2 and LBL1 are believed to operate in separate, but overlapping, pathways (Henderson et al., 2006), understanding the identity of RGD2 may also shed light on the intersection of different pathways in maize leaf development. Identifying *RGD2* via positional cloning was one of the primary goals of this study. Upon identifying *RGD2* as an *AGO7*-like gene, the focus of the study centered on the role of *RGD2* function in *t*a-siARF biogenesis and in re-evaluating the role of this pathway in maize leaf dorsiventral polarity. Additionally, this study began to evaluate downstream targets of *t*a-siARF function.

REFERENCES

Adenot X., Elmayan T., Lauressergues D., Boutet S., Bouche N., Gasiciolli V., and Vaucheret H. 2006. DRB4-dependant *TAS3 trans*-acting siRNAs control leaf morphology through AGO7. *Curr. Biol*. 18: 758-762.

Aida M., Ishida T., and Tasaka M. 1999. Shoot apical meristem and cotyledon formation during *Arabidopsis* embryogenesis: interaction among the *CUP-SHAPED COTYLEDON* and *SHOOT MERISTEMLESS* genes. *Development*. 126: 1563-1570.

Aida M., Ishida T., Fukaki H., Fujisawa H., and Tasaka M. 1997. Genes involved in organ separation in *Arabidopsis*, an analysis of the cup-shaped cotyledon mutant. *Plant Cell*. 9: 841-857.

Allen, E., Xie, Z., Gustafson, A.M., and Carrington, J.C. 2005. microRNA-directed phasing during *trans*-acting siRNA biogenesis in plants. *Cell*. 121: 207-221.

Baima, S., Possenti, M., Matteucci, A., Wisman, E. Altamura, M.M., Ruberti, I. and Morelli, G. 2001. The *Arabidopsis* ATHB-8 HD-ZIP protein acts as a differentiation-promoting transcription factor of the vascular meristems. *Plant Physiol*. 126: 643-655.

Becraft P.W., Bongard Pierce D.K., Sylvester A.W., Poethig R.S., and Freeling M. 1990. The *liguleless-1* gene acts tissue specifically in maize leaf development. *Dev. Biol*. 141: 220-232.

Belles-Boix E., Hamant O., Witiak S.M., Morin H., Traas J., and Pautot V. 2006. *KNAT6*: An *Arabidopsis* homeobox gene involved in meristem activity and organ separation. *Plant Cell*. 18: 1900-1907.

Bennett S.R.M., Alvarez J., Bossinger G., and Smyth D.R. 1995. Morphogenesis in *pinoid* mutants of *Arabidopsis thaliana*. *Plant J.* 8: 505-520.

Berger Y., Harpaz-Saad S., Brand A., Melnik H., Sirding N., Alvarez J.P., Zinder

M., Samach A., Eshed Y., and Ori N. 2009. The NAC-domain transcription factor GOBLET specifies leaflet boundaries in compound tomato leaves. *Development*. 136: 823-832.

Bolduc N. and Hake S. 2009. The maize transcription factor KNOTTED1 directly regulates the gibberellin catabolism gene *ga2ox1*. *Plant Cell.* 21: 1674-1658.

Bommert P., Lunde C., Nardmann J., Vollbrecht E., Running M., Jackson D., Hake S., and Werr W. 2005. *thick tassel dwarf1* encodes a putative maize ortholog of the Arabidopsis CLAVATA1 leucine-rich repeat receptor-like kinase. *Development* 132: 1235–1245

Brand U., Fletcher J.C., Hobe M., Meyerowitz E.M, and Simon R. 2000. Dependence of stem cell fate in *Arabidopsis* on a feedback loop regulated by CLV3 activity. *Science*. 289: 617-619.

Brooks III L.B., Strable J., Zhang X., Ohtsu K., Zhou R., Sarkar A., Hargreaves S., Elshire R.J., Eudy D., Pawlowska T., Ware D., Janick-Buckner D., Buckner B., Timmermans M.C.P., Schnable P.S., Nettleton D., and Scanlon M.J. 2009. Microdissection of Shoot Meristem Functional Domains. *PLoS Genet*. 5: e1000476.

Byrne, M.E., Barley, R., Curtis, M., Arroyo, J.M., Dunham, M., Hudson, A., and Martienssen, R.A. 2000. *Asymmetric leaves1* mediates leaf patterning and stem cell function in *Arabidopsis*. *Nature*. 408: 967-971.

Byrne M.E., Simorowski J., and Martienssen R.A. 2002. *ASYMMETRIC LEAVES1* reveals knox gene redundancy in *Arabidopsis*. *Development.* 129: 1957–1965.

Candela H., Johnston R., Gerhold A., Foster T., and Hake S. 2008. The *milkweed pod1* gene encodes a KANADI protein that is required for abaxial/adaxial patterning in maize leaves. *Plant Cell*. 20: 2073-2087.

Chaffey N. 2000. Physiological anatomy and function of the membranous grass ligule. *New Phytologist*. 1: 5-21.

Clark SE., Williams R.W., and Meyerowitz E.M. 1997. The CLAVATA1 gene encodes a putative receptor kinase that controls shoot and floral meristem size in *Arabidopsis*. *Cell*. 89: 575-585.

Dinney J.R., Yadegari R., Fischer R.L., Yanofsky M.F., and Weigel D. 2004. The role of *JAGGED* in shaping lateral organs. *Development*. 131: 1101-1110.

Donner T.J., Sherr I., and Scarpella E. 2009. Regulation of preprocambial cell state acquisition by auxin signaling in *Arabidopsis* leaves. *Development*. 136: 3235-3246.

Emery, J.F., Floyd, S.K., Alvarez, J., Eshed, Y., Hawker, N.P., Izhaki, A., Baum, S.F., and Bowman, J.L. 2003. Radial patterning of *Arabidopsis* shoots by Class III *HD-ZIP* and *KANADI* genes. *Curr.Biol*. 13: 1768-1774.

Eshed, Y., Izhaki, A., Baum, S.F., Floyd, S.K., and Bowman, J.L. 2004. Asymmetric leaf development and blade expansion in *Arabidopsis* are mediated by KANADI and YABBY activities. *Development*. 131: 2997-3006.

Evans M.M.S. 2007. The *indeterminate gametophyte1* gene of maize encodes a LOB domain protein required for embryo sac and leaf development. *Plant Cell*. 19: 46-62.

Fagard, M., Boutet, S., Morel, J.B., Bellini, C. and Vaucheret, H. 2000. AGO1, QDE-2, and RDE-1 are related proteins required for post-transcriptional gene silencing in plants, quelling in fungi, and RNA interference in animals. *Proc. Natl. Acad. Sci. USA*. 97: 11650-11654.

Fahlgren N., Montgomery T., Howell M., Allen E., Dvorak S., Alexander A., and Carrington J. 2006. Regulation of *AUXIN RESPONSE FACTOR3* by *TAS3* ta-siRNA affects developmental timing and patterning in *Arabidopsis*. *Curr. Biol*. 16: 939-944.

Fletcher J.C., Brand U., Running M.P., Simon R., and Meyerowitz E.M. 1999. Signaling of cell fate decisions by CLAVATA3 in *Arabidopsis* shoot meristems. *Science*. 283: 1911-1914.

Foster T., Hay A., Johnston R., and Hake S. 2004. The establishment of axial

patterning in the maize leaf. *Development*. 131: 3921-3929.

Foster T., Yamaguchi J., Wong B.C., Veit B., and Hake S. 1999. *Gnarley* is a dominant mutation in the *knox4* homeobox gene affecting cell shape and identity. *Plant Cell.* 11: 1239–1252.

Fowler J.E., and Freeling M. 1996. Genetic analysis of mutations that alter cell fates in maize leaves: *Dominant Liguleless* mutations. *Dev. Genet.* 18: 198–222

Freeling M., and Lane B. 1994. "The Maize Leaf" in *The Maize Handbook*. pp17-28. eds M. Freeling and V. Walbot. Springer-Verlag, NY

Friml J., Wisniewska J., Benkova E., Mendgen K., and Palme K. 2002. Lateral relocation of auxin efflux regulator PIN3 mediates tropism in *Arabidopsis*. *Nature*. 415: 806-809.

Friml J., Yang X., Michniewicz M., Weijers D., Quint A., Tietz O., Benjamins R., Ouwerkerk P.B., Ljung K., Sandberg G., Hooykaas P.J.J., Palme K., and Offringa R. 2004. A PINOID-dependent binary switch in apical-basal PIN polar targeting directs auxin efflux. *Science*. 306: 862-865.

Fu, Y., Xu, L., Xu, B., Yang, L., Ling, Q., Wang, H., and Huang, H. 2007. Genetic interactions between leaf polarity-controlling genes and ASYMMETRIC LEAVES1 and 2 in Arabidopsis leaf patterning. *Plant Cell Physiol*. 48: 724-735.

Furutani M., Vernoux T., Traas J., Kato T., Tasaka M., and Aida M. 2004. *PIN-FORMED1* and *PINOID* regulate boundary formation and cotyledon development in *Arabidopsis* embryogenesis. *Development*. 131: 5021-5030.

Gälweiler L., Guan C., Müller A., Wisman E., Mendgen K., Yephremov A., and Palme K. 1998. Regulation of polar auxin transport by AtPIN1 in *Arabidopsis* vascular tissue. *Science*. 282: 2226-2230.

Garcia, D., Collier, S.A., Byrne, M.E., and Martienssen, R.A. 2006. Specification of leaf polarity in *Arabidopsis* via the *trans*-acting siRNA pathway. *Curr. Biol*. 9: 933-

938.

Gasciolli V., Mallory A.C., Bartel D.P., and Vaucheret H. 2005. Partially redundant functions of *Arabidopsis* DICER-like enzymes and a role for DCL4 in producing *trans*-acting siRNAs. *Curr. Biol*. 15: 1494-1500.

Giulini A., Wang J., and Jackson D. 2004. Control of phyllotaxy by the cytokinin-inducible response regulator homologue *ABPHYL1*. *Nature*. 430: 1031-1034.

Gómez-Mena C., and Sablowski R. 2008. *ARABIDOPSIS THALIANA HOMEOBOX GENE1* establishes the basal boundaries of shoot organs and controls stem growth. *Plant Cell.* 20: 2059-2072.

Guilfoyle T.J., and Hagen G. 2007. Auxin response factors. *Curr. Opin. Plant Biol.* 10: 453-460.

Ha C.M., Jun J.H., Nam H.G., and Fletcher J.C. 2004. BLADE-ON-PETIOLE encodes a BTB/POZ domain containing protein required for leaf morphogenesis in *Arabidopsis thaliana*. *Plant Cell Physiol*. 45: 1361-1370.

Ha C.M., Jun J.H., Nam H.G., and Fletcher J.C. 2007. *BLADE-ON-PETIOLE1* and *2* control *Arabidopsis* lateral organ fate through regulation of LOB domain and adaxial-abaxial polarity genes. *Plant Cell.* 19: 1809-1825.

Hay, A., Barkoulas, M., and Tsiantis, M. 2006. ASYMMETRIC LEAVES1 and auxin activities converge to repress *BREVIPEDICELLUS* expression and promote leaf development in *Arabidopsis. Development* 133: 3955-3961.

Hay A., and Hake S. 2004. The dominant mutant *Wavy auricle in blade1* disrupts patterning in a lateral domain of the maize leaf. *Plant Physiol.* 135: 300-308.

Hay A., Kaur H., Phillips A., Hedden P., Hake S., and Tsiantis M. 2002. The gibberellin pathway mediates KNOTTED1-type homeobox function in plants with different body plans. *Curr. Biol.* 12: 1557-1565.

Henderson, D.C., Muehlbauer, G.J., and Scanlon, M.J. 2005. Radial leaves of the

maize mutant *ragged seedling2* retain dorsiventral anatomy. *Dev. Biol*. 282: 455-466.

Henderson, D.C., Zhang, X., Brooks III, L., and Scanlon, M.J. 2006. RAGGED SEEDLING2 is required for expression of KANADI2 and REVOLUTA homologues in the maize shoot apex. *Genesis*. 44: 372-382.

Hunter C., Sun H., and Poethig R.S. 2003. The *Arabidopsis* heterochronic gene *ZIPPY* is an ARGONAUTE family member. *Curr. Biol*. 13: 1734-1739.

Hunter C., Willmann M.R., Wu G., Yoshikawa M., de la Luz Gutierrez-Nava M., and Poethig R.S. 2006. Trans-acting siRNA-mediated repression of ETTIN and ARF4 regulates heteroblasty in *Arabidopsis*. *Development*. 133: 2973-2981.

Husbands A.Y., Chitwood D.H., Plavskin Y., and Timmermans M.C.P. 2009. Signals and prepatterns: new insights into organ polarity in plants. *Genes Dev.* 23: 1986-1997.

Iwakawa, H., Iwasaki, M., Kojima, S., Ueno, Y., Soma, T., Tanaka, H., Semiarti, E., Machida, Y., and Machida, C. 2007. Expression of the *ASYMMETRIC LEAVES2* gene in the adaxial domain of Arabidopsis leaves represses cell proliferation in this domain and is critical for the development of properly expanded leaves. *Plant J*. 51: 173-184.

Jackson D., and Hake S. 1998. Control of phyllotaxy in maize by the *abphyl1*gene. *Development*. 126: 315-323.

Jeong S., Trotochaud A.E., and Clark S.E. 1998. The *Arabidopsis* CLAVATA2 gene encodes a receptor-like protein required for the stability of the CLAVATA1 receptor-like kinase. *Plant Cell*. 11: 1925-1934.

Juarez M.T., Kui J.S., Thomas J., Heller B.A., and Timmermans M.C.P. 2004a. microRNA-mediated repression of *rolled leaf1* specifies maize leaf polarity. *Nature*. 428: 84-88.

Juarez M.T., Twigg R.W., and Timmermans M.C.P. 2004b. Specification of

adaxial cell fate during maize leaf development. *Development*. 131: 4533-4544.

Jun J.H., Ha C.M., and Fletcher J.C. 2010. BLADE-ON-PETIOLE1 coordinates organ determinacy and axial polarity in *Arabidopsis* by directly activating ASYMMETRIC LEAVES2. *Plant Cell*. 22: 62-76.

Kerstetter, R.A., Bollman, K., Taylor, R.A., Bomblies, K., and Poethig, R.S. 2001. *KANADI* regulates organ polarity in *Arabidopsis. Nature*. 411: 706-709.

Kerstetter R.A., Laudencia-Chingcuanco D., Smith L.G., and Hake S. 1997. Loss of function mutations in the maize homeobox gene, *knotted1*, are defective in shoot meristem maintenance. *Development.* 124: 3045–54.

Kidner C., and Martienssen R. 2004. Spatially restricted microRNA directs leaf polarity through ARGONAUTE1. *Nature*. 428: 81-84.

Kidner C.A., and Timmermans M.C. 2007. Mixing and matching pathways in leaf polarity. *Curr. Opin. Plant Biol.* 10: 13-20.

Kurihara, Y., Takashi, Y., Watanabe, Y. 2006. The interaction between DCL1 and HYL1 is important for efficient and precise processing of pri-miRNA in plant microRNA biogenesis. *RNA.* 12: 206-212.

Kwon C.S., Hibara K., Pfluger J., Bexhani S., Metha H., Aida M., Tasaka M., and Wagner D. 2006. A role for chromatin remodeling in regulation of CUC gene expression in the *Arabidopsis* cotyledon boundary. *Development*. 133: 3223-3230.

Lanet E., Delannoy E., Sormani R., Floris M., Brodersen P., Crete P., Voinnet O. and Robaglia C. 2009. Biochemical evidence for translational repression by *Arabidopsis* microRNAs. *Plant Cell*. 21: 1762-1768.

Laufs P., Peaucelle A., Morin H., and Traas J. 2004. MicroRNA regulation of the CUC genes is required for boundary size control in *Arabidopsis* meristems. *Development*. 131: 4311-4322.

Laux T., Mayer K.F., Berger J., and Jurgens G. 1996. The WUSCHEL gene is

required for shoot and floral meristem integrity in Arabidopsis. *Development.* 122: 87–96.

Lee B., Johnston R., Yang Y., Gallavotti A., Kojima M., Travencolo B.A.N., Costa L.F., Sakakibara H., and Jackson D. 2009. Studies of *aberrant phyllotaxy1* mutants of maize indicate complex interactions between auxin and cytokinin signaling in the shoot apical meristem. *Plant Physiol*. 150: 205-216.

Leibfried A., To J.P.C., Busch W., Stehling S., Kehle A., Demar M., Kieber J.J., and Lohmann J.U. 2005. WUSCHEL controls meristem function by direct regulation of cytokinin-inducible response regulators. *Nature*. 438: 1172–1175

Li, H., Xu, L., Wang, H., Yuan, Z., Cao, X., Yang, Z., Zhang, D., Xu, Y., and Huang, H. 2005. The putative RNA-dependent RNA polymerase RDR6 acts synergistically with ASYMMETRIC LEAVES1 and 2 to repress *BREVIPEDICELLUS* and microRNA165/166 in *Arabidopsis* leaf development. *Plant Cell*. 17: 2157-2171.

Lin, W., Shuai, B., Springer, P.S. 2003. The *Arabidopsis LATERAL ORGAN BOUNDARIES*-domain gene *ASYMMETRIC LEAVES2* functions in the repression of *KNOX* gene expression and in adaxial-abaxial patterning. *Plant Cell*. 15: 2241-2252.

Lincoln C., Long J., Yamaguchi J., Serikawa K., and Hake S. 1994. A *Knotted1*-like homeobox gene in *Arabidopsis* is expressed in the vegetative meristem and dramatically alters leaf morphology when overexpressed in transgenic plants. *Plant Cell*. 6: 1859-1876.

Long J.A., Moan E.I., Medford J.I., and Barton M.K. 1996. A member of the KNOTTED class of homeodomain proteins encoded by the *SHOOTMERISTEMLESS* gene of *Arabidopsis*. *Nature*. 379: 66-69.

Mallory A.C., Dugas D.V., Bartel D.P., and Bartel B. 2004. MicroRNA regulation of NAC-domain targets is required for proper formation and separation of adjacent

embryonic, vegetative, and floral structures. *Curr. Biol.* 14: 1035-1046.

Mallory, A.C., Reinhart, B.J., Jones-Rhoades, M.W., Tang, G., Zamore, P.D., Barton, M.K., and Bartel, D.P. 2004. MicroRNA control of *PHABULOSA* in leaf development: importance of pairing to the microRNA 5' region. *EMBO Journal*. 23: 3356-3364.

Mallory A.C., and Vaucheret H. 2009. ARGONAUTE1 homeostasis invokes the coordinate action of the microRNA and siRNA pathways. *EMBO Reports*. 10: 521-526.

Mayer, K.F., Schoof, H., Haecker, A., Lenhard, M., Jurgens, G., and Laux, T. 1998. Role of WUSCHEL in regulating stem cell fate in the *Arabidopsis* shoot meristem. *Cell*. 95: 805-815.

McConnell, J.R., Emery, J., Eshed, Y., Bao, N., Bowman, J., and Barton, M.K. 2001. Role of *PHABULOSA* and *PHAVOLUTA* in determining radial patterning in shoots. *Nature*. 411: 709-713.

McManus, M.T., Petersen, C.P., Haines, B.B., Chen, J., and Sharp, P.A. 2002. Gene silencing using micro-RNA designed hairpins. *RNA* 6: 842-850.

Mele G., Ori N., Sato Y., and Hake S. 2003. The *knotted1*-like homeobox gene *BREVIPEDICELLUS* regulates cell differentiation by modulating metabolic pathways. *Genes Dev.* 17: 2088-2093.

Montgomery T.A., Howell M.D., Cuperus J.T., Li D., Hansen J.E., Alexander A.L., Chapman E.J., Fahlgren N., Allen E., and Carrington J.C. 2008. Specificity of ARGONAUTE7-miR390 interaction and dual functionality in *TAS3 trans*-acting siRNA formation. *Cell*. 133: 128-141.

Muehlbauer G.J., Fowler J.E., Girard L., Tyers R., Harper L., and Freeling M. 1999. Ectopic expression of the maize homeobox gene *liguleless3* alters cell fates in the leaf. *Plant Physiol.*119: 651–662.

Muehlbauer G.J., Fowler J.E., and Freeling M. 1997. Sectors expressing the homeobox gene *liguleless3* implicate a time-dependent mechanism for cell fate acquisition along the proximal-distal axis of the maize leaf. *Development*. 124: 5097-5106.

Müller R., Bleckmann A., and Simon R. 2008. The receptor kinase CORYNE of *Arabidopsis* transmits the stem cell-limiting signal CLAVATA3 independently of CLAVATA1. *Plant Cell*. 20: 934-946.

Müller R., Borghi L., Kwiatkowska D., Laufs P., and Simon R. 2006. Dynamic and compensatory responses of *Arabidopsis* shoot and floral meristems to CLV3 signaling. *Plant Cell*. 18: 1188-1198.

Nagasaki H., Itoh J., Hayashi K., Hibara K., Satoh-Nagasawa N., Nosaka M., Mukouhata M., Ashikari M., Kitano H., Matsuoka M., Nagato Y., and Sato Y. 2007. The small interfering RNA production pathway is required for shoot meristem initiation in rice. *Proc. Natl. Acad. Sci. USA*. 104: 14867-14871.

Nardmann J., Ji J., Werr W., and Scanlon M.J. 2004. The maize duplicate genes *narrow sheath1* and *narrow sheath2* encode a conserved homeobox gene function in a lateral domain of shoot apical meristems. *Development*. 131: 2827-2839.

Nogueira, F.T.S., Madi, S., Chitwood, D.H., Juarez, M.T. and Timmermans, M.C.P. 2007. Two small regulatory RNAs establish opposing fates of a developmental axis. *Genes & Development* 21: 750-755.

Nogueira F.T., Chitwood, D.H., Madi, S., Ohtsu, K., Schnable, P.S., Scanlon, M.J., and Timmermans, M.C. 2009. Regulation of small RNA accumulation in the maize shoot apex. *PLoS Genet*. 5: e1000320.

Ogawa M., Shinohara H., Sakagami Y., and Matsubayashi Y. 2008. *Arabidopsis* CLV3 peptide directly binds CLV1 ectodomain. *Science*. 319: 294.

Ohno C.K., Reddy G.V., Heisler M.G., and Meyerowitz E.M. 2004. The

Arabidopsis JAGGED gene encodes a zinc finger protein that promotes leaf tissue development. *Development*. 131: 1111-1122.

Ohyama K., Shinohara H., Ogawa-Ohnishi M., and Matsubayashi Y. 2009. A glycopeptide regulating stem cell fate in *Arabidopsis thaliana*. *Nat. Chem. Biol.* 5: 578-580.

Okushima Y., Overvoorde P.J., Arima K., Alonso J.M., Chan A., Chang C., Ecker J.R., Hughes B., Lui A., Nguyen D., Onodera C., Quach H., Smith A., Yu G., and Theologis A. 2005. Functional genomic analysis of the *AUXIN RESPONSE FACTOR* gene family members in *Arabidopsis thaliana*: Unique and overlapping functions of *ARF7* and *ARF19*. *Plant Cell*. 17: 444-463.

Osakabe Y., Miyata S., Urao T., Seki M., Shinozaki K., and Yamaguchi-Shinozaki

K. 2002. Overexpression of Arabidopsis response regulators, ARR4/ATRR1/IBC7 and ARR8/ATRR3, alters cytokinin responses differentially in the shoot and in callus formation. *Biochem Biophys Res Commun.* 293: 806–815.

Ostuga, D., DeGuzman, B., Prigge, M.J., Drews, G.N., and Clark, S.E. 2001. *REVOLUTA* regulates meristem initiation at lateral positions. *Plant J*. 25: 223-236.

Palatnik J.F., Allen E., Wu X., Schommer C., Schwab R., Carrington J.C., and Weigel D. 2003. Control of leaf morphogenesis by microRNAs. *Nature*. 425: 257-263.

Pekker, I., Alvarez, J.P., and Eshed, Y. 2005. Auxin response factors mediate *Arabidopsis* organ asymmetry via modulation of KANADI activity. *Plant Cell*. 17: 2899-2910.

Peragine A., Yoshikawa M., Wu G., Albrecht H.L., and Poethig R.S. 2004. SGS3 and SGS2/SDE1/RDR6 are required for juvenile leaf development and the production of *trans*-acting siRNAs in *Arabidopsis*. *Genes Dev.* 18: 2368-2379.

Phelps-Durr, T.L., Thomas, J., Vahab, P., and Timmermans, M.C.P. 2005. Maize *rough sheath2* and its *Arabidopsis* orthologue *ASYMMETRIC LEAVES1* interact with HIRA, a predicted histone chaperone, to maintain *knox* gene silencing and determinacy during organogenesis. *Plant Cell*. 17: 2886-2898.

Prigge, M.J., Ostuga, D., Alonso, J.M., Ecker, J.R., Drews, G.N., and Clark, S.E. 2005. Class III Homeodomain-leucine zipper gene family members have overlapping, antagonistic, and distinct roles in *Arabidopsis* development. *Plant Cell*. 17: 61-76.

Ramirez J., Bolduc N., Lisch D., and Hake S. 2009. Distal expression of *knotted1* in maize leaves leads to reestablishment of proximal/distal patterning and leaf dissection. *Plant Physiol.* 151: 1878-1888.

Reddy G.V., and Meyerowitz E.M. 2005. Stem-cell homeostasis and growth dynamics can be uncoupled in the *Arabidopsis* shoot apex. *Science*. 310: 663-667.

Reinhardt, D., Frenz, M., Mandel, T., Kuhlemeier, C. 2005. Microsurgical and laser ablation analysis of leaf positioning and dorsoventral patterning in tomato. *Development*. 132: 15-26.

Reinhardt D., Mandel T., and Kuhlemeier C. 2000. Auxin regulates the initiation and radial position of plant lateral organs. *Plant Cell*. 12: 507-518.

Reinhardt D., Pesce E.-R., Stieger P., Mandel T., Baltensperger K., Bennett M., Traas J., Friml J., and Kuhlemeier C. 2003. Regulation of phyllotaxis by polar auxin transport. *Nature*. 426: 255-260.

Reinhart B.J., Weinstein E.G., Rhoades M.W., Bartel B., and Bartel D.P. 2002. MicroRNAs in plants. *Genes Dev*. 16: 1616-1626.

Riou-Khamlichi, C., Huntley, R., Jacqmard, A., and Murray, J.A. 1999. Cytokinin activation of *Arabidopsis* cell division through a D-type cyclin. *Science*. 283: 1541-1544.

Sakamoto, T., Kamiya, N., Ueguchi-Tanaka, M., Iwahori, S., and Matsuoka, M.

2001. KNOX homeodomain protein directly suppresses the expression of a gibberellin biosynthetic gene in the tobacco shoot apical meristem. *Genes Dev*. 15: 581-590.

Scanlon M.J. 2000. NARROW SHEATH1 functions from two meristematic foci during founder-cell recruitment in maize leaf development. *Development*. 127: 4573-4585.

Scanlon M.J., and Freeling M. 1997. Clonal sectors reveal that a specific meristematic domain is not utilized in the maize mutant *narrow sheath*. *Dev. Biol.* 182: 52-66.

Scanlon M.J., Schneeberger R.G., and Freeling M. 1996. The maize mutant *narrow sheath* fails to establish leaf margin identity in a meristematic domain. *Development*. 122: 1683-1691.

Schneeberger R.G., Becraft P.W., Hake S., and Freeling M. 1995. Ectopic expression of the *knox* homeobox gene *rough sheath1* alters cell fate in the maize leaf. *Genes Dev.* 9: 2292–2304.

Schoof H., Lenhard M., Haecker A., Mayer K.F, Jurgens G., and Laux T. 2000. The stem cell population of *Arabidopsis* shoot apical meristems is maintained by a regulatory loop between the CLAVATA and WUSCHEL genes. *Cell*. 100: 635-644.

Serrano-Cartagena, J., Robles, P., Ponce, M.R., and Micol, J.L. 1999. Genetic analysis of leaf form mutants from the *Arabidopsis* Information Service collection. *Molecular & General Genetics*. 261: 725-739.

Sessions A., Nemhauser J.L., McCall A., Roe J.L., Feldmann K.A., Zambryski P.C. 1997. *ETTIN* patterns the *Arabidopsis* floral meristem and reproductive organs. *Development*. 124: 4481-4491.

Shani, E., Yanai, O., and Ori, N. 2006. The role of hormones in shoot apical meristem function. *Curr. Opin. in Plant Biol*. 9: 484-489.

Siegfried, K.R., Eshed, Y., Baum, S.F., Otsuga, D., Drews, G.N., and Bowman,

J.L. 1999. Members of the *YABBY* gene family specify abaxial cell fate in *Arabidopsis. Development*. 126: 4117-4128.

Sinha N., and Hake S. 1994. The *Knotted* leaf blade is a mosaic of blade, sheath, and auricle identities. *Dev. Genet.* 15: 401–14

Souer E., Van Houwelingen A., Kloos D., Moi J., Koes R. 1996. The NO APICAL MERISTEM gene of petunia is required for pattern formation in embryos and flowers and is expressed at meristem and primordia boundaries. *Cell*. 85: 159-170.

Sussex, I.M. 1951. Experiments on the cause of dorsiventrality in leaves. *Nature*. 167: 651-652.

Taguchi-Shiobara F., Yuan Z., Hake S., and Jackson D. 2001. The *fasciated ear2* gene encodes a leucine-rich repeat receptor-like protein that regulates shoot meristem proliferation in maize. *Genes. Dev*. 15: 2755–2766

Timmermans, M.C.P., Schultes, N.P., Jankovsky, J.P., and Nelson, T. 1998. *Leafbladeless1* is required for dorsoventrality of lateral organs in maize. *Development*. 125: 2813-2823.

Timmermans, M.C.P., Hudson, A., Becraft, P.W., and Nelson, T. 1999. ROUGH SHEATH2: A myb protein that represses *knox* homeobox genes in maize lateral organ primordia. *Science* 284: 151-153.

Tsiantis, M., Schneeberger, R., Golz, J.F., Freeling, M., and Langdale, J.A. 1999. The maize *rough sheath2* gene and leaf development programs in monocot and dicot plants. *Science* 284: 154-156.

Ueno, Y., Ishikawa, T., Watanabe, K., Terakura, S., Iwakawa, H., Okada, K., Machida, C., and Machida, Y. 2007. Histone deacetylases and *ASYMMETRIC LEAVES2* are involved in the establishment of polarity in leaves of *Arabidopsis*. *Plant Cell*. 19: 445-457.

van der Graaff E., Dulk-Ras A.D., Hooykaas P.J., and Keller B. 2000. Activation

tagging of the *LEAFY PETIOLE* gene affects leaf petiole development in *Arabidopsis thaliana*. *Development*. 127: 4971-4980.

Veit B., Briggs S.P., Schmidt R.J., Yanofsky M.F., and Hake S. 1998. Regulation of leaf initiation by the *terminal ear1* gene of maize. *Nature*. 393: 166-168.

Vollbrecht E., Reiser L., and Hake S. 2000. Shoot meristem size is dependent on inbred background and presence of the maize homeobox gene, *knotted1*. *Development.* 127: 3161–3172.

Vroemen C.W., Mordhorst A.P., Albrecht C., Kwaaitaal M.A.C.J., and de Vries S.C. 2003. The *CUP-SHAPED COTYLEDON3* gene is required for boundary and shoot meristem formation in *Arabidopsis*. *Plant Cell*. 15: 1563-1577.

Wagner, D. 2003. Chromatin regulation of plant development. *Current Opinion in Plant Biology*. 6: 20-28.

Waites, R. and Hudson, A. 1995. *phantastica*: a gene required for dorsoventrality of leaves in *Antirrhinum majus*. *Development*. 121: 2143-2154.

Wu G., Lin W-c., Huang T., Poethig R., Springer P., and Kerstetter R. 2008. KANADI1 regulates adaxial-abaxial polarity in *Arabidopsis* by directly repressing the transcription of *ASYMMETRIC LEAVES2*. *Proc. Natl. Acad. Sci. USA.* 105: 16392-16397.

Xie Z., Allen E., Wilken A., and Carrington J.C. 2005. DICER-LIKE4 functions in *trans*-acting small interfering RNA biogenesis and vegetative phase change in *Arabidopsis thaliana*. *Proc. Natl. Acad. Sci. USA.* 102: 12984-12989.

Yamamoto, M. and Yamamoto, K.T. 1998. Effects of natural and synthetic auxins on the gravitropic habit of roots in two auxin-resistant mutants of *Arabidopsis*, *axr1* and *axr4*: Evidence for defects in the auxin influx mechanism of *axr4*. *Journal of Plant Research*. 112: 391-396.

Yanai, O., Shani, E., Dolezal, K., Tarkowski, P., Sablowski, R., Sandberg, G.,

Samach, A., and Ori, N. 2005. *Arabidopsis* KNOXI proteins activate cytokinin biosynthesis. *Current Biology*. 15: 1566-1571.

Zhou, G.K., Kubo, M., Zhong, R., Demura, T., and Ye, Z.H. 2007. Overexpression of miR165 affects apical meristem formation, organ polarity establishment and vascular development in *Arabidopsis*. *Plant & Cell Physiology*. 48: 391-404.

Zhu Y., Wang Y., Li R., Song X., Wang Q., Huang S., Jin J.B., Liu C.-M., and Lin J. 2010. Analysis of interactions among the CLAVATA3 receptors reveals a direct interaction between CLAVATA2 and CORYNE in Arabidopsis. *Plant J*. 61: 223-233.

CHAPTER 2

ragged seedling2 encodes an ARGONAUTE7-like protein required for mediolateral expansion, but not dorsiventrality, of maize leaves[1]

[1] Douglas R.N., Wiley D., Sarkar A., Springer N., Timmermans M.C.P., and Scanlon M.J. Submitted to *Plant Cell*

Abstract

Leaves are produced from the flank of the shoot apical meristem and are dorsiventrally asymmetric from inception. Mutations perturbing dorsiventral cell-fate acquisition can lead to the formation of radial leaves that lack adaxial/abaxial polarity. However, mutations in the maize (*Zea mays*) gene *ragged seedling2* (*rgd2*) condition radial leaves that maintain dorsiventral polarity. Positional cloning reveals that *rgd2* encodes an ARGONAUTE7 (AGO7)-like protein required to produce *t*a-siARF, a *trans*-acting small interfering RNA that targets abaxialized *auxin response factor3a* (*arf3a*) transcripts for degradation. Previous studies implicated a role for *t*a-siARF during dorsiventral patterning of monocot leaves. Here we show that *arf3a* transcripts hyper-accumulate but remain abaxialized in rgd2 mutant apices, revealing that *t*a-siARF function is not required for *arf3a* polarization. RGD2 also functions to regulate the accumulation and localization of miR390 in maize shoot apices. Similar to the abaxialized maize mutant leafbladeless1 (lbl1), rgd2 mutants exhibit ectopic accumulation of the abaxial identity factor miR166 in adaxial domains. These data reveal that hyper-accumulation of *arf3a* and miR166 is insufficient to condition abaxialized leaf phenotypes in maize. Finally, transcripts of a maize *ago1* paralog over-accumulate in lbl1 but not in rgd2 mutants, suggesting that upregulation of *ago1* combined with ectopic accumulation of miR166 contribute to the formation of abaxialized leaves in the lbl1 mutant. A revised model for the role of small RNAs during dorsiventral patterning of maize leaves is discussed.

Introduction

Shoot apical meristems (SAMs) are comprised of a group of indeterminate cells that give rise to all the above ground organs of the plant. The angiosperm SAM harbors stem cells that maintain the meristem by replacing cells lost during organogenesis. Leaves are initiated from the flank of the SAM, a position-dependent process whereby

cells at the SAM periphery are recruited to become leaf founder cells (Poethig, 1984). As the founder cells are recruited and switch to determinate growth, leaf primordia are elaborated from the SAM along three main axes: the mediolateral axis (medial midrib to lateral margin), the proximodistal axis (proximal sheath to distal blade), and the dorsiventral axis (adaxial/abaxial). Maize (*Zea mays*) leaves are dorsiventrally flattened and harbor distinct tissue types on their adaxial (upper) and abaxial (lower) surfaces. In contrast, radial leaf mutants are deficient in mediolateral development and typically lose either adaxial or abaxial epidermal patterning, with a concomitant switch from collateral (xylem is adaxial, phloem is abaxial) to amphicribral (phloem surrounds xylem) or amphivasal (xylem surrounds phloem) vascular patterning (Waites and Hudson, 1995; Timmermans et al., 1998; McConnell et al., 2001; Zhong and Ye, 2004; Eshed et al., 2004). Inspired by the *Antirrhinum majus* radial leaf mutant phantastica1, a model for dorsiventral patterning was adapted to leaf development whereby the juxtaposition of adaxial and abaxial tissue types is required to organize the mediolateral and proximodistal axes of growth (Koch and Meinhardt, 1994; Waites and Hudson, 1995). Widespread support for this model is provided by phenotypic and molecular analyses of a number of radial leaf mutants from *Arabidopsis*, rice, tobacco, tomato and maize (reviewed in Kidner and Timmermans, 2007).

Unlike any previously described radial leaf mutants that are deficient in abaxial or adaxial patterning, the maize mutant ragged seedling2 (rgd2) develops radial leaves that maintain dorsiventral polarity (Henderson et al., 2005). Previous work has suggested that RGD2 function may be required to either interpret or respond to a proposed dorsiventral juxtaposition signal that initiates mediolateral development (Waites and Hudson, 1995; Henderson et al., 2005). Although the mechanisms whereby this leaf patterning response is elaborated are still not fully understood,

several microRNAs (miRNAs) and *trans*-acting small interfering RNAs (*t*a-siRNAs) are proposed to play important roles in establishing dorsiventral polarity in developing leaves (Nagasaki et al., 2007; Nogueira et al., 2007; reviewed in Husbands et al., 2009).

MiRNA biogenesis requires DICER-LIKE1 function to process stem-loop miRNA precursors into functional small RNAs (Reinhart et al., 2002). The processed miRNA combines with an ARGONAUTE (AGO) in an RNA-induced silencing complex (RISC) that can then target complimentary mRNA sequences for silencing, either via cleavage of the target transcript or by translational inhibition (Fagard et al., 2000; Lanet et al., 2009). MiR166 is required to spatially restrict the accumulation of adaxial-determining *hd-zipIII* transcripts in both *Arabidopsis* and maize (McConnell et al., 2001; Juarez et al. 2004). Dominant mutations that disrupt the miR166 binding site of *hd-zipIII* genes but preserve the protein coding sequence lead to radial leaf phenotypes wherein abaxial epidermal characteristics are lost (McConnell et al., 2001; Juarez et al. 2004).

The production of *t*a-siRNAs is a plant-specific process that utilizes components from both miRNA and siRNA biogenesis pathways. Biogenesis of *t*a-siRNAs begins with RISC-mediated cleavage of a non-protein coding *t*a-siRNA precursor (*tas*) transcript (Yoshikawa et al., 2005; Allen et al., 2005; Adenot et al, 2006; Fahlgren et al., 2006). Whereas the majority of small RNA-cleaved transcripts are summarily degraded, the *tas* cleavage product is stabilized and processed into a double stranded RNA (dsRNA), which requires SUPPRESSOR-OF-GENE SILENCING3 (SGS3) and RNA-DEPENDENT RNA POLYMERASE6 (RDR6) function (Allen et al., 2005; Nogueira et al., 2007). The resultant dsRNA undergoes phased cleavage by DICER-LIKE4 (DCL4) to yield mature 21-nucleotide *t*a-siRNAs (Allen et al., 2005; Figure 2.1).

,

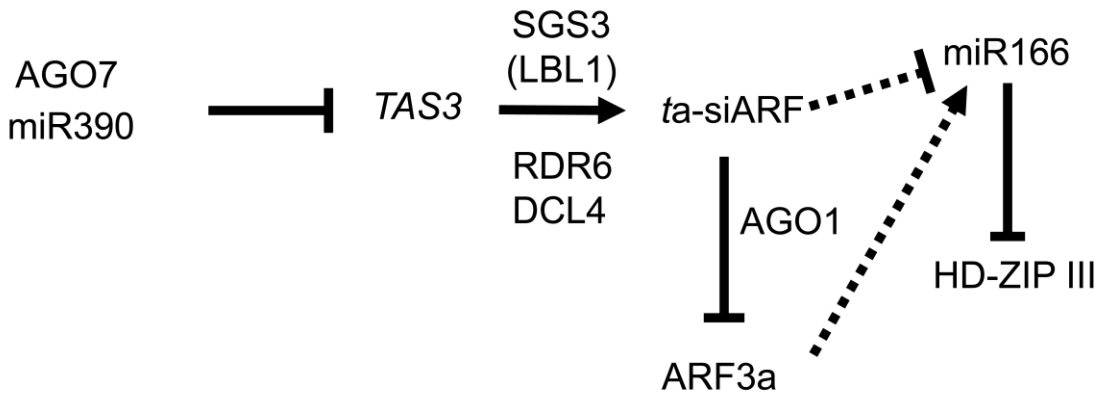

Figure 2.1. Proposed model for the role of small regulatory RNAs in dorsiventral patterning.

Model modified from Kidner and Timmermans (2007). Details provided in text. AGO7/RGD2: ARGONAUTE7/RAGGED SEEDLING2; miR390: microRNA 390; SGS3/LBL1: SUPPRESSOR-OF-GENE SILENCING3/LEAFBLADELESS1; RDR6: RNA-DEPENDANT RNA POLYMERASE6; DCL4: DICER-LIKE4; AGO1: ARGONAUTE1; ARF3a: AUXIN RESPONSE FACTOR3a; miR166: microRNA 166; HD-ZIPIII: family of adaxial identity factors.

Four *tas* gene families (*tas1, tas2, tas3, tas4*) are found in *Arabidopsis* whereas *tas3* is the lone *tas* family as yet described in maize (Nogueira et al., 2007). Post transcriptional cleavage of *tas3* precursor genes requires a specialized RISC containing miR390 and AGO7/ZIPPY (ZIP), whereupon SGS3-RDR6-DCL4 function processes the *tas3* cleavage product into 21-bp *t*a-siRNAs, a subset of which are called *t*a-siARFs (Peragine et al., 2004; Allen et al., 2005; Montgomery et al., 2008). As a small RNA substrate bound by AGO1 during post-transcriptional cleavage of the transcription factors *auxin response factor3/ettin* (*arf3/ett*) and *arf4*, *t*a-siARF regulates vegetative phase change in *Arabidopsis* shoots (Allen et al., 2005; Hunter et al., 2006). Subsequently, *t*a-siARF was shown to function redundantly to regulate organ polarity, wherein *arf3/ett* and *arf4* are abaxial determinants (Pekker et al., 2005; Garcia et al., 2006; Fahlgren et al., 2006).

Genetic analyses in maize and rice have demonstrated a primary role for *t*a-siARF during dorsiventral leaf patterning; mutations in this *t*a-siRNA pathway generate shootless embryos or filamentous, abaxialized leaf phenotypes (Nogueira et al., 2007; Nagasaki et al., 2007; Nogueira et al., 2009). In contrast, *Arabidopsis* mutants in the *tas3 t*a-siRNA pathway show no defects in leaf polarity but render a precocious switch from juvenile to adult-staged leaves (Hunter et al., 2003; Peragine et al., 2004). *Leafbladeless1* (*lbl1*) encodes the maize homolog of SGS3 (Nogueira et al., 2007). Macroscopically, lbl1 and rgd2 have very similar mutant phenotypes (Timmermans et al., 1998; Henderson et al., 2005). However, closer inspection reveals that whereas severe lbl1 radial leaves lose adaxial epidermal characteristics, rgd2 radial leaves maintain dorsiventral polarity. Recessive alleles of *lbl1* exhibit reduced levels of *t*a-siARF biogenesis and elevated levels of *arf3a*, which are purported to promote miR166 accumulation and condition an abaxialized phenotype (Figure 2.1; Nogueira et al., 2007; Nogueira et al., 2009). Surprisingly, rgd2;lbl1

double mutants have a synergistic shootless phenotype, suggesting that RGD2 and LBL1 operate in overlapping pathways, yet also perform some non-redundant functions (Henderson et al., 2006).

Here, we show that *rgd2* encodes a maize ARGONAUTE7-like protein required for *t*a-siARF biogenesis and down-regulation of *arf3a* transcripts. Surprisingly, *arf3a* transcript accumulation remains abaxialized in rgd2 and lbl1 mutants, revealing that *t*a-siARF function is not required for *arf3a* polarization. RGD2 function is also required for proper localization and down-regulation of miR390 and miR166 in maize shoot apices. Combined with previous genetic and phenotypic analyses of the rgd2-R mutation, these data suggest that *arf3a* and miR166 over-accumulation is insufficient to confer the loss of dorsiventral polarity in maize leaves. An *ago1* paralog hyper-accumulates in lbl1-rgd1, but not in rgd2-R mutants. Taken together, these findings suggest that LBL1 regulates miR166 localization in a separate pathway that does not require RGD2 function, and the combined over-accumulation of *ago1* together with ectopic miR166 triggers abaxialized leaf phenotypes that are not observed in rgd2 mutants.

Results

Positional cloning of *rgd2*

A mapping population of 189 highly introgressed individuals (see Materials and Methods) was used to genetically map the *rgd2-R* mutation to within a 0.52 centimorgan interval on maize chromosomal bin 1.04. This interval is flanked by the markers IDP1473 and CAP276M21, and comprised approximately 1.2 mega-base pairs on contig 19 of the maize genome (Figure 2.2A and Table 2.1; Maize Sequence Release 4a.53, October 2009). Among the 40 predicted genes within this interval, a maize homolog (GRMZM2G365589) of *Arabidopsis ago7/zip* was investigated as a candidate *rgd2* gene.

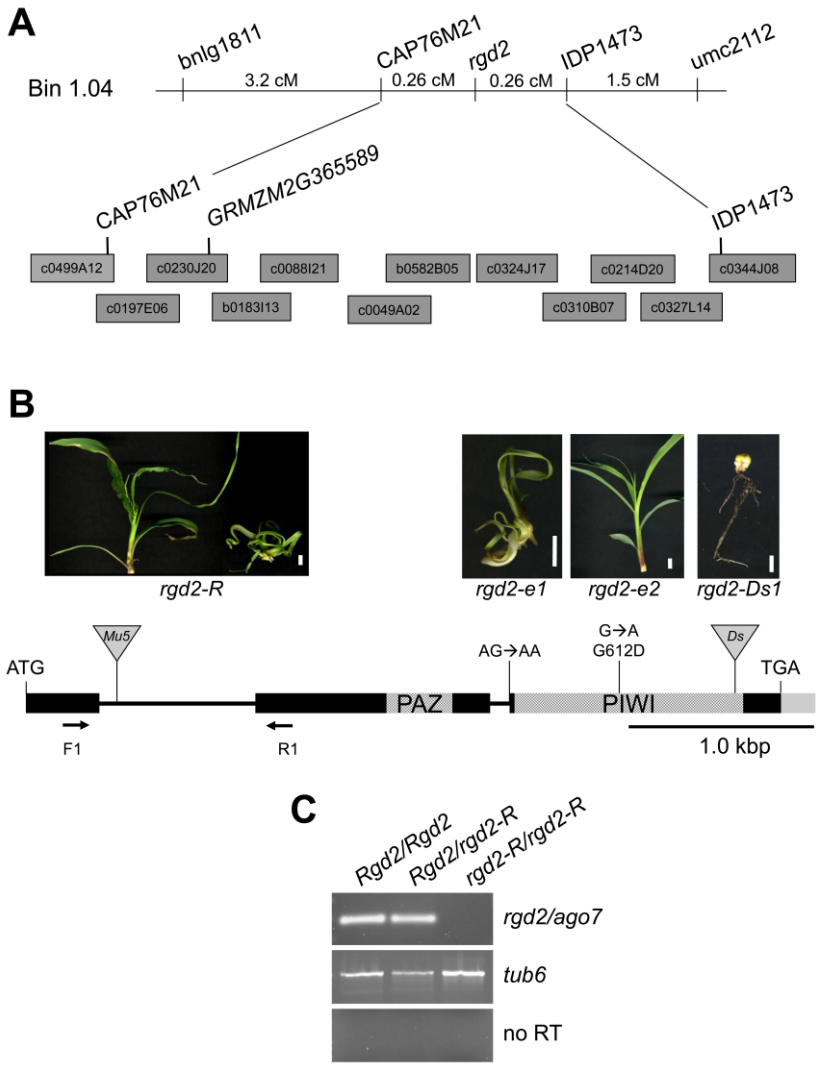

Figure 2.2. Positional cloning and characterization of *rgd2* alleles.

(A) Positional cloning of *rgd2*. *rgd2-R* was mapped to bin 1.04 using SSR markers (names) and fine mapped to an interval flanked by CAP76M21 and IDP1473. Candidate gene analysis revealed an *argonaute7*-like locus, GRMZM2G365589, on maize BAC c0230J20.
(B) Gene structure of *rgd2* wild type and mutant alleles. The r*gd2* open reading frame consists of three exons (black boxes) and shows a high degree of similarity to *argonaute7*. Shaded boxes show the approximate positions of the predicted PAZ and PIWI protein domains. Solid gray box represents 3' UTR. Inverted triangles mark the locations of transposon insertions in the *rgd2-R* and *rgd2-Ds1* alleles. Point mutations in the EMS-induced alleles, *rgd2-e1* and *rgd2-e2*, are denoted. Images of representative phenotypes of *rgd2* mutant alleles are above each lesion. Bars = 1 cm.
(C) RT-PCR analysis of *rgd2* transcripts. Primers F1 and R1, which flank the first intron, were utilized in *rgd2* transcript analyses of rgd2-R mutants, wild type siblings and heterozygous siblings. No transcripts were detected in rgd2-R mutants after 42 cycles. RT-PCR with *tub6* primers served as the control.

Table 2.1. Primers used in this study

Developed Markers for Positional Cloning of *rgd2*

Name	Accession	Forward Primer	Reverse Primer
CAP76M21	AC216276	TCTTCCCCTCTCAACTTATGGCT	TGCTCTAACAGGTGTCCTATTCCA
IDPc0499A12[a]	AC197028	TCGGAGAGAATTGAAGGGCTAAA	GGGCTAAAATTCCACATTAGGGC
IDPb0183I13[a]	AC217651	TGGTGTGATTCCATGTCCAC	TCATGCAAGTTGCTACCTCG

rgd2 Primers

Primer Name	Primer Sequence
F1	CTGCTGTTCCCCAAGGTG
R1	TGGTTCTCGTGAATGAAGCA
R2	CTGCTGGAAGGCTAACGAAG
*Mu*TIR	AGAGAAGCCAACGCCAWCGCCTCY

In Situ Hybridization Probes

Locus	Accession	Forward Primer	Reverse Primer	Size
rgd2	GQ918490	AACTCAAATGTCCTCTCGGG	ACGCGATATATGGGCAAAGA	2488-bp
tas3a	AC211570	GCTCAGGAGGGATAGAAGGG	CTGATCCCAAACTAGCTGGC	522-bp
arf3a	AC204859	AACCATTTTCTGCTGGTTCG	CACACTACGCAACACAGCCT	1355-bp

RNA Gel Blot Hybridization Probe

Locus ID	Accession	Forward Primer	Reverse Primer	Size
ago1	AY109385	GGATTTTGCTCTTGAGCCTG	GGCCTTTCTAATGGCATCAA	700-bp

qRT-PCR Primers

Locus ID	Accession	Forward Primer	Reverse Primer
miR166a	AY501431	GGGTACGTACATGCAAATCTGA	TCCTCCTCTCTTCAGTCGTCTT
miR166c	AY501433	AGGCTTCATTCCCCTCAAGT	GACAGAAAGATCGAGTCGCC
miR166h	AC200627	AGATACCATGCACACGAACATC	GAAATGAAGTGTAGCTAGCAAGGAT
miR166i	AC195814	CTTCCAAGATTGCTTTGTCAGTCGT	GTACAAACTATTCGCTTGCGTTCA
arf3a	AC204859	CTAGGTTTTCCTACCGTTGCTCAG	GACAAACATTGCGCGTCTATCCTC
tas3a	AC211570	GCTCAGGAGGGATAGAAGGG	TCTTTCCCACTACATGCAGGA
ago1	AY110984	CTGCTGGTGTTGGGAATGTT	GCTCTGCCTTAACAGCATCA
tub6	L10633	ATGCTTGGCGTTTGAGGTTC	CACGTCGCTGTCAATTGCTT
ubq	S94464	TAAGCTGCCGATGTGCCTGCGTCG	CTGAAAGACAGAACATAATGAGCACA

[a]Marker not mentioned in text

The rgd2-R mutation arose in a *Mutator* (*Mu*) transposon-mutagenized background (Henderson et al., 2005); the *ago7* candidate gene was used as a probe in a DNA gel blot hybridization to search for a gene-specific *Mu* insertion in rgd2-R mutant plants. As compared to the inbred lines Mo17 and B73, rgd2-R mutants contained an approximately 1.6-kbp insertion in the maize *ago7*-like gene (Figure 2.2B and Figure 2.3). Analyses of genomic PCR products obtained using an *ago7*-specific primer and a degenerate *Mu* transposon primer (*MuTIR*) revealed the presence of a *Mu5* (Talbert et al., 1989) transposon located 96-base pairs into the first intron of the *rgd2-R* allele of *ago7*. Attempts to span the *Mu5* insertion site using *ago7*-specific primers (F1 and R1) in reverse transcriptase PCR (RT-PCR) of cDNA derived from rgd2-R mutants failed (Figure 2.2C), suggesting that the *Mu5* transposon is improperly spliced from *ago7* transcripts of rgd2-R mutants. RT-PCR analyses using an *ago7*-specific primer (F1) and the *MuTIR* primer yielded an aberrant *ago7* cDNA fragment in which the *Mu5* terminus was spliced directly into the first exon of *ago7*, indicating that *rgd2-R* is a null mutation.

Identification of three additional mutant alleles verified that *rgd2* is an *ago7*-like maize gene (Figure 2.2B). Two alleles were obtained via EMS mutagenesis; *rgd2-e1* conditions a severe phenotype and contains a canonical G to A transition at the last base pair of the second intron. A predicted null allele, *rgd2-e1* produces a mis-spliced transcript containing a premature stop codon that is predicted to eliminate the conserved PIWI domain of RGD2 (described below). A second EMS allele with a relatively mild ragged seedling phenotype, *rgd2-e2* contains a G to A transition in the third exon that is predicted to cause a glycine to aspartic acid missense substitution at amino acid 612 (Figure 2.2B). A fourth mutant allele, *rgd2-Ds1*, contains a ~1.5-kbp *Dissociation* (*Ds*) transposon insertion at base pair 3635 of the third exon. In the W22

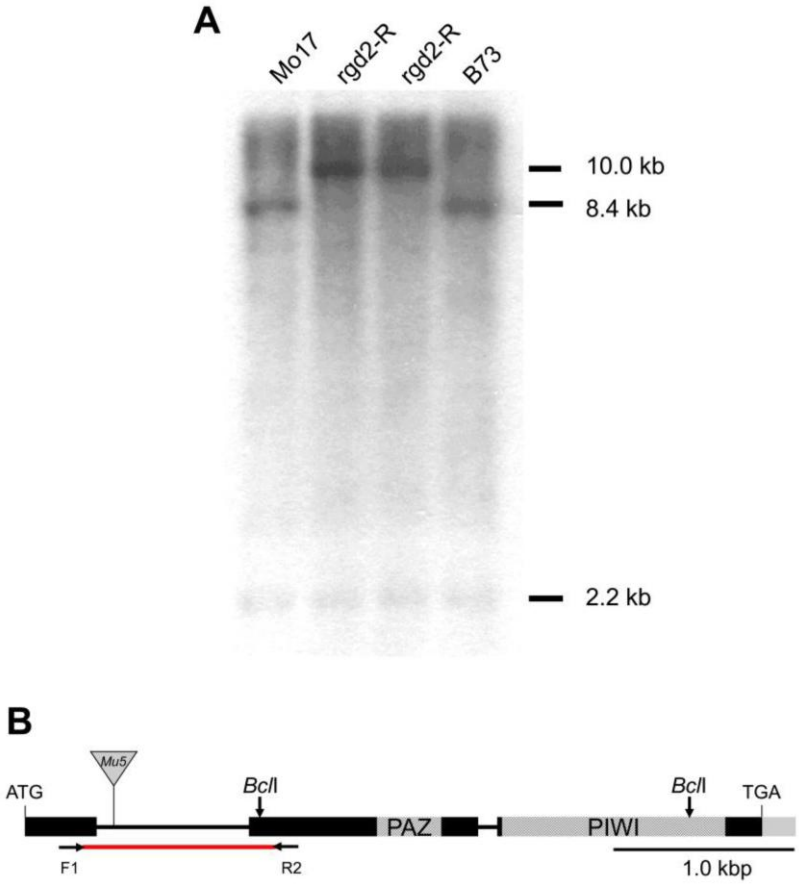

Figure 2.3. DNA gel-blot analysis of maize *ago7.*

(**A**) Genomic DNA digested with *Bcl*I was hybridized to a 1.2-kbp fragment of maize *ago*. A 1.6-kbp insertion is detected in the *rgd2-R* allele of *ago7.*
(**B**) Map of the maize *ago7* gene, showing location of *Bcl*I restriction sites, the location of the *ago7*probe (red underline) and PCR primers utilized to amplify this fragment, and the *Mu5* insertion in the *rgd2-R* mutant allele.

inbred genetic background wherein *rgd2-Ds1* arose, plants homozygous for this allele are shootless (Figure 2.2B). Notably, the *rgd2-R* allele is also shootless when introgressed into W22 (data not shown). The independent origin of these four *rgd2* mutations, all of which contain lesions in the *ago7*-like locus (GRMZM2G365589), verifies that *rgd2* (GenBank Accession GQ918490) encodes an AGO7-like protein in maize.

Like its homologs in *Arabidopsis* (AGO7/ZIP) and rice [SHOOT ORGANIZATION2/SHOOTLESS4 (SHO2/SHL4)], the *rgd2* locus contains three exons and is predicted to encode a protein of 1032 amino acids (Hunter et al., 2003; Nagasaki et al.; 2007). RGD2 shares 61% identity/76% similarity with AGO7/ZIP and 76% identity/85% similarity with SHO2/SHL4 (Figure 2.4). RGD2 also contains the highly conserved PAZ domain (87.7% identity with SHO2, 62.3% identity with AGO7) and the PIWI domain (86.6% identity with SHO2, 69.0% identity with AGO7). PAZ domains are important for recognizing the 3' end of small RNAs, while PIWI domains function during endonucleolytic slicing of target transcripts (reviewed in Vaucheret, 2008).

RGD2 is required for miR390 localization

As an AGO7-like protein, RGD2 is predicted to regulate maize dorsiventral patterning via *t*a-siARF biogenesis (Figure 2.1; Nogueira et al., 2009). *In situ* hybridization of seedling apices revealed that *rgd2* transcript accumulation is not polarized (Figures 2.5A and 2.5B). Unlike the adaxial accumulation observed for *ago7* orthologs from *Arabidopsis* and rice (Itoh et al., 2008; Chitwood et al., 2009), *rgd2* transcripts are evenly accumulated throughout the adaxial and abaxial regions of the youngest leaf primordium (P0-P1) and weakly in the SAM. In older leaf primordia (P2-P6), transcripts are localized to the margins and vascular bundles. No transcript accumulation was detected using a *rgd2* sense control (Figure 2.5C).

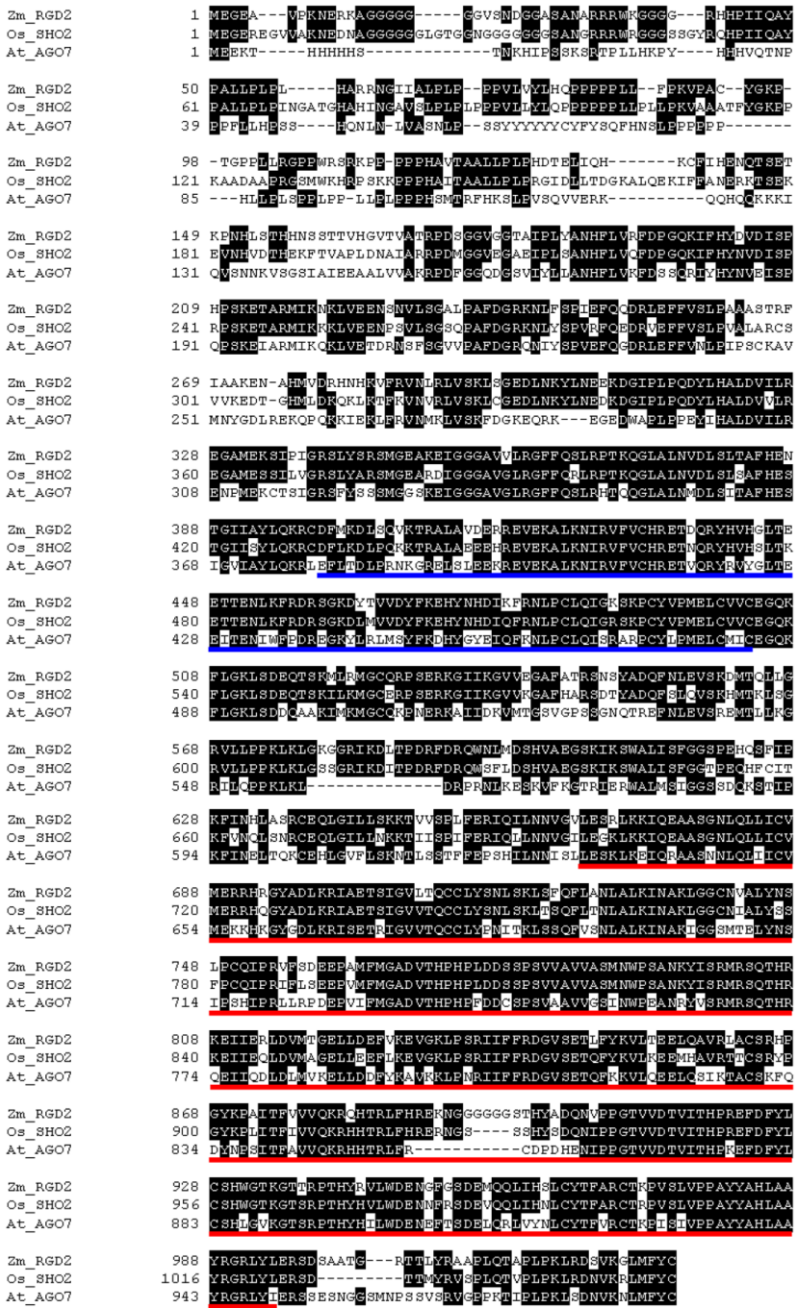

Figure 2.4. Amino acid alignment of RGD2, AGO7 and SHO2.

Predicted amino acid sequences of *Zea mays* RGD2, *Arabidopsis thaliana* AGO7, and *Oryza sativa* SHO2 were aligned using ClustalW. RGD2 shares 61% overall identity with AGO7 and 76% overall identity with SHO2. Black boxes denote identical amino acids for a given position. The blue bar marks the PAZ domain (87.7% identity with SHO2 and 62.3% identity with AGO7) and the red bar demarcates the PIWI domain (86.6% identity with SHO2 and 69.0% identity with AGO7).

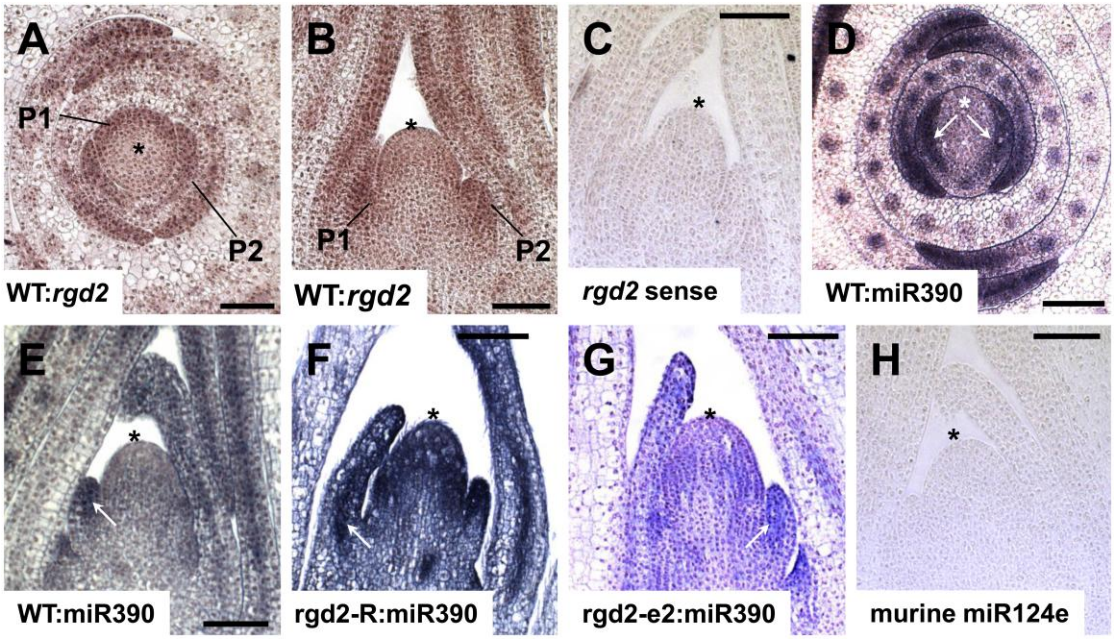

Figure 2.5. *In situ* hybridization analysis of *rgd2* and miR390 accumulation in rgd2 mutants and wild type sibling apices.

(A) and **(B)** Accumulation pattern of *rgd2* in the shoot apical meristem (*) and leaf primordia (P1, P2, etc.).
(A) Transverse wild type shoot apex.
(B) Longitudinal wild type shoot apex.
(C) Sense control for *rgd2*
(D) to **(G)** Accumulation pattern of miR390.
(D) Transverse wild type shoot apex.
(E) Longitudinal wild type shoot apex.
(F) Longitudinal rgd2-R shoot apices show ectopic miR390 expression throughout the shoot apical meristem crown and leaf primordia.
(G) Longitudinal rgd2-e2 shoot apex.
(H) An LNA probe for murine miR124e was used as a sense control for miR390 accumulation.
Bars = 100 µm; arrows point to areas of transcript accumulation.

Co-immunoprecipitation analyses in *Arabidopsis* showed that AGO7 selectively interacts with miR390 (Montgomery et al., 2008). Small RNA gel-blot hybridizations were utilized to analyze the effect of the *rgd2-R* mutation on miR390 accumulation in maize shoot apices. As shown in Figure 2.6A, miR390 levels are significantly elevated in rgd2-R mutant apices compared to wild type siblings. In order to determine if the rgd2-R mutation affects the tissue specificity of miR390 accumulation, locked-nucleic acid (LNA) probes complimentary to miR390 were utilized for *in situ* hybridizations of maize seedling shoot apices. As previously described and shown in Figures 2.5D and 2.5E, miR390 accumulates in adaxial domains of wild type maize leaf primordia, but is not detected in the crown of the SAM (Nogueira et al., 2009). Polarized accumulation of miR390 is maintained in the rgd2-R mutant leaf primordia, however, marked miR390 over-accumulation is observed in the crown of the rgd2-R mutant SAM as compared to wild type siblings (Figure 2.5F and Figure 2.7). In contrast, miR390 accumulation in the weakly phenotypic rgd2-e2 mutant is similar to that observed in wild type apices; very little miR390 is detected within the SAM crown (Figure 2.5G). An LNA probe complimentary to murine miR124e was used as a negative control for all LNA *in situ* hybridizations and no signal was detected in maize tissues (Figure 3H).

RGD2 is required for *t*a-siARF biogenesis and regulation of *arf3a* transcripts

AGO7 and miR390 are required to cleave the non-protein coding *tas3* transcripts that serve as precursors to *t*a-siARFs, small RNAs that regulate *arf3a* transcript accumulation (Figure 2.1; Allen et al., 2005; Pekker et al., 2005; Hunter et al., 2006; Montgomery et al., 2008). While mature *t*a-siARF transcripts are shown to accumulate adaxially in maize leaf primordia (Nogueira et al., 2007), the accumulation pattern of the *tas3a* precursor is undescribed. Transcripts of miRNA precursor genes

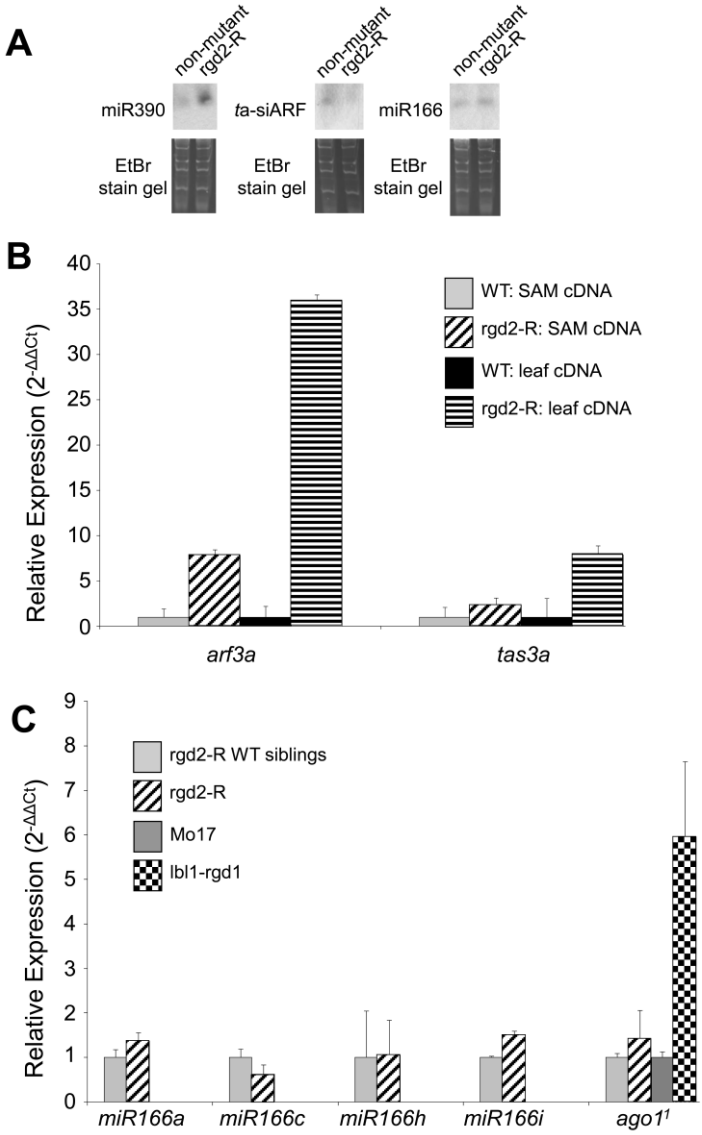

Figure 2.6. Accumulation analyses of transcripts involved in the *t*a-siARF pathway.

(A) Small RNA gel blot hybridization of miR390, miR166 and *t*a-siARF in wild type and rgd2-R shoot apices.
(B) qRT-PCR analysis of *arf3a* and *tas3a* in laser-microdissected leaf primordia and shoot apical meristems from wild type and rgd2-R mutants. Accumulation was normalized to *ubq*. Three biological replicates were used per experiment. Error bars denote one standard error.
(C) qRT-PCR analysis of miR166 precursors in laser-microdissected shoot apical meristems from wild type and rgd2-R mutants. An *ago1* paralogue ([1]GenBank Accession AY110984) was analyzed in wild type, rgd2-R mutant, and lbl1-ref mutant 14-day old seedlings. Accumulation was normalized to *tub6*. Each experiment used three biological replicates. Error bars denote one standard error.

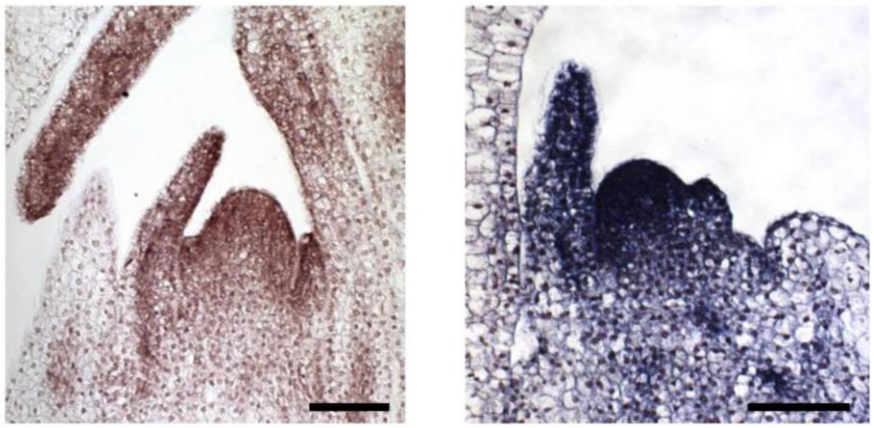

Figure 2.7. Additional *in situ* hybridization analyses of miR390 accumulation in rgd2-R mutant apices. Bar = 100 μm.

are predicted to form a stem-loop secondary structure that prevents hybridization of probes complimentary to the 21-bp miRNA sequence contained within the precursor RNA. Unlike miRNAs however, the *tas3a* transcript is not predicted to form secondary structure preventing the binding of a *t*a-siARF LNA probe to two complimentary sites found within the *tas3a* mRNA (Nogueira et al., 2007). Thus, a probe complimentary to *ta*-siARF is also expected to hybridize to *tas3a* precursor transcripts. As predicted, equivalent signals are detected in the abaxial regions of wild type leaf primordia following *in situ* hybridization to either a *tas3a* antisense probe *or* to a 16-bp LNA probe that is complimentary to the mature *t*a-siARF (Figures 2.8A-C). Previous studies revealed that precursor *tas3a* transcripts accumulate to much higher levels than mature *t*a-siARF (Allen et al., 2005; Lu et al., 2006). Taken together, these data suggest that the signal obtained following *in situ* hybridization of the *t*a-siARF LNA probe corresponds to *tas3a* precursor transcripts, which accumulate in abaxial leaf domains when RGD2 function is intact (Figure 2.8A-C); no accumulation is detected with a *tas3a* sense probe (Figure 2.8E). In contrast, the *t*a-siARF LNA probe identifies *tas3a* precursor transcripts in both adaxial and abaxial domains of rgd2-R leaf primordia, wherein RGD2 function is mutated (Figure 2.8D). These data suggest that *tas3a* transcripts initially accumulate throughout maize leaf primordia and are preferentially cleaved to generate *ta*-siARF in adaxial leaf domains by RGD2/miR390 activity, whereupon intact *tas3a* transcripts persist in abaxial regions.

Quantitative RT-PCR (qRT-PCR) confirmed that *tas3a* transcripts over-accumulate by 2.7-fold in rgd2-R mutant apices, and by 7.86-fold in rgd2-R leaf primordia (P1-P4) as compared to wild type siblings (Figure 2.6B). Hyper-accumulation of *tas3a* transcripts in rgd2-R apices may reflect inefficient processing of *tas3a* precursors into *t*a-siARF in the mutant shoots. To test this hypothesis, the accumulation of *t*a-siARF in rgd2-R and wild type apices was compared using small

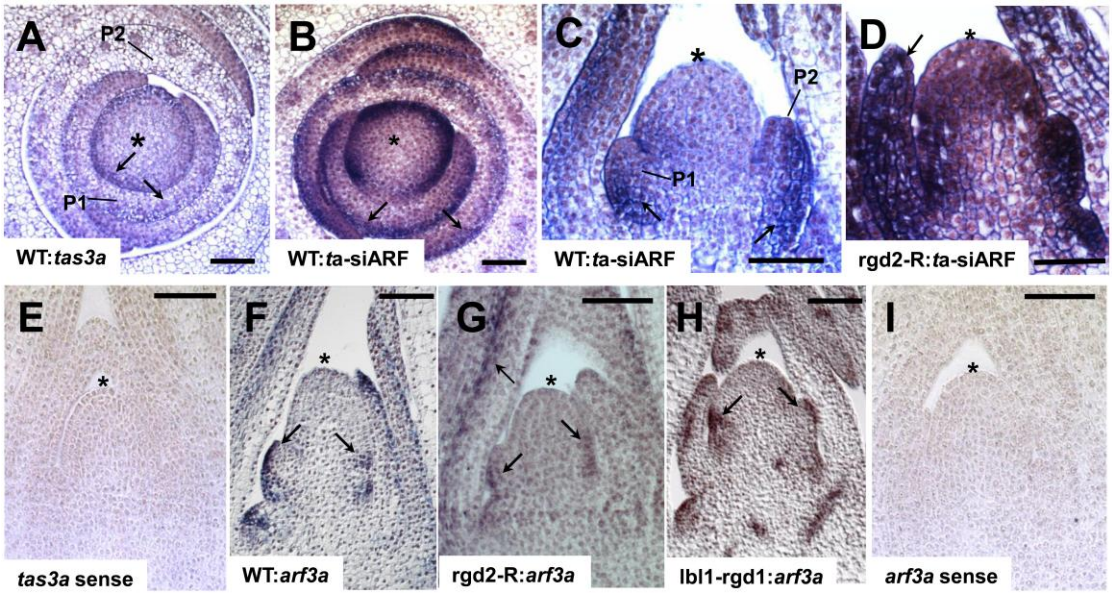

Figure 2.8. *In situ* hybridization analysis of *tas3a* and *arf3a* in wild type, rgd2-R and lbl1-rgd1 mutants.

(A) Accumulation of *tas3a* in a wild type apex transverse section.
(B) to **(D)** Accumulation pattern of a *t*a-siARF LNA probe.
(B) Transverse section of a wild type apex is similar to that seen with a *tas3a* probe.
(C) Longitudinal section of a wild type shoot apical meristem (*) and leaf primordia (P1, P2, etc.)
(D) Longitudinal section of a rgd2-R mutant apex shows ectopic expression in the shoot apical meristem and the leaf primordia.
(E) Sense control for *tas3a*.
(F) to **(H)** Accumulation pattern of *arf3a*.
(F) Longitudinal wild type apex exhibits accumulation in abaxial domains of leaf primordia.
(G) Longitudinal rgd2-R mutant apex. *arf3a* accumulation is observed only in abaxial regions of leaf primordia.
(H) Longitudinal lbl1-rgd1 mutant apex. *arf3a* accumulation remains abaxialized.
(I) Sense control for *arf3a*.
Bars = 100 µm. Arrows point to areas of accumulation.

RNA gel-blot hybridization. A 16-bp LNA probe complimentary to *t*a-siARF detects a small RNA of the expected size in total RNA extracted from wild type apices. In contrast, *t*a-siARF hybridization is dramatically reduced in RNA derived from rgd2-R mutant shoot apices (Figure 2.6A).

Proper biogenesis of *t*a-siARF is required to regulate *arf3a* accumulation levels in maize (Nogueira et al., 2007). Therefore, it was expected that *arf3a* transcripts would also be elevated in rgd2-R mutants owing to the absence of *t*a-siARF. Using cDNA prepared from laser microdissected (LM) SAM-P1 and leaf primordia (P1-P4) tissue, the accumulation of *arf3a* was examined by qRT-PCR. As expected, *arf3a* transcript accumulation is elevated in rgd2-R mutant SAMs (7.81-fold) and leaf primordia (35.89-fold) (Figure 2.6B) as compared to wild type siblings.

Whereas *ARF3/ETT* transcripts accumulate throughout leaf primordia in *Arabidopsis*, accumulation of ARF3/ETT protein is only detected in abaxial domains (Pekker et al., 2005; Chitwood et al., 2009). *In situ* hybridization analyses of wild type shoot apices confirmed that *arf3a* transcripts in maize are preferentially abaxialized (Figure 2.8F), while no accumulation is detected using a sense probe (Figure 2.8I). Unexpectedly, *arf3a* transcript accumulation remains abaxialized in rgd2-R mutant leaves (Figure 2.8G). An equivalent *arf3a* accumulation pattern was also observed in lbl1-rgd1 mutants (Figure 2.8H), suggesting that *ta-siARF* biogenesis is not required to polarize *arf3a* accumulation within abaxial domains of maize leaf primordia.

RGD2 regulates abaxial localization of miR166

Previous studies have suggested that miR166 accumulation is negatively regulated by *t*a-siARF and/or positively regulated by ARF3a (Figure 2.1; Nogueira et al., 2007; Nogueira et al., 2009). In lieu of these findings, the accumulation of *miR166* precursor loci was examined in rgd2-R mutant and wild type SAM-P1 tissue by LM-

qRT-PCR. Of the nine *miR166* precursor loci identified in the maize genome, four (*miR166a, miR166c, miR166h, and miR166i*) were previously shown to exhibit abnormal transcript accumulation in lbl1 mutant shoots (Nogueira et al., 2007). However, the accumulation of these *miR166* precursor transcripts is not significantly increased in rgd2-R mutant apices as compared to wild type siblings (Figure 2.6C). In contrast, small RNA gel-blot hybridization reveals that the 21-bp mature miR166 accumulates to approximately two-fold higher levels in rgd2-R mutant apices (Figure 2.6A).

The tissue-specific accumulation of mature miR166 was examined by *in situ* hybridization using a LNA probe. In wild type apices miR166 accumulates in abaxial regions of young leaf primordia, but is excluded from the SAM and from the pith directly below the SAM (Juarez et al., 2004; Figure 2.9A). Whereas lbl1 mutants accumulate miR166 throughout the abaxial and adaxial domains of young leaf primordia and below the SAM (Juarez et al., 2004; Nogueira et al., 2007), rgd2-R mutants also exhibit ectopic miR166 accumulation in adaxial leaf domains but do not accumulate miR166 in the pith directly below the SAM (Figure 2.9B).

Recent studies have shown that SGS3 is required for siRNA-directed cleavage of *ago1* transcripts in *Arabidopsis* (Mallory and Vaucheret, 2009). Using cDNA from 14-day old maize seedlings, qRT-PCR was carried out in rgd2-R and lbl1-rgd1 mutant backgrounds. In congruence with *Arabidopsis*, a maize *ago1* paralog (GenBank Accession AY110984) accumulates nearly six-fold higher in lbl1-rgd1 mutants as compared to rgd2-R mutant and wild type plants (Figure 2.6C).

Discussion

rgd2 encodes AGO7 function in maize

rgd2-R is a recessively-inherited mutant that is defective in mediolateral leaf development. Mutant plants often have radial leaves that, unlike other radial leaf

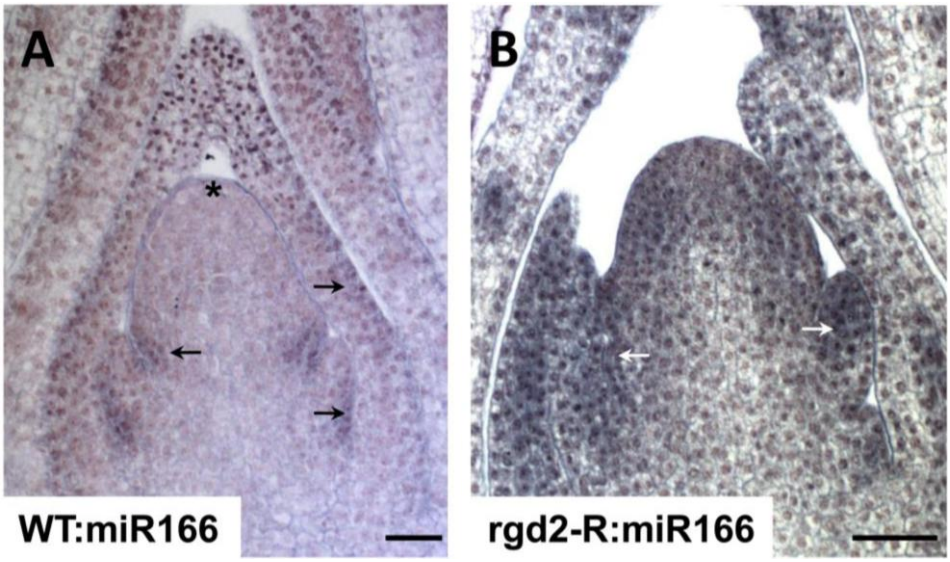

Figure 2.9. *In situ* hybridization analysis of miR166 in wild type and rgd2-R mutants.

(A) and (**B)** Accumulation of miR166 in shoot apices.
(A) Longitudinal section of a wild type apex shows miR166 accumulation in abaxial regions of leaf primordia (indicated by arrows).
(B) Longitudinal section of rgd2-R mutant apex shows ectopic accumulation of miR166 in adaxial regions of leaf primordia and the crown the the meristem (arrows). Bars = 50 µm. Asterisk (*) denotes shoot apical meristem.

mutants, maintain dorsiventral anatomy. No net loss of adaxial or abaxial characteristics is observed in rgd2-R mutant leaves (Henderson et al., 2005). The *rgd2* gene is identified as an *ago7*-like gene (GRMZM2G365589) using a positional cloning approach; several non-complementing *ago7* mutant alleles were isolated to verify the identity of *rgd2* (Figures 2.2A and 2.2B). The *rgd2-R* reference allele harbors a *Mu5* transposable element within intron 1, and RT-PCR analyses of rgd2-R mutants fail to amplify wild type transcripts that span the exon 1-exon 2 boundary (Figure 2.2C). These data suggest that *rgd2-R* is a null allele. In *Arabidopsis* AGO7 is implicated in the formation of *t*a-siARFs, which are required to down-regulate the abaxial identity factors *arf3* and *arf4* (Allen et al., 2005; Pekker et al., 2005; Hunter et al., 2006). As predicted for a null allele of *ago7*, rgd2-R mutants are defective in *t*a-siARF biogenesis (Figure 2.6A) and show a concomitant increase in *arf3a* transcript accumulation (Figure 2.6B).

RGD2 is required to localize miR390 in maize shoot apices

Elegant and detailed co-immunoprecipitation analyses in *Arabidopsis* demonstrated that AGO7 forms a RISC exclusively with miR390 (Montgomery et al., 2008). Although the accumulation of *rgd2* and miR390 transcripts overlaps in young leaf primordia and developing vasculature, miR390 is adaxial (Noguiera et al., 2007; Figures 2.5D and 2.5E) whereas *rgd2* accumulation is apolar (Figures 2.5A and 2.5B). Adaxial accumulation of miR390 is maintained in rgd2-R mutant leaf primordia, however marked over-accumulation of miR390 is observed within the crown of the mutant SAM (Figures 2.5F, 2.6A, and 2.7).

Layer-specific LM-qRT-PCR has shown that maize *miR390* precursor transcripts are expressed in the outer cell layer (L1) of the SAM, but not in the L2 (Nogueira et al., 2009). Intriguingly, *in situ* hybridizations detect mature miR390 accumulation in both the L1 and L2 (Nogueira et al., 2009; Figure 2.5E). One

possible explanation for this phenomenon is that *miR390* precursor transcripts are processed more rapidly in the L2 than the L1; a second proposal is that mature miR390 is mobile and traffics from the L1 to the L2. Although *t*a-siRNAs are shown to act non-cell autonomously (Chitwood et al., 2009), several studies examining the localization of artificial miRNAs and miRNAs with non-native promoters concluded that miRNAs act cell-autonomously (Schwab et al., 2006; Alvarez et al., 2006; Tretter et al., 2008). Still other studies have suggested that miR166 and miR390 may traffic in the shoot apex (Juarez et al., 2004; Kidner and Martienssen, 2004; Nogueira et al., 2009). Our analyses of differential rgd2 mutant alleles support a scenario wherein miR390 acts non-cell autonomously, and RGD2 functions to restrict its mobility into the crown of the maize shoot apex.

The conserved PAZ domains of AGO proteins recognize and bind the 3' ends of small RNAs (Ma et al., 2004; Lingel et al.; 2004; Hutvagner and Simard, 2008). The unspliced *Mu* insertion in *rgd2-R* transcripts is expected to disrupt or eliminate the PAZ domain from RGD2, thereby preventing the binding of miR390, which over-accumulates ectopically in the rgd2-R mutant SAM crown (Figure 2.5F). In contrast, rgd2-e2 mutants harbor a point mutation in the PIWI domain that causes a missense amino acid substitution; the PAZ domain is predicted to be unaltered (Figure 2.2B). Unlike rgd2-R mutants, rgd2-e2 mutants do not show ectopic miR390 over-accumulation within the SAM crown (Figure 2.5G). Likewise, miR390 accumulation is unchanged in lbl1 mutants (Noguiera et al., 2009), indicating that *t*a-siARF function is not required for proper localization of miR390. Taken together, these data suggest that an intact PAZ domain is correlated with normal miR390 accumulation in the maize SAM. We speculate that RGD2 is required to bind miR390 and restrict it from trafficking into the crown of the SAM (Figure 2.10).

Polarized degradation of *tas3a* is patterned by localization of miR390

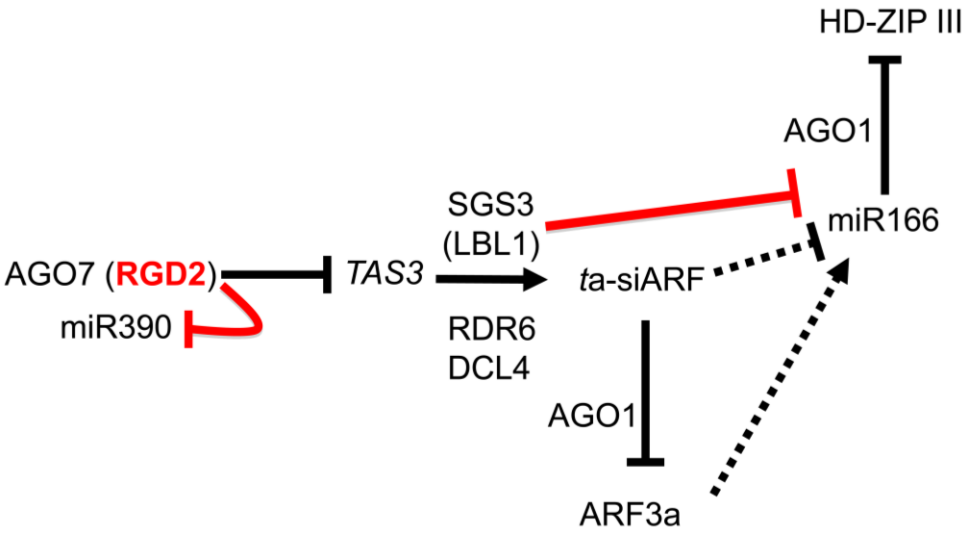

Figure 2.10. Revised model for the role of small regulatory RNAs in dorsiventral patterning.

rgd2 is the maize homolog of *Arabidopsis ago7* and is required to regulate miR390 accumulation and localization in the maize shoot apex. RGD2 and LBL1/SGS3 are both required to regulate miR166 accumulation levels. Like LBL1, RGD2 is required to properly localize miR166, suggesting miR166 polarization requires *t*a-siARF function. Although rgd2 mutants over accumulate miR166 and *arf3a*, miR166 is properly localized, resulting in no net loss of dorsiventral patterning in rgd2 mutants. However in lbl1 mutants, the ectopic accumulation of miR166 combined with the hyper-accumulation of *ago1* may account for the abaxialized mutant leaf phenotype. Abbreviations as described in Figure 1.

An *in situ* hybridization probe that recognizes *tas3a* precursor transcripts was used to determine their accumulation pattern in wild type shoot apices (Figure 2.6A). Wild type apices showed *tas3a* accumulation only in abaxial regions of leaf primordia, which is consistent with the biogenesis and function of *t*a-siARF in adaxial domains. An equivalent *in situ* hybridization signal is detected using a 16-bp LNA probe, which contains two complimentary sites in the *tas3a* transcript (Figures 2.8B and 2.8C). In lieu of previous analyses revealing that *t*a-siARF accumulates to lower levels than most miRNAs (Allen et al., 2005; Lu et al., 2006), these data strongly suggest that the signals obtained with the *t*a-siARF LNA probe are derived from *tas3a* transcript accumulation, not *t*a-siARF accumulation.

Unlike wild type siblings, *t*a-siARF LNA *in situ* hybridization analyses of rgd2-R mutants detect *tas3a* accumulation throughout the abaxial and adaxial domains of mutant leaf primordia (Figure 2.8D). These data suggest that the failure to process *tas3a* precursor transcripts into mature *t*a-siARF results in the ectopic accumulation of intact *tas3a* transcripts in rgd2-R mutant primordia. Both the overabundance of *tas3a* transcripts and the failure to detect *t*a-siARF in rgd2 mutant shoots support this hypothesis (Figures 2.6A and 2.6B). AGO7 and miR390 are both required to cleave *tas3a* and begin the process of *t*a-siARF biogenesis (Montgomery et al., 2008). Although *rgd2* accumulation is not polarized, miR390 is restricted to adaxial domains of maize leaf primordia (Figures 2.5A-D). These data indicate that the abaxial accumulation pattern of *tas3a* in wild type leaves is patterned by the adaxial expression of miR390, not by RGD2 *per se*. By the same token, the ectopic *tas3a* accumulation observed in adaxial domains of rgd2-R mutant leaf primordia is the likely result of failure to incorporate previously adaxialized miR390 into a functional RISC that normally converts *tas3a* into *t*a-siARF.

Up-regulation of both *arf3a* and miR166 is insufficient to confer an abaxialized leaf phenotype in maize

ARF3/ETT is an abaxial identity factor in *Arabidopsis* (Pekker et al., 2005), although the absence of arf3 mutants and/or *t*a-siARF insensitive lines has hindered analyses of ARF3 function in maize. *Arf3a* accumulation is detected in abaxial regions of wild type maize (Figure 2.8F). Although the *rgd2-R* mutation confers marked over-accumulation of *arf3a* in the SAM and in young leaf primordia (Figure 2.6B), the accumulation pattern remains abaxialized (Figure 2.8G) and dorsiventral polarity is maintained in mutant radial leaves (Henderson et al., 2005). A similar pattern of abaxialized *arf3a* over-accumulation is observed in lbl1-rgd1 mutants, which are also defective in *t*a-siARF biogenesis (Figure 2.8H). Therefore, like the adaxialized expression of miR390, the abaxial accumulation of *arf3a* transcripts is regulated independently of *t*a-siARF biogenesis. Moreover, rgd2-R mutants retain dorsiventral leaf polarity (Henderson et al., 2005), suggesting that *t*a-siARF biogenesis is not an essential requirement for leaf polarity in maize.

Over-expression of a *t*a-siARF-insensitive *arf3/ett* transcript recapitulates the zip-2/ago7 mutant phenotype in *Arabidopsis* (Hunter et al., 2006), which might suggest that the rgd2-R mutant phenotype is conditioned entirely by *arf3a* over-accumulation. However, mutations in orthologous *t*a-siARF biogenesis genes condition disparate phenotypes in maize and *Arabidopsis* (Mourrain et al., 2000; Hunter et al., 2003; Peragine et al., 2004; Timmermans et al., 1998; Henderson et al., 2005), and in the absence of a maize *t*a-siARF insensitive line this hypothesis remains quite speculative. On the other hand, the lack of abaxialized leaf phenotypes in rgd2 mutants clearly indicates that *arf3a* over-accumulation alone is not sufficient to disrupt dorsiventral leaf patterning in maize.

LBL1 encodes the maize SGS3 (Nogueira et al., 2007), and is thereby

predicted to function directly downstream of RGD2 during *t*a-siARF biogenesis (Figure 2.1). Unlike rgd2 mutants however, *lbl1* mutations confer severe disruptions in dorsiventral patterning and abaxialized, radial leaf phenotypes (Timmermans et al., 1998; reviewed in Chitwood et al., 2007). Furthermore instead of epistasis, rgd2;lbl1 double mutants display synergistic shootless phenotypes, which suggest that RGD2 and/or LBL1 perform non-overlapping functions outside of *t*a-siARF biogenesis (Henderson et al., 2006). Similar to lbl1 and the rice ago7 mutant sho2, rgd2-R mutant shoot apices exhibit ectopic over-accumulation of miR166 in adaxial leaf domains, although lbl1 also accumulates ectopic miR166 at the base of the SAM (Nogueira et al., 2007; Nagasaki et al., 2007; Figure 2.8B; Figure 2.9B). As such, our findings are consistent with suggested models wherein *t*a-siARF negatively regulates the expression of the abaxial-determinant miR166 (Figure 2.1; Nogueira et al., 2007, Nagasaki et al., 2007; Nogueira et al., 2009). Thus, despite the fact that rgd2 and lbl1 mutants both over-express *arf3a* and ectopically accumulate miR166, they condition disparate leaf phenotypes. These data, when considered in light of the synergistic rgd2;lbl1 double mutant phenotype, strongly suggest that LBL1 performs additional functions contributing to maize leaf polarity, outside of the *t*a-siARF biogenesis pathway.

In addition to its role during *t*a-siARF biogenesis, *Arabidopsis* SGS3 is also required for production of *ago1* siRNAs that down-regulate the accumulation of *ago1* mRNA in conjunction with miR168 (Mallory and Vaucheret, 2009). Unlike AGO7, AGO1 binds numerous miRNA species, including miR166. Our data demonstrate that lbl1-ref mutants over-accumulate an *ago1* paralog, whereas rgd2-R mutants do not (Figure 2.6C). Recent studies have shown that a maize *ago1*-like transcript accumulates in a gradient within leaf primordia, with higher accumulation in adaxial domains (Brooks et al., 2009). Intriguingly, miR166 accumulates ectopically in

adaxial leaf domains of lbl1 mutants, in a pattern that overlaps with *ago1* accumulation. We propose that up-regulation of *ago1* in lbl1 mutants (Figure 2.6C), in conjunction with the ectopic over-accumulation of miR166, may result in enhanced post-transcriptional degradation of adaxial identity factor *hd-zip III* genes. This increase in miR166 activity may explain why lbl1 mutants lose adaxial identity, while rgd2 mutants do not. Additionally, *Arabidopsis* SGS3 functions during viral defense and in additional siRNA pathways besides *t*a-siRNA biosynthesis (Mourrain et al., 2000; Peragine et al., 2004; Borsani et al., 2005). We propose a revised model (Figure 2.10) wherein additional functions of LBL1 outside of *t*a-siARF biogenesis contribute to the abaxialized phenotypes observed in lbl1 mutants and to the synergistic, shootless phenotype seen in rgd2;lbl1 double mutants (Henderson et al., 2006).

The interplay of several small RNAs is critical to the dorsiventral patterning of maize leaves (reviewed in Kidner and Timmermans, 2007; Chitwood et al., 2007). Future studies probing the mechanisms of miR390 polarization and its RGD2-mediated localization will enhance our understanding of the role of regulatory RNAs during leaf development. In addition, identification and analyses of arf3a mutants in maize may help decipher the convergent and divergent mechanisms by which *t*a-siARF regulates the development of monocots and eudicot shoots.

Methods

Plant Materials

The *rgd2-R* mutation arose in a *Mutator* transposon line (Henderson et al., 2005), and was introgressed into the maize inbred Mo17 genetic background for at least four-to-five generations to generate the mapping population utilized in this study. Primers for novel molecular markers developed during this study are listed in Table 2.1.

Ethylmethylsulfonate (EMS)-mutagenized Mo17 pollen was crossed onto *rgd2-R* heterozygous individuals to obtain additional mutant alleles of *rgd2* as described

(Neuffer, 1993). One EMS allele, *rgd2-e1*, was identified in a non-complementation screen of ~6200 F1 plants. However, the *rgd2-R*/*rgd2-e1* heterozygous plant was seedling lethal and the lesion was not recoverable for further genetic analyses. An additional mutant allele of *rgd2, rgd2-e2,* was obtained via screens of ~3000 M2 EMS-mutagenized families in the B73 inbred background. An M2 family segregated a filamentous leaf phenotype and was mapped to bin 1.04 using bulk segregant analyses. The *rgd2-Ds1*allele was identified in a large-scale transposon mutagenesis program utilizing the transposons *Activator* and *Dissociation* (Ahern et al., 2009). Analyses of the *lbl1-rgd1* allele were performed in the Mo17 genetic background.

***In situ* hybridizations**

Samples from 14 day seedlings were fixed, processed, sectioned and hybridized to gene specific probes as described (Jackson, 1991) with modifications as described (Juarez et al., 2004). Double-digoxigenin (DIG) labeled LNA probes complimentary to miR390, miR166, and *ta*-siARF were purchased from Exiqon (Vedbaek, Denmark). Five picomoles of LNA probe were used per slide; hybridizations were performed at 50°C and washes were performed at 55°C. The *rgd2* and *tas3a* probes (Table 2.1) were DIG-labeled (Roche) according to manufacturer's instructions. All samples were imaged on a Zeiss Axio Imager Z1m microscope (Thornwood, New York) using a five-megapixel Zeiss AxioCam MRc5 (Thornwood, New York) and AxioVision Release 4.6 software.

Small RNA Blot Hybridization

MiRNA blots were performed as described (Allen et al., 2004). Fifteen hand-dissected apices (shoot apex plus six leaf primordia) were pooled for each wild type and rgd2-R mutant sample; RNA was extracted using the TRIzol lysis method and prepared for Northern transfer as described (Fu et al., 2002). Approximately 20 µg of total RNA was loaded per lane. Twenty-one base pair oligonucleotide probes

complimentary to miR390 and miR166 were end-labeled with ^{32}P. Double-DIG labeled LNA *ta*-siARF probes were as described above. Hybridizations and washes were performed at 42°C.

qRT-PCR

SAM or leaf primordia (P1-P4) tissue was harvested by laser microdissection, and cDNA was synthesized from amplified RNA as described in Zhang et al. (2007). Gene-specific primers were designed (Table 2.1) for use with SYBR-Green (Quanta) in qRT-PCR as described (Zhang et al., 2007). Three biological replicates were examined, and samples were normalized to *beta-6 tubulin* (accession L10633) or *ubiquitin* (accession S94464) expression as described using Bio-Rad iQ5 Version 1.0 software (Livak and Schmittgen, 2001; Zhang et al., 2007).

Accession Numbers

Sequence data can be found in the GenBank data library under the following accession numbers: BAC c0230J20 (AC206196), *rgd2* (GQ918490).

Acknowledgements

We thank Marja Timmermans and Dan Chitwood for assistance with small RNA *in situ* hybridizations; Xiaolan Zhang donated LM SAM cDNA and Dave Henderson provided helpful discussions of the data. We thank Erik Vollbrecht, Tom Brutnell, and Kevin Ahern for identifying the *rgd2-Ds1* allele. Scott Tingey and Amanda Jones provided physical mapping information that expedited the positional cloning of *rgd2*, and Taiowa Montgomery offered technical advice on small RNA gel-blot hybridizations. This work was supported by the National Science Foundation (grant #IOS-0649810 to M.J.S.).

REFERENCES

Adenot X., Elmayan T., Lauressergues D., Boutet S., Bouche N., Gasiciolli V., and Vaucheret H. 2006. DRB4-dependant *TAS3 trans*-acting siRNAs control leaf morphology through AGO7. *Curr. Biol*. 18: 758-762.

Ahern K.R., Deewatthanawong P., Schares J., Muszynski M., Weeks R., Vollbrecht E., Duvick J., Brendel V.P., and Brutnell T.P. 2009. Regional mutagenesis using *Dissociation* in maize. *Methods*. 49: 248-254.

Allen E. Xie Z., Gustafson A.M., Sung G.H., Spatafora J.W., and Carrington J.C. 2004. Evolution of microRNA genes by inverted duplication of target gene sequences in Arabidopsis thaliana. *Nat. Genet*. 36: 1282-1290.

Allen E., Xie Z., Gustafson A.M., and Carrington J.C. 2005. microRNAs-directed phasing during *trans*-acting siRNA biogenesis in plants. *Cell*. 121: 207-221.

Alvarez J.P., Pekker I., Goldshmidt A., Blum E., Amsellem Z., and Eshed Y. 2006. Endogenous and synthetic microRNAs stimulate simultaneous, efficient, and localized regulation of multiple targets in diverse species. *Plant Cell*. 18: 1134-1151.

Borsani O., Zhu J., Verslues P.E., Sunkar R., and Zhu J.K. 2005. Endogenous siRNAs derived from a pair of natural *cis*-antisense transcripts regulate salt tolerance in *Arabidopsis*. *Cell*. 123: 1279-1291.

Brooks III L.B., Strable J., Zhang X., Ohtsu K., Zhou R., Sarkar A., Hargreaves S., Elshire R.J., Eudy D., Pawlowska T., Ware D., Janick-Buckner D., Buckner B., Timmermans M.C.P., Schnable P.S., Nettleton D., and Scanlon M.J. 2009. Microdissection of Shoot Meristem Functional Domains. *PLoS Genet*. 5: e1000476.

Chitwood D.H., Nogueira F.T.S., Howell M.D., Montgomery T.A., Carrington J.C., and Timmermans M.C.P. 2009. Pattern formation via small RNA mobility. *Genes Dev*. 23: 549-554.

Eshed Y., Izhaki A., Baum S.F., Floyd S.K., and Bowman J.L. 2004. Asymmetric leaf development and blade expansion in *Arabidopsis* are mediated by KANADI and YABBY activities. *Development*. 131: 2997-3006.

Fagard M., Boutet S., Morel J.B., Bellini C., and Vaucheret H. 2000. AGO1, QDE-2, and RDE-1 are related proteins required for post-transcriptional gene silencing in plants, quelling in fungi, and RNA interference in animals. *Proc. Natl. Acad. Sci. USA*. 97: 11650-11654.

Fahlgren N., Montgomery T., Howell M., Allen E., Dvorak S., Alexander A., and Carrington J. 2006. Regulation of *AUXIN RESPONSE FACTOR3* by *TAS3* ta-siRNA affects developmental timing and patterning in *Arabidopsis. Curr. Biol*. 16: 939-944.

Fu S., Meeley R., and Scanlon M.J. 2002. *Empty pericarp2* encodes a negative regulator of the heat shock response and is required for maize embryogenesis. *Plant Cell*. 14: 3119-3132.

Garcia D., Collier S.A., Byrne M.E., and Martienssen R.A. 2006. Specification of leaf polarity in *Arabidopsis* via the *trans*-acting siRNA pathway. *Curr. Biol*. 16: 933-938.

Henderson D.C., Muehlbauer G.J., and Scanlon M.J. 2005. Radial leaves of the maize mutant *ragged seedling2* retain dorsiventral anatomy. *Dev. Biol*. 282: 455-466.

Henderson D.C., Zhang X., Brooks L., and Scanlon M.J. 2006. RAGGED SEEDLING2 is required for normal expression of KANADI2 and REVOLUTA homologues in the maize shoot apex. *Genesis*. 44: 372-382.

Hunter C., Sun H., and Poethig S.R. 2003. The *Arabidopsis* heterochronic gene *ZIPPY* is an *ARGONAUTE* family member. *Curr. Biol*. 13: 1734-1739.

Hunter C., Willmann M.R., Wu G., Yoshikawa M., de la Luz Gutierrez-Nava M., and Poethig S.R. 2006. Trans-acting siRNA-mediated repression of ETTIN and ARF4 regulates heteroblasty in *Arabidopsis*. *Development*. 133: 2973-2981.

Husbands A.Y., Chitwood D.H., Plavskin Y., and Timmermans M.C. 2009. Signals and prepatterns: new insights into organ polarity in plants. *Genes Dev*. 23: 1986-1997.

Hutvagner G., and Simard M.J. 2008. Argonaute proteins: key players in RNA silencing. *Nat. Rev. Mol. Cell Biol*. 9: 22-32.

Itoh J., Sato Y., and Nagato Y. 2008. The SHOOT ORGANIZATION2 gene coordinates leaf domain development along the central-marginal axis in rice. *Plant Cell Physiol*. 49: 1226-1236.

Jackson, D. 1991. In situ hybridization in plants. In *Molecular Plant Pathology: A Practical Approach*, D.J. Bowles, S.J. Gurr, and M. McPherson, eds (Oxford, UK: Oxford University Press), UK, pp. 163–174.

Juarez M.T., Kui J., Thomas J., Heller B. and Timmermans M.C.P. 2004. microRNAs-mediated repression of *rolled leaf1* specifies maize leaf polarity. *Nature*. 428: 84-88.

Koch A.J. and Meinhardt H. 1994. Biological pattern-formation – From basic mechanisms to complex structures. *Rev Mod Phys*. 66: 1481-1507.

Kidner C.A. and Martienssen R.A. 2004. Spatially restricted microRNA directs leaf polarity through *ARGONAUTE1*. *Nature*. 428: 81-84.

Kidner C.A. and Timmermans M.C.P. 2007. Mixing and matching pathways in leaf polarity. *Curr. Opin. Plant Biol*. 10: 13-20.

Lanet E., Delannoy E., Sormani R., Floris M., Brodersen P., Crete P., Voinnet O. and Robaglia C. 2009. Biochemical evidence for translational repression by *Arabidopsis* microRNAs. *Plant Cell*. 21: 1762-1768.

Lingel A., Simon B., Izaurralde E., and Sattler M. 2004. Nucleic acid 3'-end recognition by the Argonaute2 PAZ domain. *Nat. Struct. Mol. Biol*. 11: 576-577.

Livak K.J., and Schmittgen T.D. 2001. Analysis of relative gene expression data

using real-time quantitative PCR and the 2(-Delta Delta C(T)) Method. *Methods*. 25: 402–408.

Lu C., Kulkarni K., Souret F.F., MuthuValliappan R., Tej S.S., Poethig R.S., Henderson I.R., Jacobsen S.E., Wang W., Green P.J., and Meyers B.C. 2006. MicroRNAs and other small RNAs enriched in the *Arabidopsis* RNA-dependent RNA polymerase-2 mutant. *Genome Res.* 16: 1276-1288.

Ma J.B., Ye K., and Patel D.J. 2004. Structural basis for overhang-specific small interfering RNA recognition by the PAZ domain. *Nature*. 429: 318-322.

Mallory A.C., and Vaucheret H. 2009. ARGONAUTE1 homeostasis invokes the coordinate action of the microRNA and siRNA pathways. *EMBO Reports*. 10: 521-526.

McConnell, J.R., Emery, J., Eshed, Y., Bao, N., Bowman, J., and Barton, M.K. 2001. Role of PHABULOSA and PHAVOLUTA in determining radial patterning in shoots. *Nature*. 411: 709-713.

Montgomery T.A., Howell M.D., Cuperus J.T., Li D., Hansen J.E, Alexander A.L., Chapman E.J., Fahlgren N., Allen E., and Carrington J.C. 2008. Specificity of ARGONATUE7-miR390 interaction and dual functionality in TAS3 trans-acting siRNA formation. *Cell*. 133: 128-141.

Mourrain P., Beclin C., Elmayan T., Feuerbach F., Godon C., Morel J.B., Jouette D., Lacombe A.M., Nikic S., Picault N., Remoue K., Sanial M., Vo T.A., and Vaucheret H. 2000. Arabidopsis *SGS2* and *SGS3* genes are required for posttranscriptional gene silencing and natural virus resistance. *Cell*. 101: 533-542.

Nagasaki H., Itoh J., Hayashi K., Hibara K., Satoh-Nagasawa N., Nosaka M., Mukouhata M., Ashikari M., Kitano H., Matsuoka M., Nagato Y., and Sato Y. 2007. The small interfering RNA production pathway is required for shoot meristem initiation in rice. *Proc. Natl. Acad. Sci. USA*. 104: 14867-14871.

Neuffer, M.G. 1993. Mutagenesis. In *The Maize Handbook*, M. Freeling, and V. Walbot, eds (New York: Springer), pp. 212–219

Nogueira F.T., Madi S., Chitwood D.H., Juarez M.T., and Timmermans M.C. 2007. Two small regulatory RNAs establish opposing fates of a developmental axis. *Genes Dev*. 21: 750-755.

Nogueira F.T., Chitwood, D.H., Madi, S., Ohtsu, K., Schnable, P.S., Scanlon, M.J., and Timmermans, M.C. 2009. Regulation of small RNA accumulation in the maize shoot apex. *PLoS Genet*. 5: e1000320.

Pekker I., Alvarez J., and Eshed Y. 2005. AUXIN RESPONSE FACTORS mediate *Arabidopsis* organ asymmetry via modulation of KANADI activity. *Plant Cell*. 17: 2899-2910.

Peragine A., Yoshikawa M., Wu G., Albrecht H.L., and Poethig R.S. 2004. SGS3 and SGS2/SDE1/RDR6 are required for juvenile development and the production of trans-acting siRNAs in *Arabidopsis*. *Genes Dev.* 18: 2368-2379.

Poethig R.S. 1984. Cellular parameters of leaf morphogenesis in maize and tobacco. In *Contemporary Problems of Plant Anatomy*, R.A. White, and W.C. Dickinson, eds (New York: Academic Press), pp. 235–238.

Reinhart B.J., Weinstein E.G., Rhoades M.W., Bartel B., and Bartel D.P. 2002. MicroRNAs in plants. *Genes Dev*. 16: 1616-1626.

Schwab R., Ossowski S., Riester M., Warthmann N., and Weigel D. 2006. Highly specific gene silencing by artificial microRNAs in *Arabidopsis*. *Plant Cell*. 18: 1121-1133.

Talbert L.E., Patterson G.I., and Chandler V.L. 1989. *Mu* transposable elements are structurally diverse and distributed throughout the genus *Zea*. *J. Mol. Evol.* 29: 28-39.

Timmermans M.C., Schultes N.P., Jankovsky J.P., and Nelson T. 1998.

Leafbladeless1 is required for dorsoventrality of lateral organs in maize. *Development*. 125: 2813-2823.

Tretter E.M., Alvarez J.P., Eshed Y., and Bowman J.L. 2008. Activity range of *Arabidopsis* small RNAs derived from different biogenesis pathways. *Plant Phyisol*. 147: 58-62.

Vaucheret H. 2008. Plant ARGONAUTES. *Trends Plant Sci*. 13: 350-358.

Waites R. and Hudson A. 1995. *phantastica*: a gene required for dorsoventrality of leaves in *Antirrhinum majus*. *Development*. 121: 2143-2154.

Yoshikawa M., Peragine A., Park M.Y., and Poethig R.S. 2005. A pathway for the biogenesis of *trans*-acting siRNAs in *Arabidopsis*. *Genes Dev*. 19: 2164-2175.

Zhang X., Madi S., Borsuk L., Nettleton D., Elshire R.J., Buckner B., Janick-Buckner D., Beck J., Timmermans M., Schnable P.S., Scanlon M.J. 2007. Laser microdissection of narrow sheath mutant maize uncovers novel gene expression in the shoot apical meristem. *PLoS Genet*. 3(6): e101.

Zhong R., and Ye Z.H. 2004. Amphivasal vascular bundle1, a gain-of-function mutation of the IFL1/REV gene, is associated with alterations in the polarity of leaves, stems and carpels. *Plant Cell Physiol.* 45: 369-385.

CHAPTER 3

EXAMINING DOWNSTREAM EFFECTS OF RGD2 FUNCTION[1]

[1] Douglas R.N., Zhang X., and Scanlon M.J. To be included in submission to *Proc. Natl. Acad. Sci. USA*.

Introduction

Leaves are initiated by the shoot apical meristem (SAM) and possess three main axes of development: proximodistal (base to tip), mediolateral (midrib to margin) and dorsiventral or adaxial/abaxial (upper and lower surfaces). Maize (*Zea mays*) leaves have distinct adaxial and abaxial tissue types and the leaves are flattened in the mediolateral axis to increase surface area for light capture and gas exchange. Several mutants have been identified in *Antirrhinum majus,* maize and *Arabidopsis thaliana* that condition radially symmetric leaves lacking either adaxial or abaxial identities (Waites and Hudson, 1995; Timmermans et al., 1998; McConnell et al., 2001). Examination of these radial leaf mutants has led to a model whereby the juxtaposition of adaxial and abaxial tissue types is required for mediolateral leaf development (Waites and Hudson, 1995; Timmermans et al., 1998; Candela et al., 2008). However, this model fails to explain phenotypes associated with ragged seedling2 (rgd2), which has radially symmetric leaves that maintain adaxial and abaxial tissue types (Henderson et al., 2005).

Rgd2 encodes an ARGONAUTE7 (AGO7)-like protein that is required for biogenesis of a *trans*-acting small interfering RNA (*t*a-siRNA) termed *t*a-siARF (Douglas et al., submitted; Chapter 2). The production of *t*a-siARF is a plant specific process that utilizes microRNA (miRNA) and *t*a-siRNA biogenesis components (Allen et al., 2005). *t*a-siARF production begins with the cleavage of a non-protein coding *tas3a* transcript by an RNA-induced silencing complex (RISC) comprised of miR390 and RGD2/AGO7 (Allen et al., 2005; Adenot et al, 2006; Fahlgren et al., 2006; Douglas et al., submitted). Rather than being degraded, as would happen to most transcripts cleaved by a RISC, the cleavage product is stabilized and converted into double-stranded RNA (dsRNA) in a process that requires LEAFBLADELESS1 (LBL1)/SUPPRESSOR-OF-GENE-SILENCING3 and RNA-DEPENDANT RNA

POLYMERASE6 (Allen et al., 2005; Nogueira et al., 2007). The dsRNA undergoes phased cleavage by DICER-LIKE4 to yield 21-nucleotide mature *t*a-siARFs (Allen et al., 2005).

In *Arabidopsis* and maize, *t*a-siARF forms a RISC with AGO1 to target transcripts of *auxin response factor3/ettin* (*arf3/ett*) for degradation (Peragine et al., 2004; Allen et al., 2005; Nogueira et al., 2007; Montgomery et al., 2008). Although *arf3a* and *t*a-siARF have been described as polarity determinants (Pekker et al., 2005; Garcia et al., 2006; Fahlgren et al., 2006; Nogueira et al., 2007; Nogueira et al., 2009), their specific roles in maize leaf development are unclear (Douglas et al., submitted). In non-mutant maize, *arf3a* accumulates in abaxial regions of leaf primordia (Douglas et al., submitted). Surprisingly, *arf3a* still accumulates abaxially in rgd2 and lbl1 mutants, which are deficient in *t*a-siARF biogenesis (Douglas et al., submitted). These findings suggest that *arf3a* transcripts are polarized independently of the *t*a-siARF biogenesis pathway.

Although RGD2 functions to create *t*a-siARF, downstream effects of the *t*a-siARF biogenesis pathway remain unknown. Given that the roles of *t*a-siARF and *arf3a* in maize leaf development are unclear at present; more investigation is required to elucidate their functions. In order to identify possible downstream functions for the *t*a-siARF biogenesis pathway, a microarray hybridization analysis of SAM-enriched maize cDNAs was performed utilizing laser microdissected (LM) tissue to compare transcript accumulation in non-mutant and rgd2 mutant apices (X. Zhang and M. Scanlon, unpublished data). Approximately 200 transcripts displayed differential accumulation in rgd2 mutant apices, and one particular gene with greatly reduced accumulation in rgd2 (AC211276.4_FG008) was initially selected for functional analysis (X. Zhang and M. Scanlon, unpublished data).

Transcripts for AC211276.4_FG008 accumulate in the developing vasculature,

and appears to predict the eventual location of vascular bundles in the P1 leaf primordium (X. Zhang and M. Scanlon, unpublished data). The accumulation pattern is similar but greatly reduced in rgd2 mutants, until the P5 leaf primordium. Interestingly, the accumulation pattern appears equivalent in rgd2 mutant and non-mutants starting in the P6 leaf primordium. As AC211276.4_FG008 shows no homology to known genes, it was named *punctate vascular expression1* (*pve1*) based on its accumulation pattern. A PCR-based reverse genetics technique was utilized to identify two independently derived, non-complimenting *Mutator* (*Mu*) transposon alleles of *pve1* (X. Zhang, P. Schnable, and M. Scanlon, unpublished data). Both mutant alleles of *pve1* exhibit a variety of leaf defects including narrow leaves, half leaves, split leaves, and some ectopic leaves (J. Strable and M. Scanlon, unpublished data; Figure 3.1).

The identification of *pve1* has provided an opportunity to examine a potential downstream mediator of RGD2 function. Here, we describe the coding region and structure of the non-mutant and mutant alleles of *pve1*. We verified the down regulation of *pve1* transcripts in rgd2 mutant leaf primordia by quantitative reverse-transcriptase PCR (qRT-PCR), and demonstrate that *pve1* is also downregulated by mutation in the downstream *t*a-siARF biosynthesis gene *lbl1*. We also examined the accumulation of several transcripts implicated in dorsiventral patterning of maize leaves in pve1 mutants, and propose a working model for PVE function during maize leaf development. Finally, to investigate potential downstream transcriptional effects of *t*a-siARF biogenesis, we coupled laser microdissection with Illumina RNA sequencing to search for differential accumulation of potential target genes with predicted complimentarity to microRNA 390 (miR390), miR166 and/or *t*a-siARF, the small RNAs that are known to be regulated by RGD2 function.

Figure 3.1. pve1-R mutant phenotype.

The pve1-R mutant phenotype is characterized by smaller stature, narrow leaves, half leaves, split leaves and occasional ectopic leaf outgrowths. Bar = 1 cm.

Results

The maize gene AC211276.4_FG008 (Maize Sequence Release 4a.53, October 2009) was identified via a microarray hybridization analysis of SAM-enriched cDNAs (X. Zhang and M. Scanlon, unpublished data). Owing to its unique *in situ* hybridization signal, AC211276.4_FG008 was renamed *punctate vacular expression1* (*pve1*). A PCR-based reverse genetics technique identified two independent, non-complimentary *Mu* transposon alleles of *pve1*. Previously, a *Mu8*-like transposon in base pair 684 of the pve1 gene was found to be segregating in families harboring the *pve1-M2* allele (J. Strable and M. Scanlon, unpublished data). Sequence analyses of plants homozygous for the *pve1-R* allele were found to contain a *Mu1*-like element inserted at base pair 614 of the coding region of *pve1* (Figure 3.2A). As this insertion is located within the lone exon of *pve1*, *pve1-R* is predicted to be a null allele. BLAST (Basic Local Alignment Search Tool; Altschul et al., 1990) revealed that the *pve1* locus is on chromosome 5; a paralogous gene (GRMZM2G324273) displaying 95% nucleotide identity within the predicted coding region is located on chromosome 1. The *pve1* transcript comprises an unusually long 5'-UTR (untranslated region), a single exon, and a 3'-UTR interrupted by a single intron (FIGURE 3.2), and is predicted to encode a protein of 360 amino acids with no homology to proteins of known function.

In order to corroborate the microarray hybridization data, LM-qRT-PCR analysis of non-mutant and rgd2-R mutant shoot apices was performed. As shown in Figure 3.3, *pve1* transcript accumulation is reduced in rgd2-R mutant P1-P4 leaf primordia to 0.14-fold the level detected in non-mutant siblings. Interestingly, *pve1* also only accumulates to 0.54-fold in lbl1 mutant whole seedlings as compared to

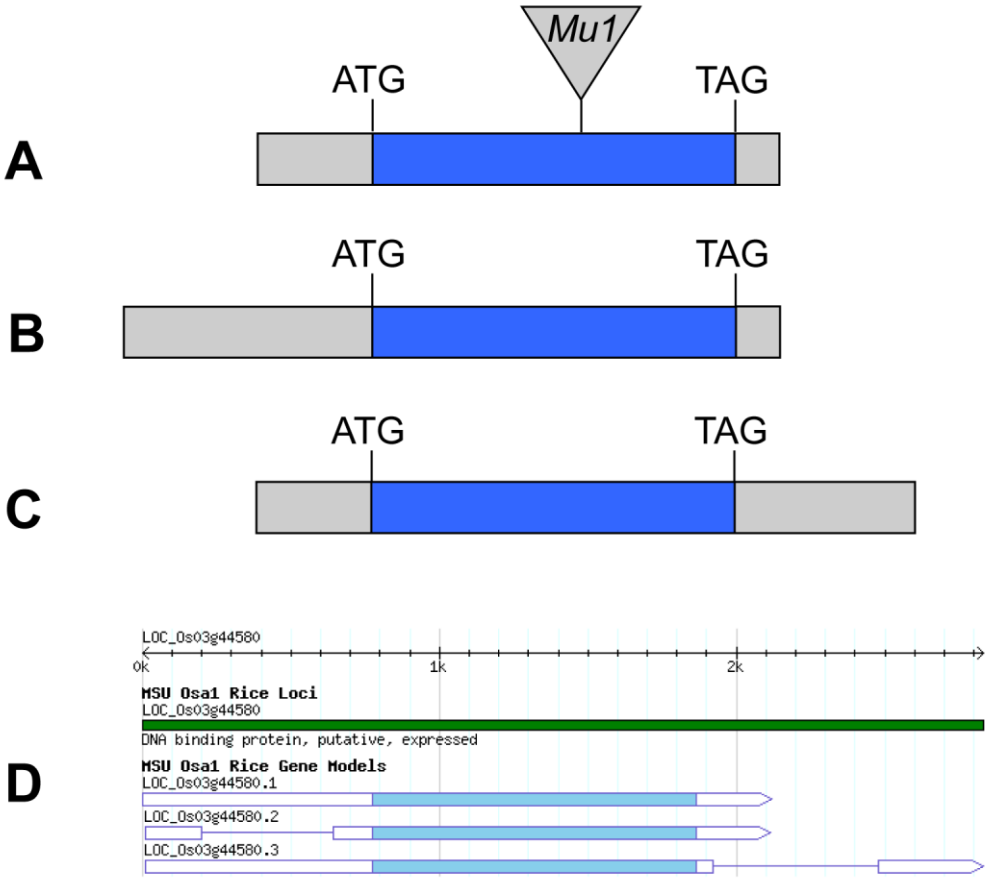

Figure 3.2. *pve1* gene structure.

(A) *pve1* has a 317-bp 5'-UTR (gray box) followed by a single 1083-bp exon (blue box). The exon is followed by a spliced 113-bp 3'-UTR (gray box). The *pve-R* allele contains a *Mutator1*-like (*Mu1*) element inserted at bp 614 of the coding region.
(B) An EST (accession EE186754) suggests that the 5'-UTR of *pve1* may extend at least 763-bp upstream of the coding region.
(C) One splice variant of *pve1* does not excise an intron in the 3'-UTR, resulting in a 3'-UTR that is 535-bp long.
(D) Rice gene models for LOC_Os03g44580, the closest rice (*Oryza sativa*) homolog to *pve1*. Image from: http://rice.plantbiology.msu.edu/cgi-bin/ORF_infopage.cgi?orf=13103.m04799

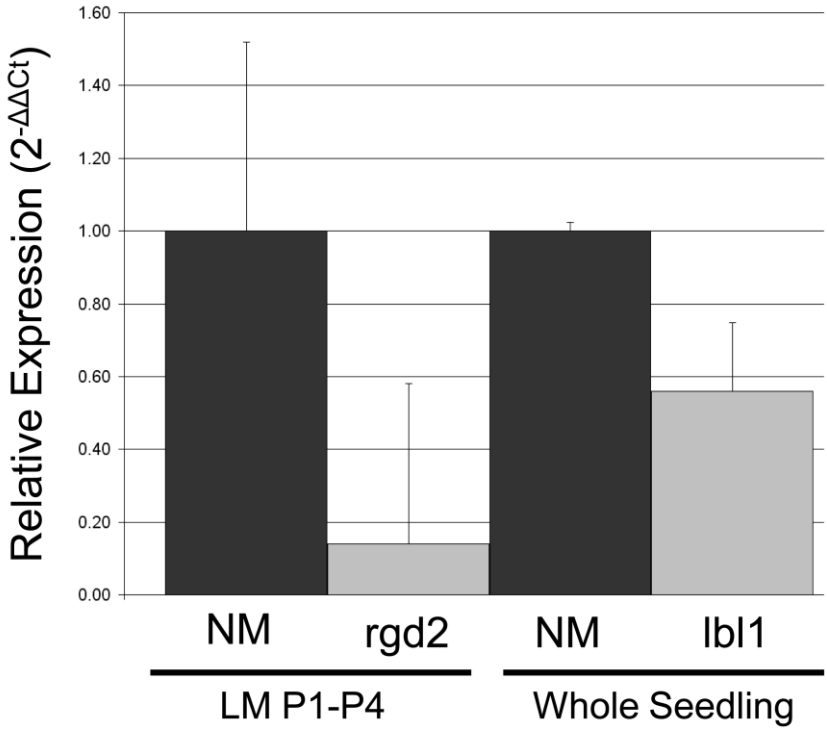

Figure 3.3 qRT-PCR of *pve1* in rgd2 and lbl1 mutants.

The accumulation levels of *punctate vascular expression1* (*pve1*) was examined in ragged seedling2 (rgd2) and leafbladeless1 (lbl1) mutants. The accumulation of *pve1* is diminished in both rgd2 and lbl1 mutants. For rgd2, RNA was harvested by using laser-microdissection (LM) of the first four leaf primordia (P1-P4) in rgd2 mutants and non-mutant (NM) siblings. For lbl1, RNA was extracted from 14 day old whole seedlings. Three biological replicates were used per genotype and all replicates were normalized to *ubiquitin* accumulation. Error bars represent one standard error.

non-mutant siblings (Figure 3.3). Several transcripts (*arf3a, tas3a, rolled leaf1 (rld1), kanadi2* (*kan2*), *ago1*, *lbl1* and *pve1*) that are implicated in establishing maize leaf

dorsiventral polarity (Henderson et al., 2006; Nogueira et al., 2007; Douglas et al., submitted) were examined via qRT-PCR analyses of pve1-R mutants to help elucidate the role of PVE1 in maize leaf development. Generally, *rld1*, *arf3a*, *tas3* and *lbl1* transcripts accumulate to lower levels in pve1-R mutants, while *ago1* transcript levels are increased over two-fold (Figure 3.4). Transcript accumulation for *kan2* is essentially unaltered in pve1-R mutants, while *pve1* accumulation is slightly lower in pve1-R mutants as compared to non-mutant siblings (Figure 3.4).

Although microarray hybridization analyses open many research possibilities, the technique does have some limitations. Microarrays are prone to type II error (false negatives) and may not efficiently detect rare transcripts (Hatfield et al., 2003). Moreover, microarrays are a closed system in that the derived data is limited to genes contained on the gene chip. For example, the SAM gene chips (Ohtsu et al., 2007) utilized in the rgd2 LM-microarray analyses contained only ~20,000 unique maize cDNAs (X. Zhang and M. Scanlon, unpublished data), therefore more than one third of the maize Filtered Gene Set (FGS; ~ 30,000 genes; Schnable et al., 2009) was unrepresented. In contrast, Illumina RNA-sequencing (RNA-seq) has the ability to detect very rare transcripts and is an open system that is not limited by a predetermined list of transcripts. In essence, our previous microarray hybridization may have failed to identify changes in the accumulation of known or predicted targets of *t*a-siARF, miR390 and/or miR166, either due to low transcript abundance or their absence from the SAM cDNA gene chips. Therefore, amplified RNA from laser-microdissected shoot apices was used for Illumina RNA sequencing to compare rgd2 mutants to non-mutant siblings (Figure 3.5). A list of all predicted targets for *t*a-siARF, miR390 and miR166 within the maize FGS was generated by Zhang et al.

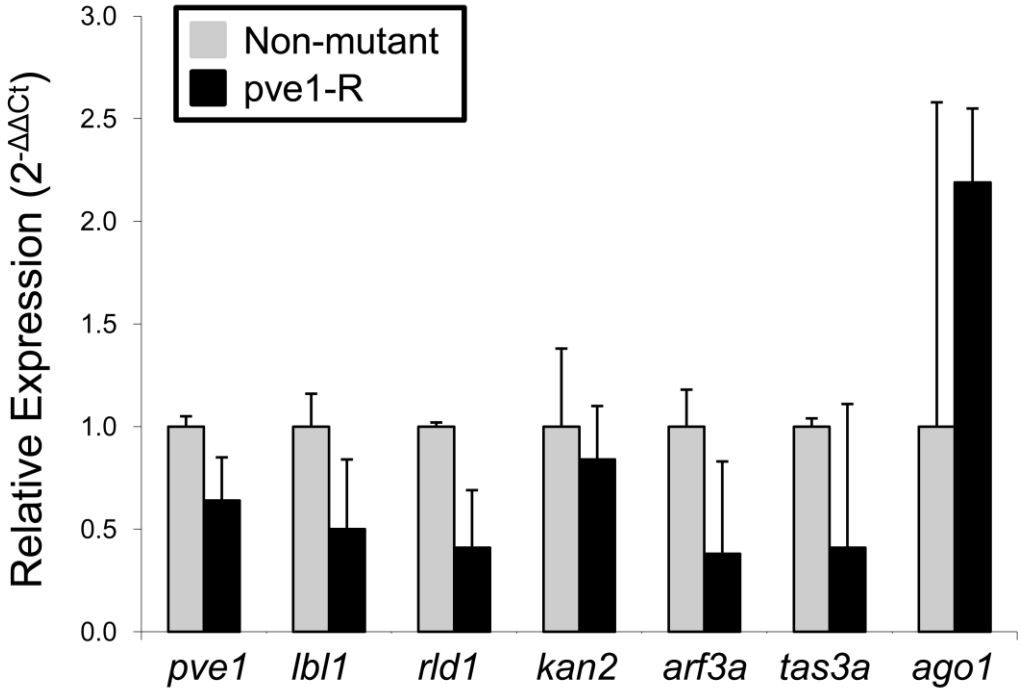

Figure 3.4. qRT-PCR of leaf development genes in pve1-R mutants.

Several genes involved in establishing maize leaf dorsiventral polarity were examined in pve1-R mutants. Three biological replicates were used for each genotype and all samples were normalized to 18s rRNA. Bars represent one standard error.

pve1: punctate vascular expression1; lbl1: leafbladeless1; rld1: rolled leaf1; kan2: kanadi2; arf3a: auxin response factor3a; ago1: argonaute1

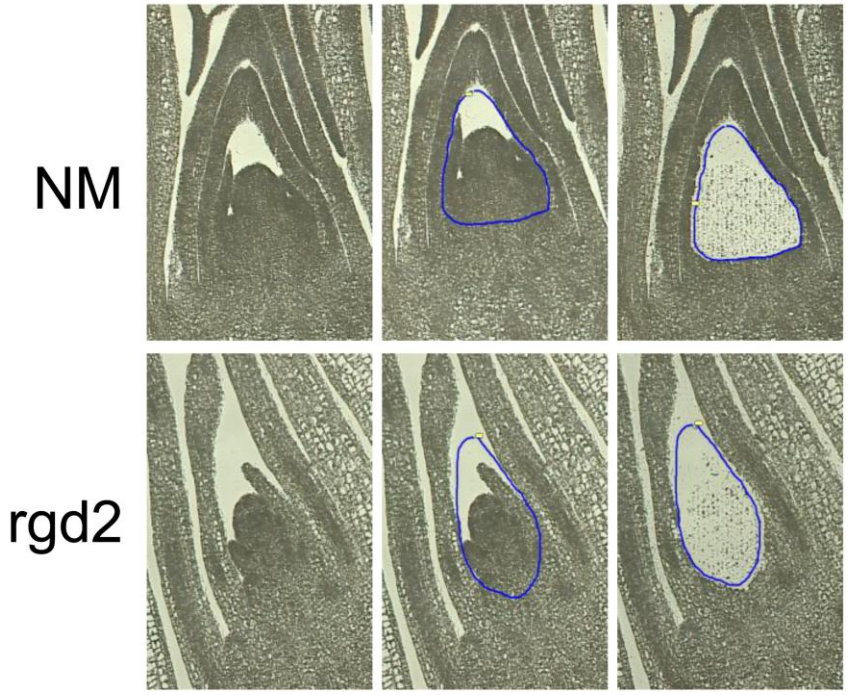

Figure 3.5 Apical regions captured by laser-microdissection for Illumina RNA sequencing.

The shoot apical meristem and first two leaf primordia were captured from non-mutant (NM) and ragged seedling2 (rgd2) mutant apices. Three or four individual apices were pooled for each biological sample and approximately 1 mm^2 of tissue was captured per sample.

(2009). Identification of differential expression of any predicted target genes and their subsequent verification by qRT- PCR and 5' rapid amplification of cDNA ends (RACE) will be performed by co-authors in the Scanlon laboratory, and will not be included as part of this dissertation.

Discussion

Laser-microdissection microarray analyses identified *pve1* as a gene of unknown function that is down-regulated in rgd2 mutant shoot apices (X. Zhang and M. Scanlon, unpublished data). qRT-PCR of microdissected P1-P4 leaf primordia confirmed that *pve1* accumulates in rgd2-R mutants to approximately 15% of the level observed in non-mutant siblings (Figure 3.3). The *pve1* gene has one exon that encodes a 360 amino acid protein of unknown function. The 5'-UTR of *pve1* is at least 317-bp in length, and may contain as many as 763-bp (Figure 3.2B). The 3'-UTR may undergo alternative splicing; some splice variants contain a 3'-UTR of 113-bp split by a 422-bp intron, while other variants do not splice out the intron and simply have a 535-bp 3'-UTR (Figure 3.2A and 3.2C). The long 5'-UTR may reflect a need for *pve1* to be rapidly and effectively translated (Fu et al., 2002), although additional experiments would be necessary to confirm this hypothesis. The observed *pve1* cDNA splice variants are similar to those found in its closest rice (*Oryza sativa*) homolog, *LOC_Os03g44580* (Figure 3.2D). A *Mu1*-like insertion was verified in the lone exon in pve1-R mutants (Figure 3.2A) by utilizing a *Mu* terminal inverted repeat primer with a *pve1* specific primer. The identification of this mutant allele permitted a molecular genetic analysis of the loss of PVE1 function in maize.

In addition to having reduced accumulation in rgd2-R mutants, *pve1* also has reduced accumulation in lbl1-R mutants (Figure 3.3), which suggests that *pve1* is regulated by *t*a-siARF, *arf3a,* or another downstream target of the *t*a-siARF biogenesis pathway rather than directly by RGD2 function. Several genes known to be involved

in the establishment of maize leaf dorsiventral polarity were examined using qRT-PCR in pve1-R mutants (Figure 3.4) and the resulting data were used to construct a working model for PVE1 function (Figure 3.6A). The down-regulation of *lbl1* and the up-regulation of *ago1* corroborate findings that LBL1 function is required to restrict *ago1* accumulation (Figure 3.4; Douglas et al., submitted). The reduction of *lbl1*and *tas3a* transcripts in pve1-R mutants suggests that PVE1 function promotes the *t*a-siARF pathway, which in turn promotes the accumulation of *pve1* (Figure 3.6B). Interestingly, *pve1* promotes the accumulation of *arf3a*, which is repressed by the *t*a-siARF pathway (Figure 3.6B). These findings suggest a complex feedback loop regulating both the *t*a-siARF pathway and *pve1*. ARF3a may down-regulate *pve1*, which in turn promotes *arf3a* in a negative feedback loop. The reduction of *rld1* transcripts in pve1-R mutants could be a result of increased miR166 levels or increased miR166 activity due to elevated *ago1* and reduced *lbl1* levels. Additional experiments are required to elucidate the connection between the *t*a-siARF pathway and the accumulation of miR166 (Figure 3.6A).

Finally, Illumina RNA sequencing of aRNA derived from laser-microdissected rgd2 mutant and non-mutant sibling apices (SAM-P2 leaf primordia; Figure 3.5) was performed to examine the regulation of known and predicted downstream, small-RNA targets of the *t*a-siARF biogenesis pathway. If any of the targets are mis-regulated in rgd2 mutants, they may become investigated with future reverse genetics approaches to further examine downstream effects of the *t*a-siARF biogenesis pathway on maize leaf development.

Materials

Plant Materials

The *pve1-R* mutant allele arose in *Mu* active lines of a mixed pedigree. The *pve1-R* allele has been introgressed into the B73 inbred line for two generations.

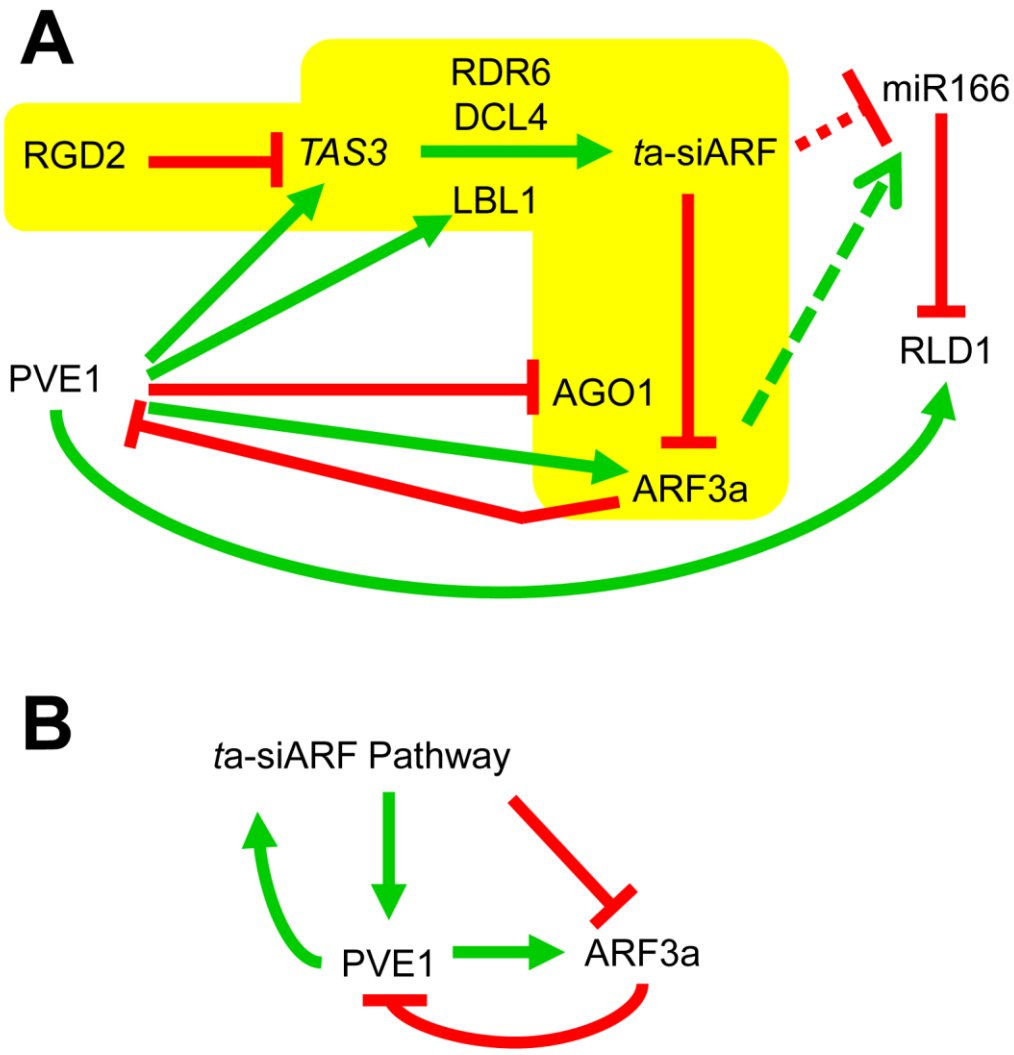

Figure 3.6. Proposed model for PVE1 function.

(A) Based on qRT-PCR data, a model is proposed whereby PVE1 functions downstream of RGD2**.** PVE1 is hypothesized to promote the accumulation of *lbl1*, *ta*-siARF, *arf3a* and *rld1* while repressing the accumulation of *ago1*. The *ta*-siARF pathway is highlighted in yellow. Dashed lines represent putative interactions. **(B)** A simplified model from part A. The *ta*-siARF pathway inhibits ARF3a accumulation and promotes PVE1, which in turn positively regulates the *ta*-siARF pathway and ARF3a.

RGD2: RAGGED SEEDLING2; RDR6: RNA-DEPENDANT RNA POLYMERASE6; DCL4: DICER-LIKE4; LBL1: LEAFBLADELESS1; AGO1: ARGONAUTE1; PVE1: PUNCTATE VASCULAR EXPRESSION1; ARF3a: AUXIN RESPONSE FACTOR3a; RLD1: ROLLED LEAF1; miR166: microRNA 166

Table 3.1. Primers used in this study

pve1 primers

Primer Set	Forward Primer	Reverse Primer	Product Size
Coding	GTGATCCAAGAGGCCGCAG	CCAGAATGCAACAGATTCCCA	1592-bp
5' UTR	CCTTCGGTTATCTGAGCTGC	AGAGGAGGAGAGGATGGCTC	489-bp
3' UTR	CCCACACATGTATGAGCCTG	CCTGAAACAAGGAGAGGACG	857-bp

qRT-PCR primers

Locus	Accession	Forward Primer	Reverse Primer
pve1	DN223697	CCCACACATGTATGAGCCTG	ACTCAGGAGAAAACTTGCGG
arf3a	AC204859	CTAGGTTTTCCTACCGTTGCTCAG	GACAAACATTGCGCGTCTATCCTC
tas3a	AC211570	GCTCAGGAGGGATAGAAGGG	TCTTTCCCACTACATGCAGGA
rld1	AY501430	CGAAGAGTGTTCCTGAAGTGCTT	GCGCAGTGCCACAGTAGTCA
kan2	CO520143	CTGGGTGTGGTGCAAGAA	CACAACGACCACCACCATCAG
ago1	AY110984	CTGCTGGTGTTGGGAATGTT	GCTCTGCCTTAACAGCATCA
lbl1	DQ832257	GCATAAGCCAGATACCTTCGAG	ACATCTACAGACTGTCCAGGCA
18s rRNA	AF168884	CTGTCGGCCAAGGCTATAGACT	TCTGTGATGCCCTTAGATGTTCTG
ubq	S94464	TAAGCTGCCGATGTGCCTGCGTCG	CTGAAAGACAGAACATAATGAGCA CA

qRT-PCR

Whole plant tissue was harvested using TRIzol reagent (Invitrogen; Carlsbad, CA) and cDNA was synthesized using SuperScript III First Strand Synthesis System (Invitrogen; Carlsbad, CA). Leaf primordia (P1-P4) tissue was harvested by laser microdissection (LM) from rgd2 mutant and non-mutant siblings, and cDNA was synthesized from amplified RNA (aRNA) as described in Zhang et al. (2007). Gene-specific primers were designed (Table 3.1) for use with SYBR-Green (Quanta) in qRT-PCR as described (Zhang et al., 2007). Three biological replicates were examined, and samples were normalized to *ubiquitin* (accession S94464) accumulation as described using Bio-Rad iQ5 Version 1.0 software (Livak and Schmittgen, 2001; Zhang et al., 2007).

Illumina RNA Sequencing

SAM and P0-P2 leaf primordia tissues were harvested from rgd2 mutants and non-mutant siblings (two replicates per genotype) using LM (Figure 3.5) and aRNA was synthesized as described in Zhang et al. (2007). Three or four individual apices were pooled per biological replicate, and approximately 1 mm^2 of tissue was harvested per replicate. Approximately 100 ng of aRNA for each replicate was processed for Illumina-based RNA-seq analysis. RNA-seq was performed by the Cornell University Life Sciences Core Laboratories Center (Ithaca, NY).

REFERENCES

Adenot X., Elmayan T., Lauressergues D., Boutet S., Bouche N., Gasiciolli V., and Vaucheret H. 2006. DRB4-dependant *TAS3 trans*-acting siRNAs control leaf morphology through AGO7. *Curr. Biol.* 18: 758-762.

Allen, E., Xie, Z., Gustafson, A.M., and Carrington, J.C. 2005. microRNA-directed phasing during *trans*-acting siRNA biogenesis in plants. *Cell*. 121: 207-221.

Altschul SF., Gish W., Miller W., Myers EW., and Lipman DJ. 1990. Basic local alignment search tool. *J Mol Biol.* 215: 403-410.

Candela H., Johnston R., Gerhold A., Foster T., and Hake S. 2008. The *milkweed pod1* gene encodes a KANADI protein that is required for abaxial/adaxial patterning in maize leaves. *Plant Cell*. 20: 2073-2087.

Fahlgren N., Montgomery T., Howell M., Allen E., Dvorak S., Alexander A., and Carrington J. 2006. Regulation of *AUXIN RESPONSE FACTOR3* by *TAS3* ta-siRNA affects developmental timing and patterning in *Arabidopsis*. *Curr. Biol*. 16: 939-944.

Fu S., Meeley R., and Scanlon M.J. 2002. *empty pericarp2* encodes a negative regulator of the heat shock response and is required for early stages of maize embryogenesis. *Plant Cell*. 14: 3119-3132.

Garcia, D., Collier, S.A., Byrne, M.E., and Martienssen, R.A. 2006. Specification of leaf polarity in *Arabidopsis* via the *trans*-acting siRNA pathway. *Curr. Biol*. 9: 933-938.

Hatfield G.W., Hung S.P., and Baldi P. 2003. Differential analysis of DNA microarray gene expression data. *Mol. Microbiol.* 47: 871-877.

Henderson, D.C., Muehlbauer, G.J., and Scanlon, M.J. 2005. Radial leaves of the maize mutant *ragged seedling2* retain dorsiventral anatomy. *Dev. Biol*. 282: 455-466.

McConnell, J.R., Emery, J., Eshed, Y., Bao, N., Bowman, J., and Barton, M.K. 2001. Role of PHABULOSA and PHAVOLUTA in determining radial patterning in

shoots. *Nature*. 411: 709-713.

Montgomery T.A., Howell M.D., Cuperus J.T., Li D., Hansen J.E., Alexander A.L., Chapman E.J., Fahlgren N., Allen E., and Carrington J.C. 2008. Specificity of ARGONAUTE7-miR390 interaction and dual functionality in *TAS3 trans*-acting siRNA formation. *Cell*. 133:128-141.

Nogueira, F.T.S., Madi, S., Chitwood, D.H., Juarez, M.T. and Timmermans, MCP. 2007. Two small regulatory RNAs establish opposing fates of a developmental axis. *Genes Dev.* 21: 750-755.

Ohtsu K., Smith M.B., Emrich S.J., Borsuk L.A., Zhou R., Chen T., Zhang X., Timmermans M.C.P., Beck J., Buckner B., Janick-Buckner D., Nettleton D.S., Scanlon M.J., and Schnable P.S. 2007. Global gene expression analysis of the shoot apical meristem of maize (*Zea mays* L.). *Plant J.* 52: 391-404.

Pekker, I., Alvarez, J.P., and Eshed, Y. 2005. Auxin response factors mediate *Arabidopsis* organ asymmetry via modulation of KANADI activity. *Plant Cell*. 17: 2899-2910.

Peragine A., Yoshikawa M., Wu G., Albrecht H.L., and Poethig R.S. 2004. SGS3 and SGS2/SDE1/RDR6 are required for juvenile leaf development and the production of *trans*-acting siRNAs in *Arabidopsis*. *Genes Dev.* 18: 2368-2379.

Schnable P.S., Ware D., Fulton R.S., Stein J.C., Wei F., Pasternak S., Liang C., Zhang J., Fulton L., Graves T.A., Minx P., Reily A.D., Courtney L., Kruchowski S.S., Tomlinson C., Strong C., Delehaunty K., Fronick C., Courtney B., Rock S.M., Belter E., Du F., Kim K., Abbott R.M., Cotton M., Levy A., Marchetto P., Ochoa K., Jackson S.M., Gillam B., Chen W., Yan L., Higginbotham J., Cardenas M., Waligorski J., Applebaum E., Phelps L., Falcone J., Kanchi K., Thane T., Scimone A., Thane N., Henke J., Wang T., Ruppert J., Shah N., Rotter K., Hodges J., Ingenthron E., Cordes M., Kohlberg S., Sgro J., Delgado B., Mead

K., Chinwalla A., Leonard S., Crouse K., Collura K., Kudrna D., Currie J., He R., Angelova A., Rajasekar S., Mueller T., Lomeli R., Scara G., Ko A., Delaney K., Wissotski M., Lopez G., Campos D., Braidotti M., Ashley E., Golser W., Kim H., Lee S., Lin J., Dujmic Z., Kim W., Talag J., Zuccolo A., Fan C., Sebastian A., Kramer M., Spiegel L., Nascimento L., Zutavern T., Miller B., Ambroise C., Muller S., Spooner W., Narechania A., Ren L., Wei S., Kumari S., Faga B., Levy M.J., McMahan L., Van Buren P., Vaughn M.W., Ying K., Yeh C.T., Emrich S.J., Jia Y., Kalyanaraman A., Hsia A.P., Barbazuk W.B., Baucom R.S., Brutnell T.P., Carpita N.C., Chaparro C., Chia J.M., Deragon J.M., Estill J.C., Fu Y., Jeddeloh J.A., Han Y., Lee H., Li P., Lisch D.R., Liu S., Liu Z., Nagel D.H., McCann M.C., SanMiguel P., Myers A.M., Nettleton D., Nguyen J., Penning B.W., Ponnala L., Schneider K.L., Schwartz D.C., Sharma A., Soderlund C., Springer N.M., Sun Q., Wang H., Waterman M., Westerman R., Wolfgruber T.K., Yang L., Yu Y., Zhang L., Zhou S., Zhu Q., Bennetzen J.L., Dawe R.K., Jiang J., Jiang N., Presting G.G., Wessler S.R., Aluru S., Martienssen R.A., Clifton S.W., McCombie W.R., Wing R.A., Wilson R.K. 2009. The B73 maize genome: complexity, diversity and dynamics. *Science*. 326: 1112-1115.

Timmermans, M.C.P., Schultes, N.P., Jankovsky, J.P., and Nelson, T. 1998. *Leafbladeless1* is required for dorsoventrality of lateral organs in maize. *Development*. 125: 2813-2823.

Waites, R. and Hudson, A. 1995. *phantastica*: a gene required for dorsoventrality of leaves in *Antirrhinum majus*. *Development*. 121: 2143-2154.

Zhang L., Chia J.M., Kumari S., Stein J.C., Liu Z., Narechania A., Maher C.A., Guill K., McMullen M.D., Ware D. 2009. A genome-wide characterization of microRNAs in maize. *PLoS Genet.* 5:e1000716.

CHAPTER 4

Summary

The Waites-Hudson model for mediolateral leaf development tied the mediolateral and dorsiventral axes together in that it states that the juxtaposition of adaxial and abaxial tissues is sufficient to trigger mediolateral outgrowth in plants harboring dorsiventrally-flattened leaf morphology (Waites and Hudson, 1995). Support for this model is provided by molecular-genetic analyses of the maize (*Zea mays*) mutants leafbladeless1 (lbl1), which has radially symmetric, abaxialized leaves, and milkweedpod1, which has ectopic outgrowths on the abaxial surface of husk leaves where new adaxial/abaxial juxtaposition points occur (Timmermans et al., 1998; Candela et al., 2008). However, the Waites-Hudson model is insufficient to explain the leaf phenotypes of the maize mutant ragged seedling2 (rgd2), which has radial leaves that maintain distinct adaxial and abaxial tissue types (Henderson et al., 2005). Observations of rgd2 mutant leaves suggest that either the Waites-Hudson model is insufficient to describe mediolateral leaf development, or RGD2 function is required for the ability to understand that adaxial and abaxial tissues are in juxtaposition (Henderson et al., 2005). The primary goal of this dissertation was to understand the molecular function of RGD2, and its contribution to mediolateral and dorsiventral patterning in maize leaves.

Despite having very different mutant phenotypes, *rgd2* and *lbl1* function in the same molecular pathway to generate *trans*-acting small interfering RNAs called *t*a-siARFs (Nogueira et al., 2007; Douglas et al., submitted). *rgd2* encodes an ARGONAUTE7 (AGO7)-like protein that forms an RNA-induced silencing complex (RISC) with microRNA 390 (miR390) to target the non-protein coding *tas3a* transcript for degradation (Douglas et al., submitted; Montgomery et al., 2008). LBL1 is a homolog of *Arabidopsis* SUPPRESSOR-OF-GENE-SILENCING3, which is believed to bind to and stabilize double-stranded RNA produced by RNA-dependant RNA POLYMERASE6, which occurs directly downstream of RGD2-

mediated *tas3a* cleavage (Nogueira et al., 2007; Elkashef and Ding, 2009; Allen et al., 2005). The *t*a-siARFs generated by this RGD2-LBL1 dependent pathway target the putative abaxial identity factor *auxin response factor3a* (*arf3a*) for degradation (Allen et al., 2005; Nogueira et al., 2006).

Upon cloning and identification of the *rgd2 gene*, the *t*a-siARF biogenesis pathway was examined to ascertain *rgd2* function and to reconcile the distinct rgd2 and lbl1 mutant phenotypes. Since AGO7 and miR390 were found to work nearly exclusively with each other to form a RISC in the eudicot *Arabidopsis* (Montgomery et al., 2008), the accumulation pattern and levels of miR390 were examined in rgd2 mutants. While miR390 ectopically accumulates in rgd2 mutant shoot apical meristems (SAM), it remains polarized in adaxial regions of young leaf primordia, suggesting that the polarization of miR390 occurs upstream of *t*a-siARF biogenesis (Douglas et al., submitted). Interestingly, *rgd2* transcripts were found to accumulate throughout young leaf primordia, which means miR390 polarization (not AGO7) establishes the boundaries of adaxialized *t*a-siARF biogenesis in maize (Douglas et al., submitted; Nogueira et al., 2007). These results are in agreement with previous work that showed miR390 remains adaxialized in lbl1 mutants (Nogueira et al., 2009).

It was also discovered that only rgd2-R mutants, which are presumed to either lack a PAZ domain or have a mis-folded PAZ domain, exhibit ectopic miR390 accumulation; rgd2-e2 mutants with an intact PAZ domain display normal miR390 accumulation (Douglas et al., submitted). As miR390 has been hypothesized to be mobile within the maize shoot apex (Nogueira et al., 2009), these data may provide a mechanism whereby miR390 movement is restricted by RGD2. Presumably, the PAZ domain of RGD2 binds to miR390 and keeps it from trafficking from leaf primordia to the SAM crown rather than sequestering miR390 precursor transcripts;

PAZ domains bind the 3' end of small RNAs (Ma et al., 2004; Lingel et al., 2004). This mechanism would imply that in rgd2-R mutants mature miR390 diffuses through plasmodesmata (or is actively transported by as-yet-unknown chaperones) into the SAM crown if RGD2 is not present. In *Arabidopsis*, green fluorescent protein with a predicted mass of 54 kDa was unable to move between the shoot apex and cotyledons (Kim et al., 2005). RGD2 is predicted to have a mass of 115.3 kDa, so any miR390 bound by RGD2 would likely be unable to move between cells.

The target of *t*a-siARF, *arf3a*, is an abaxial identity factor in *Arabidopsis* (Pekker et al., 2005; Garcia et al., 2006; Fahlgren et al., 2006), and it has been purported to play a similar role in maize based on analysis of *arf3a* in lbl1mutants (Nogueira et al., 2007). Surprisingly, *in situ* hybridization revealed that *arf3a* accumulation remains strictly abaxialized in both rgd2 and lbl1 mutants (Douglas et al., submitted). These findings indicate that *arf3a* is *not polarized* by *t*a-siARF cleavage; *arf3a* is polarized upstream of *t*a-siARF biogenesis and function. In contrast, miR166 polarization is dependant on components of the *t*a-siARF biogenesis pathway. MiR166 is an abaxial determinant that targets adaxial identity factor *HD-ZIP III* family transcripts for degradation and normally accumulates only in abaxial regions of leaf primordia (McConnell et al., 2001; Nogueira et al., 2007). In non-mutant maize miR166 accumulates in abaxial regions of young leaf primordia, but its accumulation pattern expands to encompass the entire young leaf primordia in rgd2 and lbl1 mutants (Nogueira et al., 2007; Douglas et al., submitted).

The examination of rgd2 mutants has shed new light on the role of the *t*a-siARF biogenesis pathway. Prior to this study, the pathway was believed to play a major role in establishing leaf dorsiventral polarity in maize (reviewed in Kidner and Timmermans, 2007). However, given that the putative abaxial identity factor *arf3a* remains abaxially polarized in rgd2 mutants, and since rgd2 mutants maintain

dorsiventral polarity, it seems unlikely that the main function of the *t*a-siARF biogenesis pathway in maize is to establish leaf dorsiventral polarity. Additionally, the fact that miR390 is also polarized upstream of this pathway suggests that a yet-to-be-determined factor or factors are responsible for polarizing *t*a-siARF accumulation and its target, *arf3a*. In *Arabidopsis* the *t*a-siARF biogenesis pathway is predominantly involved in vegetative phase-change; ago7 mutants exhibit leaves that undergo a precocious switch from juvenile stage to adult stage (Hunter et al., 2003). Although the possibility that rgd2 and lbl1 being phase-change mutants has largely been ignored, a closer examination of their mutant phenotypes may be warranted given that the *t*a-siARF biogenesis pathway no longer appears to be a key factor in establishing leaf dorsiventral polarity in maize.

Despite not having a clear, direct role in establishing dorsiventral polarity via modulation of *arf3a* accumulation, the *t*a-siARF biogenesis pathway does play an important role in establishing the polarized accumulation pattern of miR166 (Nogueira et al., 2007; Douglas et al., submitted). Exactly how *t*a-siARF biogenesis effects miR166 remains unknown. It is possible that *t*a-siARF represses *miR166* precursor loci, or that *arf3a* may promote *miR166*.

Future work examining downstream targets/components of the *t*a-siARF biogenesis pathway will likely offer new insights toward understanding the roles of the pathway in maize leaf development. A microarray hybridization study comparing rgd2 mutant and non-mutant sibling apices was performed to identify potential downstream targets of *rgd2* function (X. Zhang and M. Scanlon, unpublished data). A transcript with no homology to transcripts of known function was identified as being highly down-regulated in rgd2 mutants and was named *punctate vascular expression1* (*pve1*) based on its *in situ* hybridization profile (X. Zhang, M. Scanlon, unpublished data). Using a reverse genetics technique, pve1 mutants were identified,

and they should prove useful in widening our knowledge downstream of RGD2 and LBL1 function. qRT-PCR analysis of several genes involved in leaf polarity and/or the *t*a-siARF biogenesis pathway has suggested that PVE1 promotes *t*a-siARF biogenesis and *arf3a* accumulation. In turn, the *t*a-siARF biogenesis pathway enhances the accumulation of *pve1* and ARF3a represses *pve1* in an apparent negative feedback loop (R. Douglas and M. Scanlon, unpublished data; Chapter 3).

In order to search for additional targets of *t*a-siARF biogenesis-related small RNAs, and thus further expand our knowledge of leaf development, Illumina RNA sequencing of amplified RNA from rgd2 mutant and non-mutant sibling apices will be performed. Like the microarray analyses that identified *pve1* as a gene of interest, this experiment may yield additional transcripts of interest that can be subjected to a variety of reverse genetic techniques to build on established models and reveal novel molecular and genetic pathways.

REFERENCES

Allen E., Xie Z., Gustafson A.M., and Carrington J.C. 2005. microRNAs-directed phasing during *trans*-acting siRNA biogenesis in plants. *Cell*. 121: 207-221.

Candela H., Johnston R., Gerhold A., Foster T., and Hake S. 2008. The *milkweed pod1* gene encodes a KANADI protein that is required for abaxial/adaxial patterning in maize leaves. *Plant Cell*. 20: 2073-2087.

Elkashef S. and Ding S.W. 2009. Possible new RNA intermediate in RNA silencing. *Nat. Chem. Biol.* 5: 278-279.

Fahlgren N., Montgomery T., Howell M., Allen E., Dvorak S., Alexander A., and Carrington J. 2006. Regulation of *AUXIN RESPONSE FACTOR3* by *TAS3* ta-siRNA affects developmental timing and patterning in *Arabidopsis*. Curr. Biol. 16: 939-944.

Garcia D., Collier S.A., Byrne M.E., and Martienssen R.A. 2006. Specification of leaf polarity in *Arabidopsis* via the *trans*-acting siRNA pathway. *Curr. Biol*. 16: 933-938.

Henderson D.C., Muehlbauer G.J., and Scanlon M.J. 2005. Radial leaves of the maize mutant *ragged seedling2* retain dorsiventral anatomy. *Dev. Biol*. 282: 455-466.

Hunter C., Sun H., and Poethig R.S. 2003. The *Arabidopsis* heterochronic gene *ZIPPY* is an ARGONAUTE family member. *Curr. Biol*. 13:1734-1739.

Kidner C.A., and Timmermans M.C. 2007. Mixing and matching pathways in leaf polarity. *Curr. Opin. Plant Biol.* 10:13-20.

Kim I., Kobayashi K., Cho E., and Zambryski P.C. 2005. Subdomains for transport via plasmodesmata corresponding to the apical-basal axis are established during *Arabidopsis* embryogenesis. *Proc. Natl. Acad. Sci. USA.* 102: 11945-11950.

Lingel A., Simon B., Izaurralde E., and Sattler M. 2004. Nucleic acid 3'-end recognition by the Argonaute2 PAZ domain. *Nature Struct. Mol. Biol.* 11: 576-577.

Ma J., Ye K., and Patel D.J. 2004. Structural basis for overhang-specific small

interfering RNA recognition by the PAZ domain. *Nature*. 429: 318-322.

McConnell J.R., Emery J., Eshed Y., Bao N., Bowman J., and Barton M.K. 2001. Role of *PHABULOSA* and *PHAVOLUTA* in determining radial patterning in shoots. *Nature*. 411:709-713.

Montgomery T.A., Howell M.D., Cuperus J.T., Li D., Hansen J.E, Alexander A.L., Chapman E.J., Fahlgren N., Allen E., and Carrington J.C. 2008. Specificity of ARGONATUE7-miR390 interaction and dual functionality in TAS3 trans-acting siRNA formation. *Cell*. 133: 128-141.

Nogueira F.T.S., Madi S., Chitwood D.H., Juarez M.T. and Timmermans M.C.P. 2007. Two small regulatory RNAs establish opposing fates of a developmental axis. *Genes Dev.* 21: 750-755.

Nogueira F.T., Chitwood, D.H., Madi, S., Ohtsu, K., Schnable, P.S., Scanlon, M.J., and Timmermans, M.C. 2009. Regulation of small RNA accumulation in the maize shoot apex. *PLoS Genet*. 5: e1000320.

Pekker I., Alvarez J., and Eshed Y. 2005. AUXIN RESPONSE FACTORS mediate *Arabidopsis* organ asymmetry via modulation of KANADI activity. *Plant Cell*. 17: 2899-2910.

Timmermans M.C., Schultes N.P., Jankovsky J.P., and Nelson T. 1998. Leafbladeless1 is required for dorsoventrality of lateral organs in maize. *Development*. 125: 2813-2823.

Waites R. and Hudson A. 1995. *phantastica*: a gene required for dorsoventrality of leaves in *Antirrhinum majus*. *Development*. 121: 2143-2154.